APPENDIX B - GLOBAL SENSITIVITY ANALYSIS RESULTS

B.1 HMA OVER HMA

B.1.1 Alligator Cracking

Inputs main effect

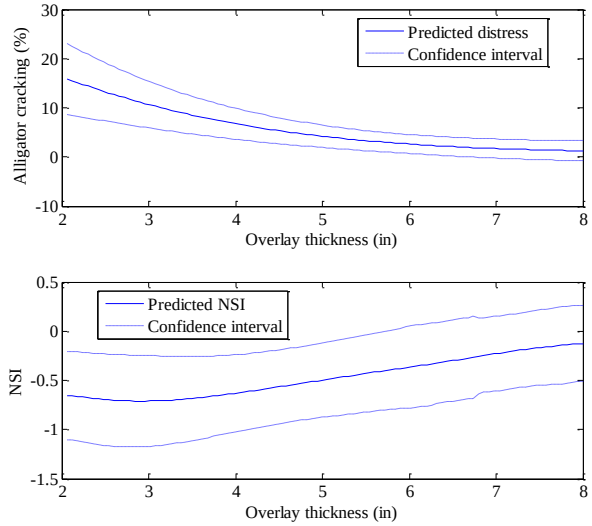

Figure B-1 Predicted alligator cracking and NSI for overlay thickness

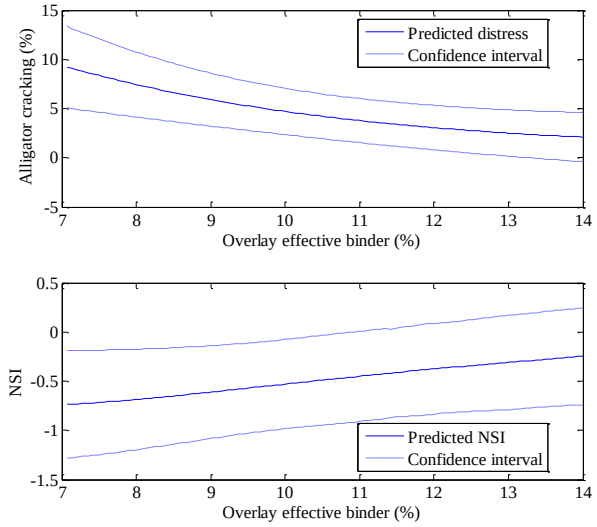

Figure B-2 Predicted alligator cracking and NSI for effective binder

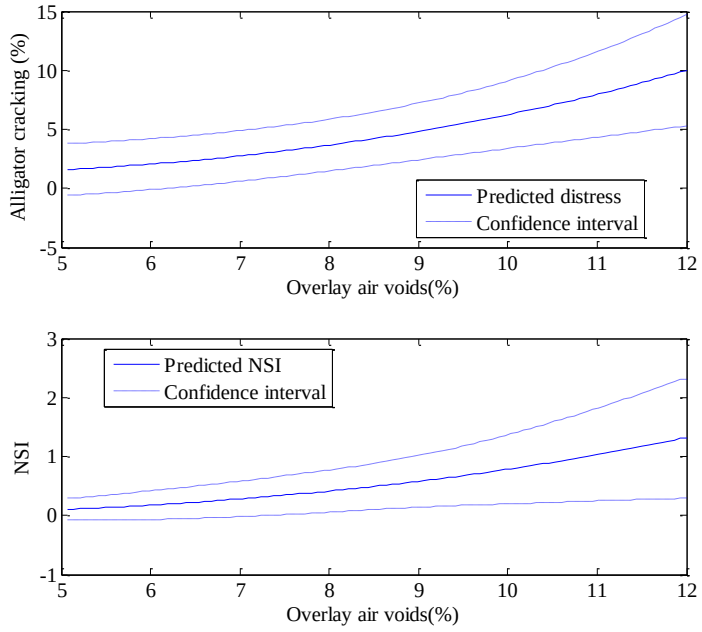

Figure B-3 Predicted alligator cracking and NSI for air voids

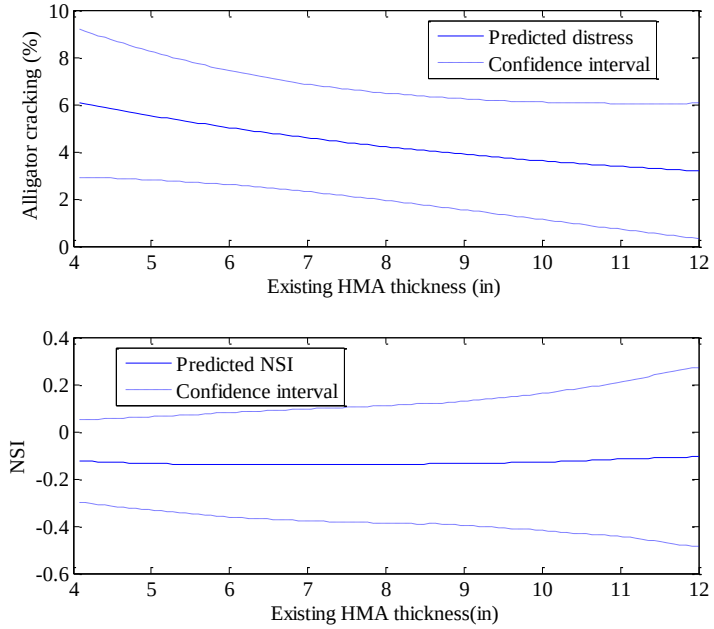

Figure B-4 Predicted alligator cracking and NSI for existing thickness

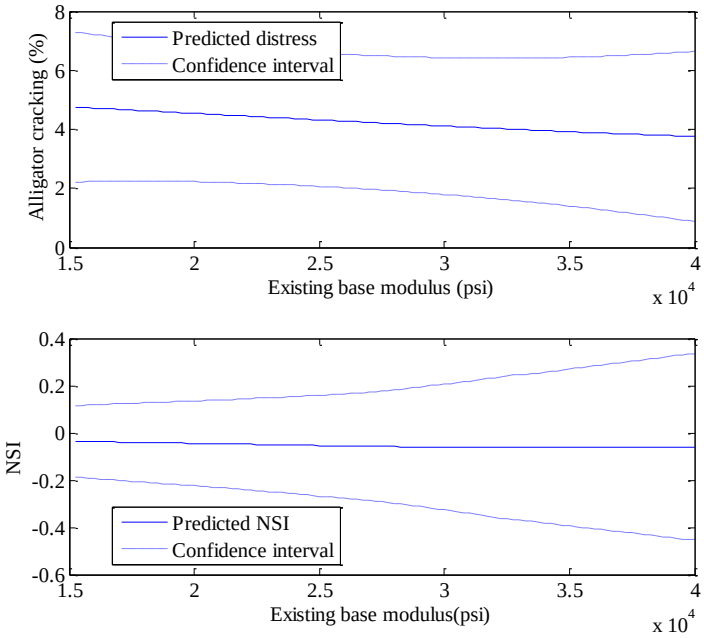

Figure B-5 Predicted alligator cracking and NSI for base modulus

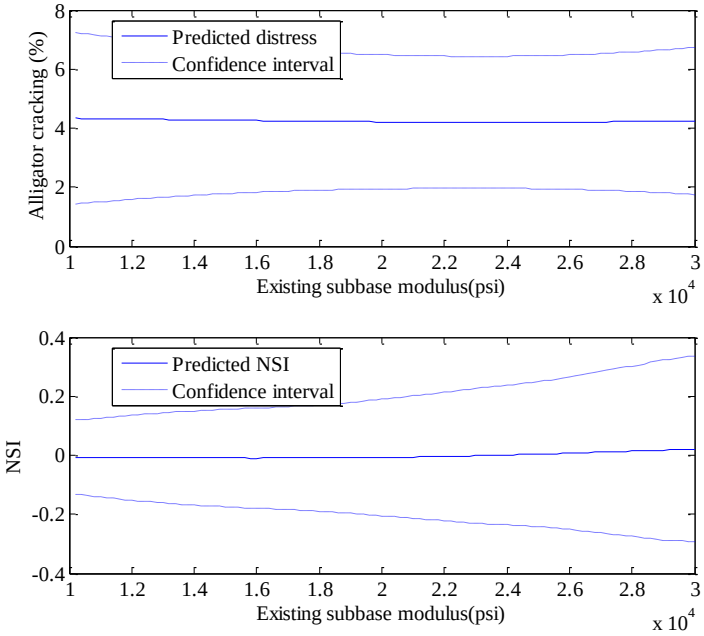

Figure B-6 Predicted alligator cracking and NSI for subbase modulus

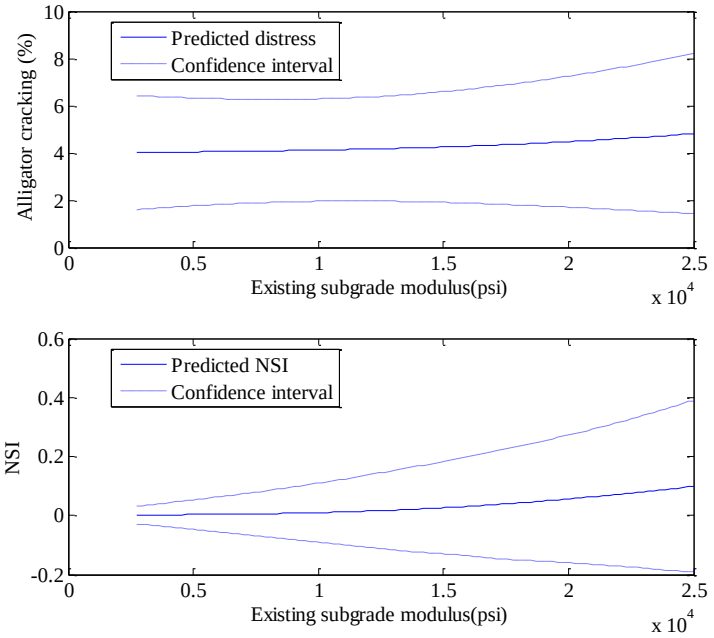

Figure B-7 Predicted alligator cracking and NSI subgrade modulus

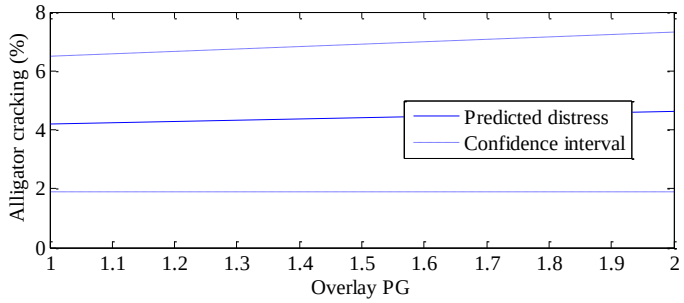

Figure B-8 Predicted alligator cracking for overlay PG

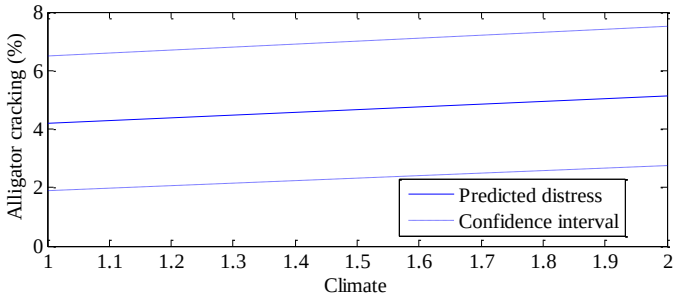

Figure B-9 Predicted alligator cracking for cliamte

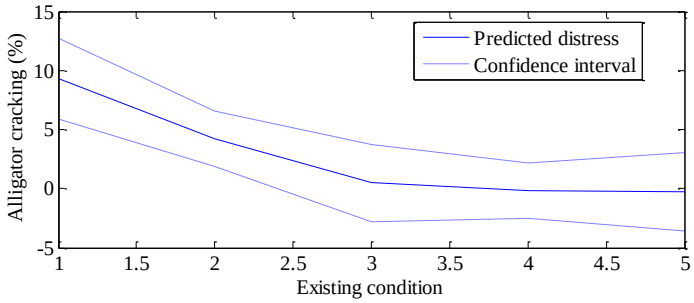

Figure B-10 Predicted alligator cracking for existing condition

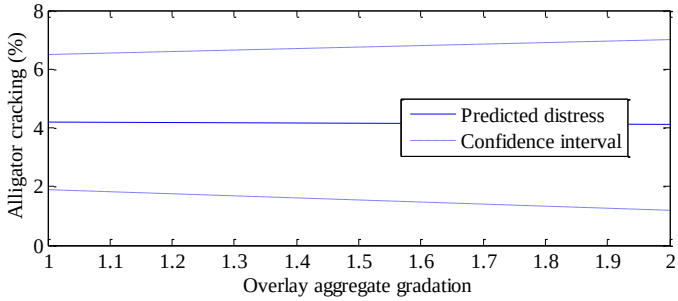

Figure B-11 Predicted alligator cracking for overlay aggregate gradation

Inputs interaction effect

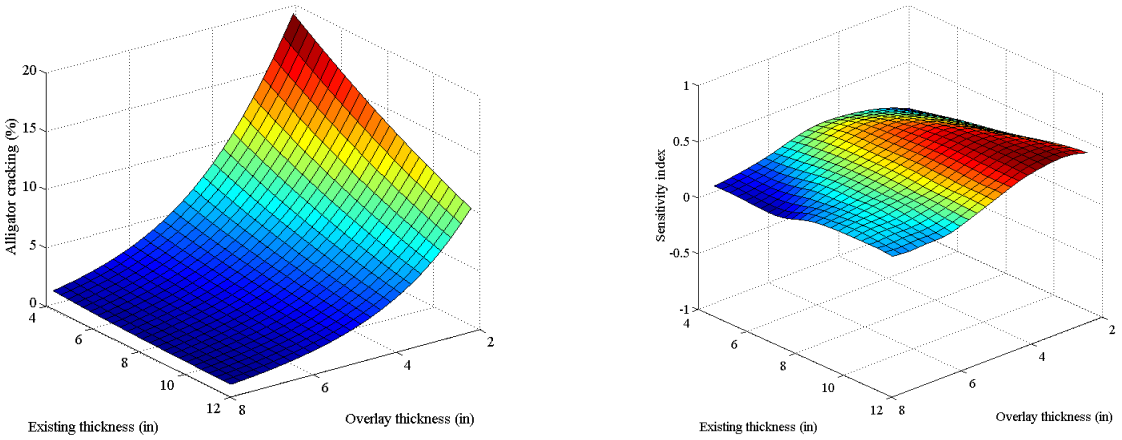

Figure B-12 Predicted interaction and NSI between existing thickness and overlay thickness

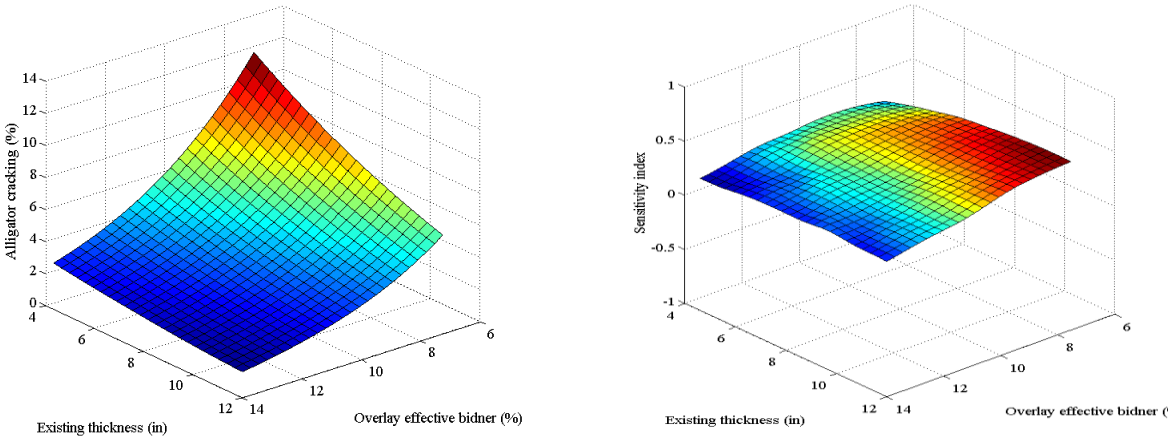

Figure B-13 Predicted interaction and NSI between existing thickness and overlay effective binder

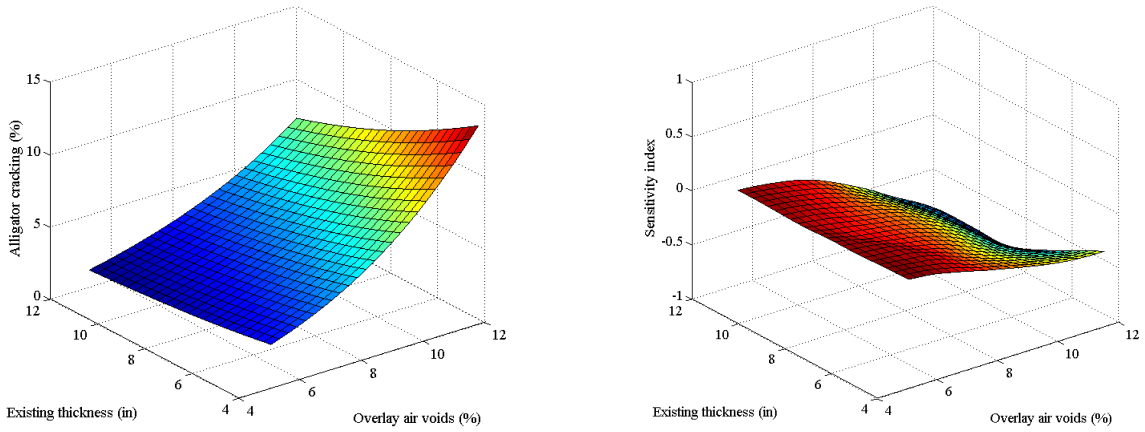

Figure B-14 Predicted interaction and NSI between existing thickness and overlay air voids

B.1.2 Longitudinal Cracking

Inputs main effect

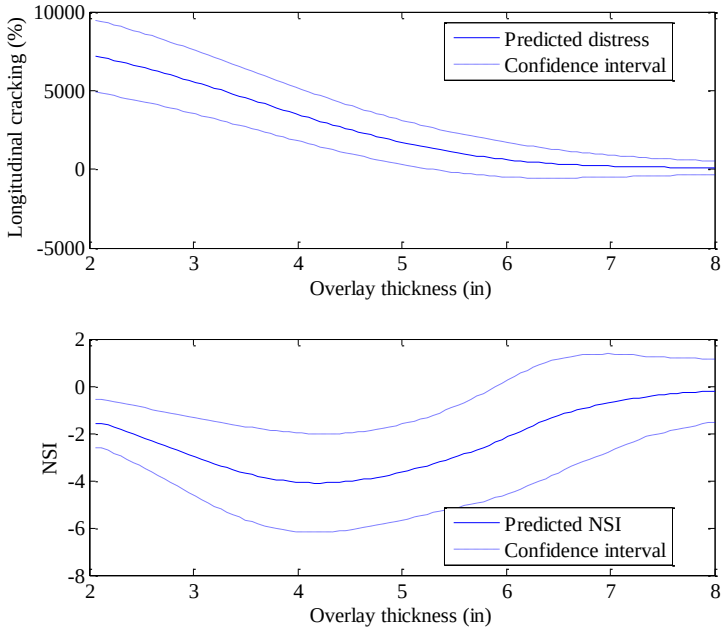

Figure B-15 Predicted longitudinal cracking and NSI for overlay thickness

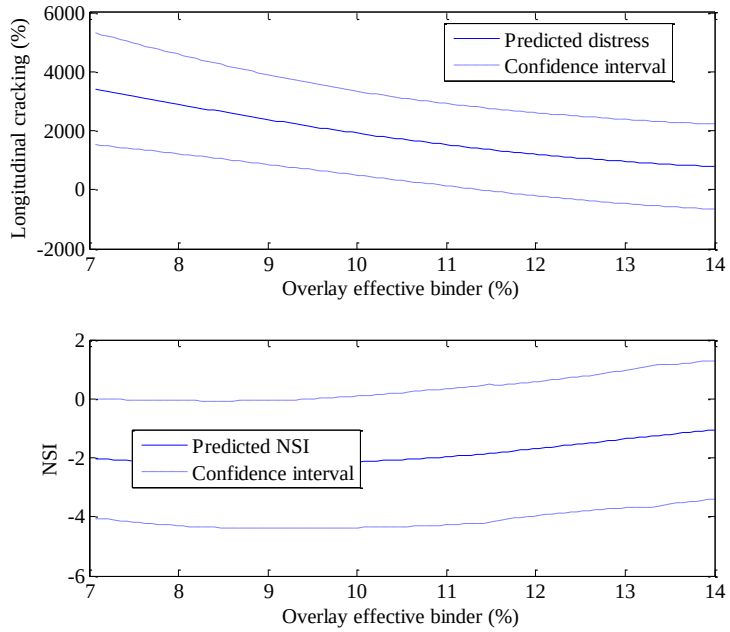

Figure B-16 Predicted longitudinal cracking and NSI for overlay effective binder

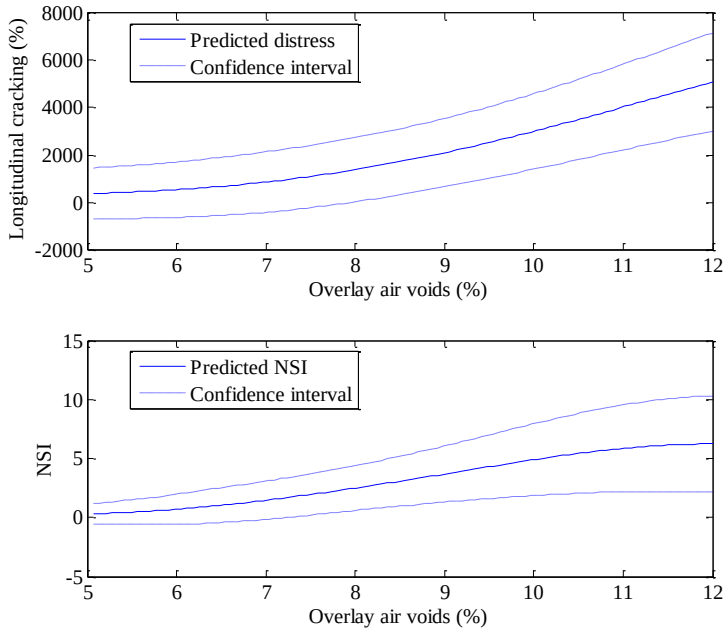

Figure B-17 Predicted longitudinal cracking and NSI for overlay air voids

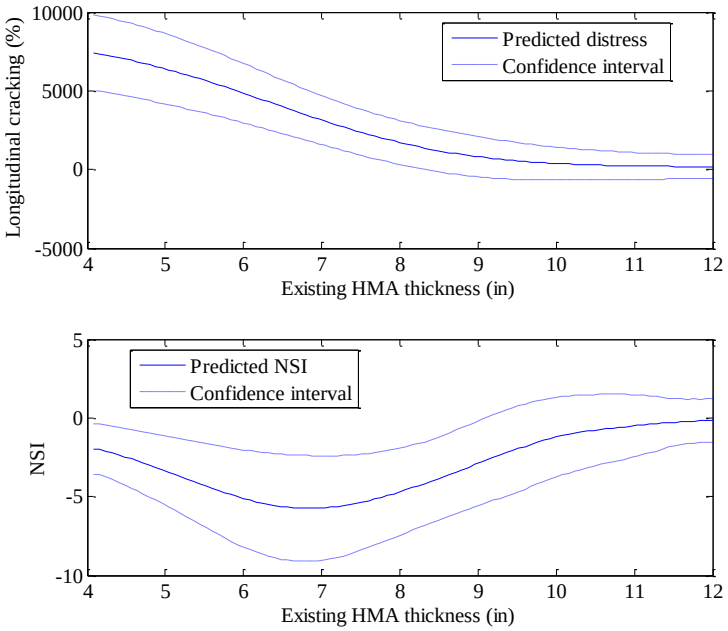

Figure B-18 Predicted longitudinal cracking and NSI for existing thickness

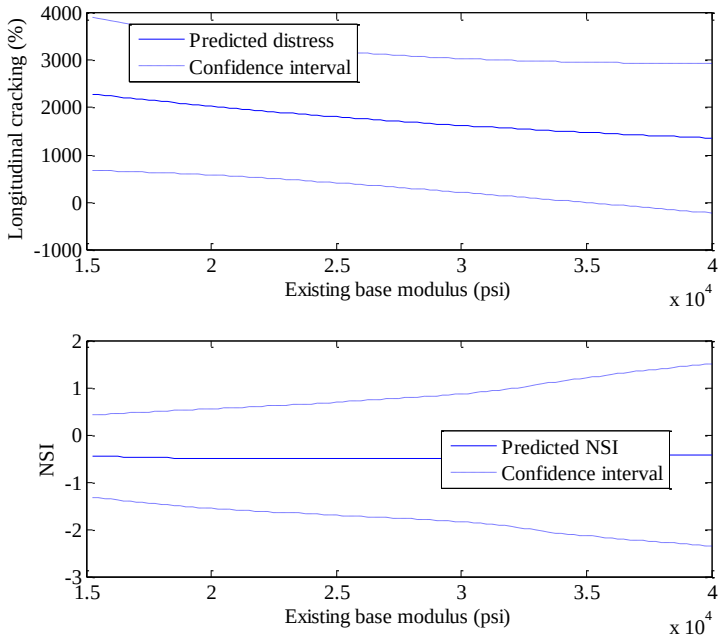

Figure B-19 Predicted longitudinal cracking and NSI for base modulus

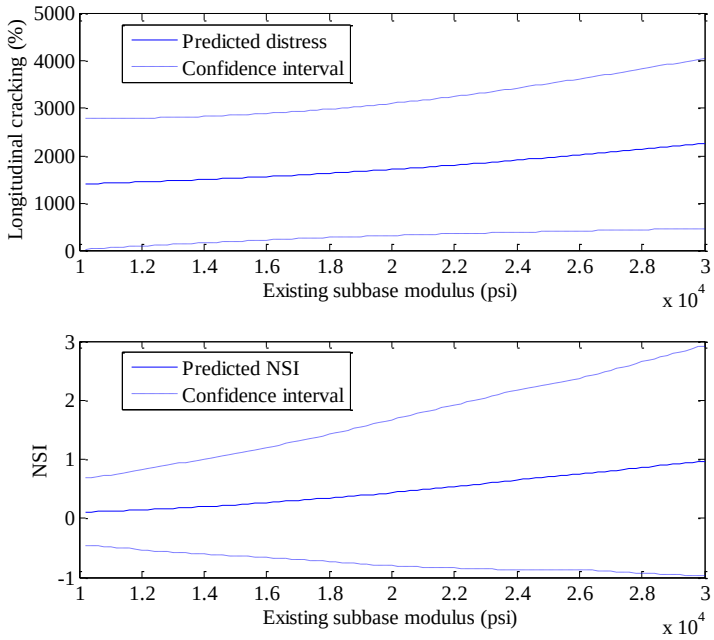

Figure B-20 Predicted longitudinal cracking and NSI for subbase modulus

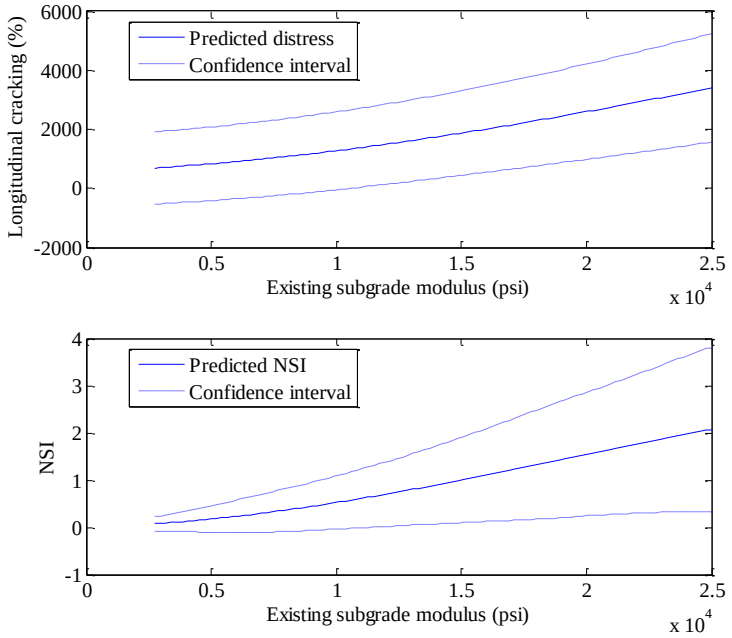

Figure B-21 Predicted longitudinal cracking and NSI for subgrade modulus

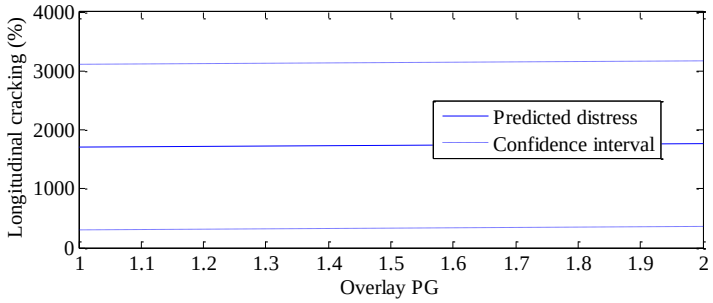

Figure B-22 Predicted longitudinal cracking for overlay PG

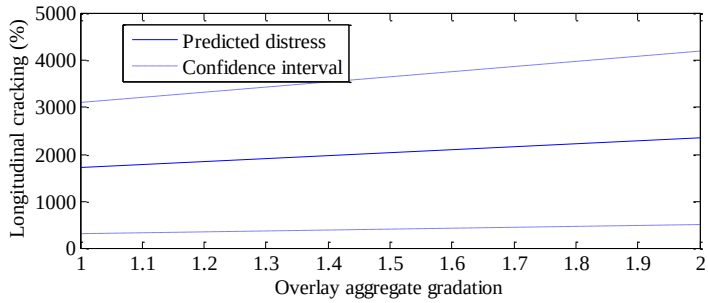

Figure B-23 Predicted longitudinal cracking for overlay aggregate gradation

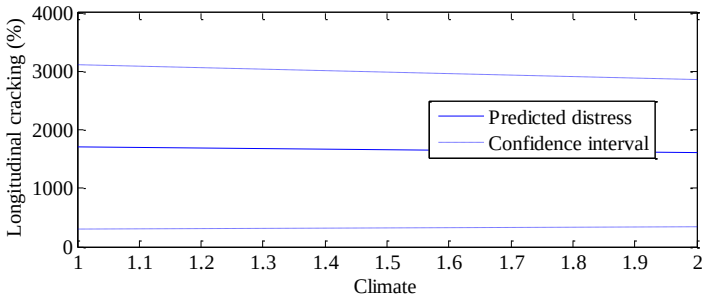

Figure B-24 Predicted longitudinal cracking for cliamte

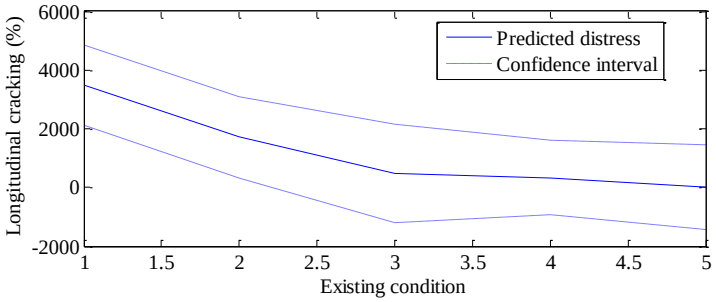

Figure B-25 Predicted longitudinal cracking for existing condition

Inputs interaction effect

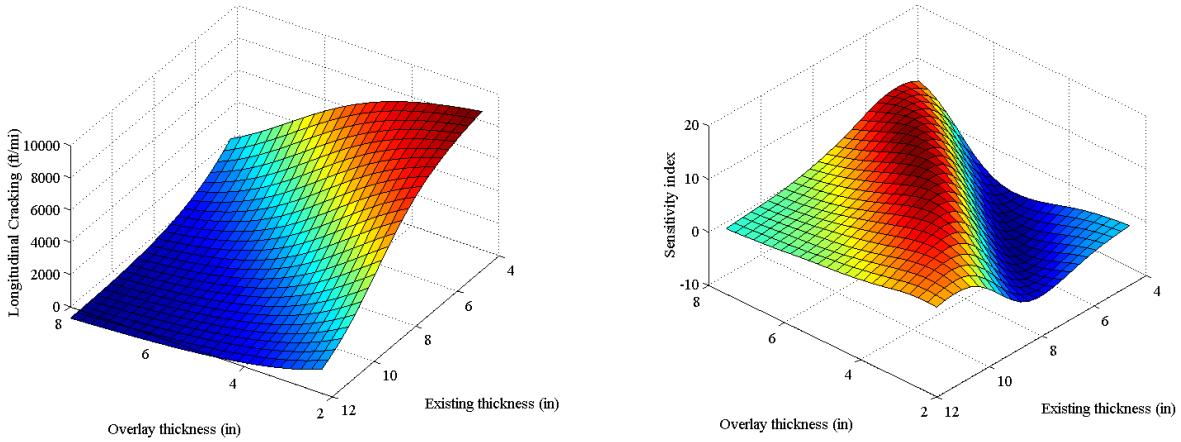

Figure B-26 Predicted interaction and NSI between existing condition and overlay thickness

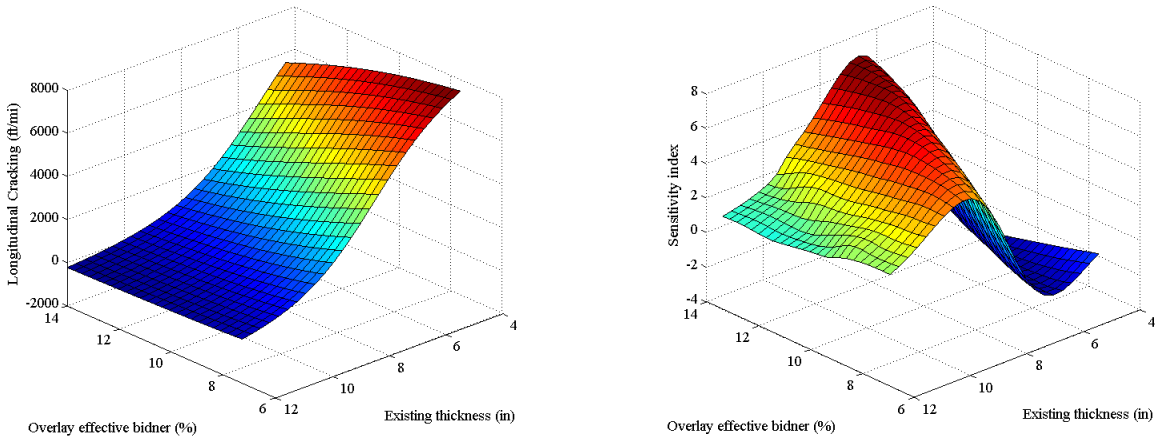

Figure B-27 Predicted interaction and NSI between existing thickness and overlay effective binder

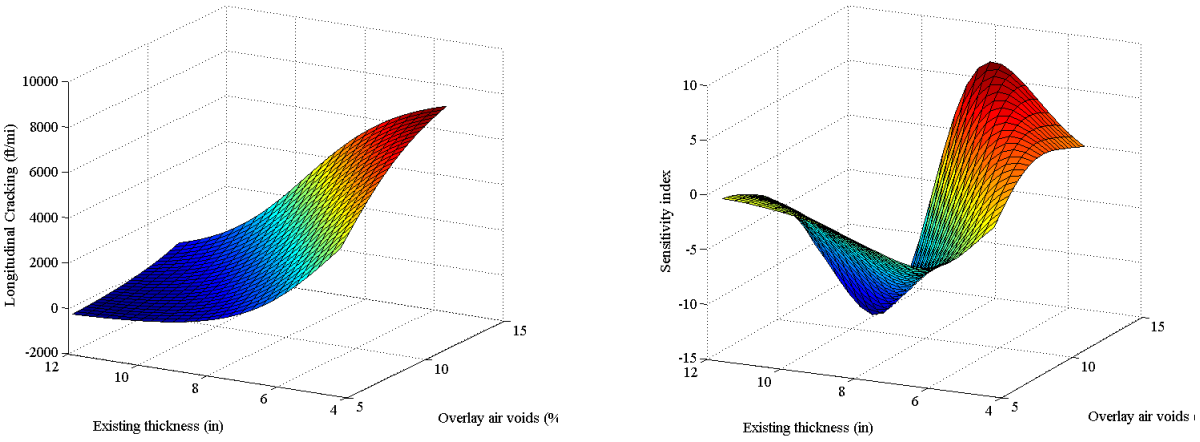

Figure B-28 Predicted interaction and NSI between existing thickness and overlay air voids

B.1.3 Rutting

Inputs main effect

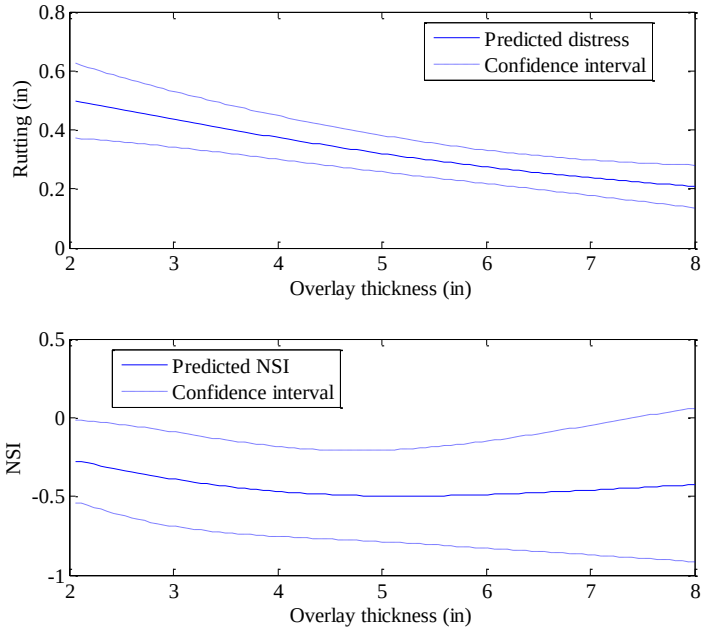

Figure B-29 Predicted rutting and NSI for overlay thickness

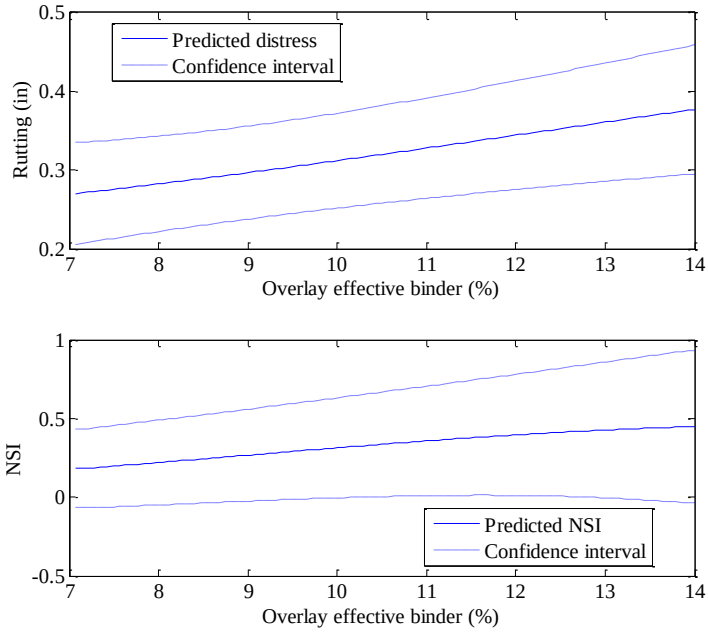

Figure B-30 Predicted rutting and NSI for overlay effective binder

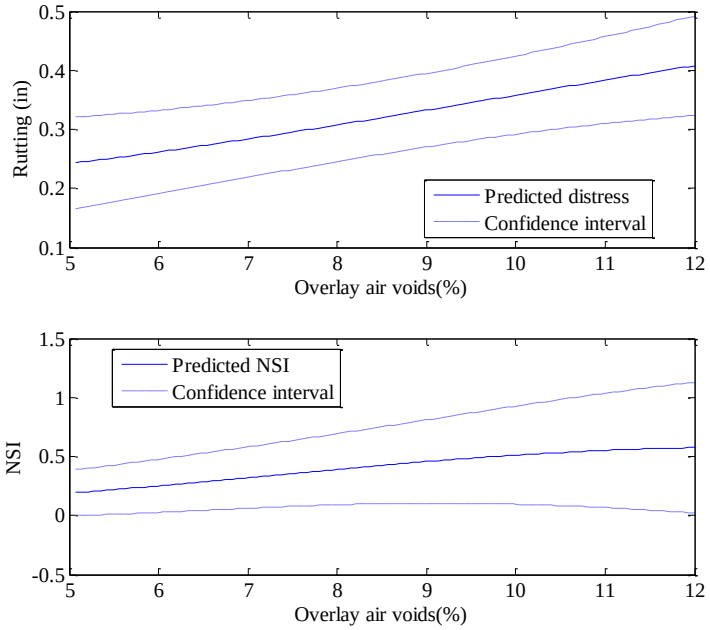

Figure B-31 Predicted rutting and NSI for overlay air voids

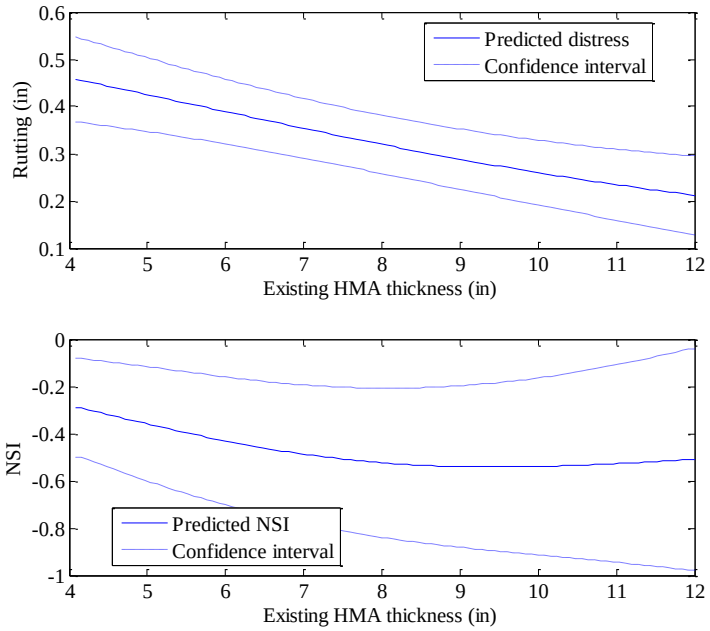

Figure B-32 Predicted rutting and NSI for existing thickness

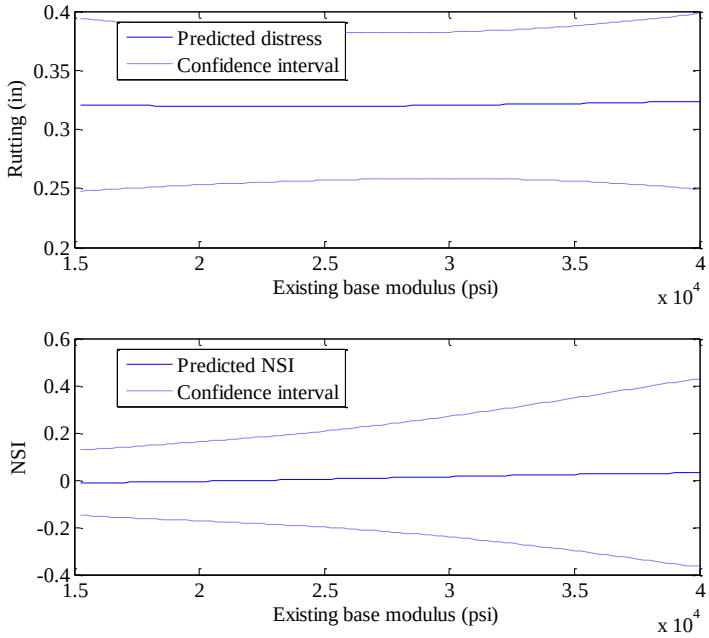

Figure B-33 Predicted rutting and NSI for base modulus

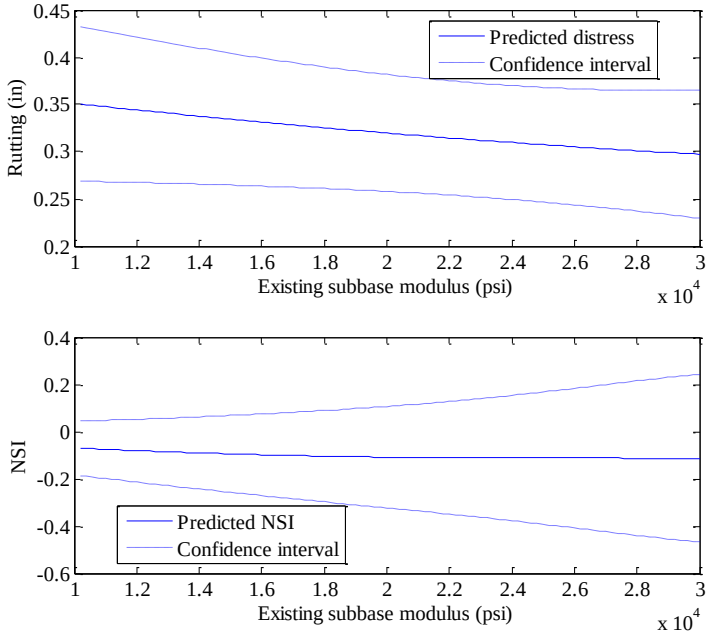

Figure B-34 Predicted rutting and NSI for subbase modulus

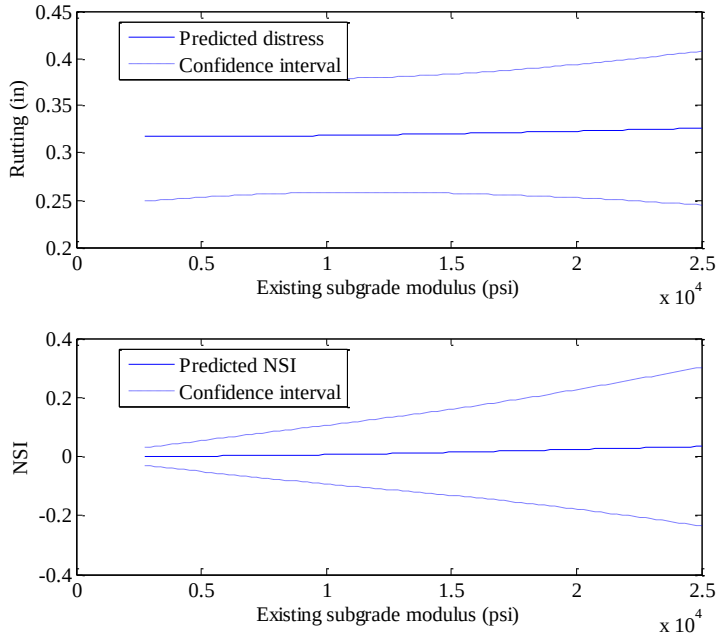

Figure B-35 Predicted rutting and NSI for subgrade modulus

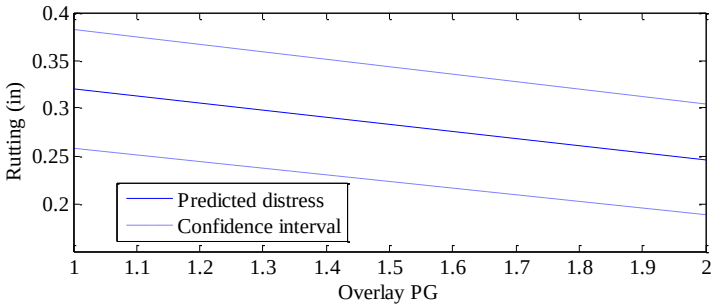

Figure B-36 Predicted rutting for overlay PG

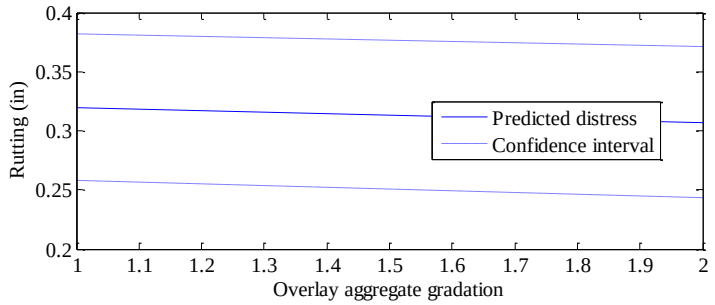

Figure B-37 Predicted rutting for overlay aggregate gradation

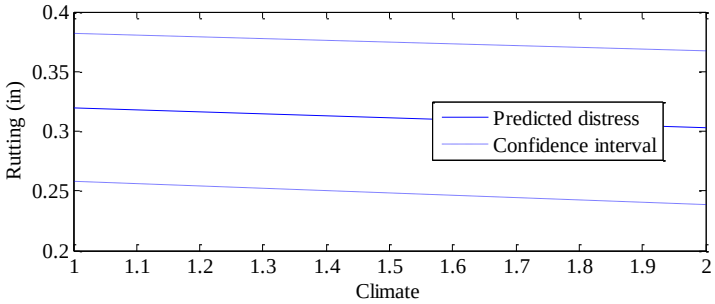

Figure B-38 Predicted rutting for climate

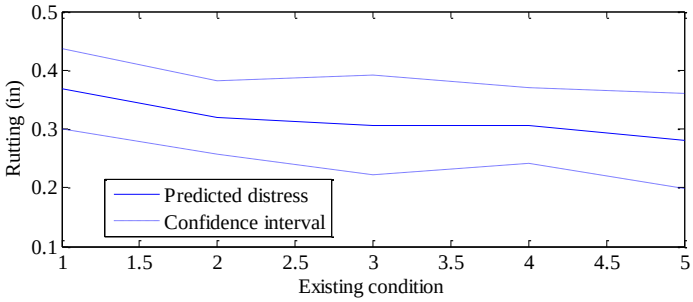

Figure B-39 Predicted rutting existing condition

Inputs interaction effect

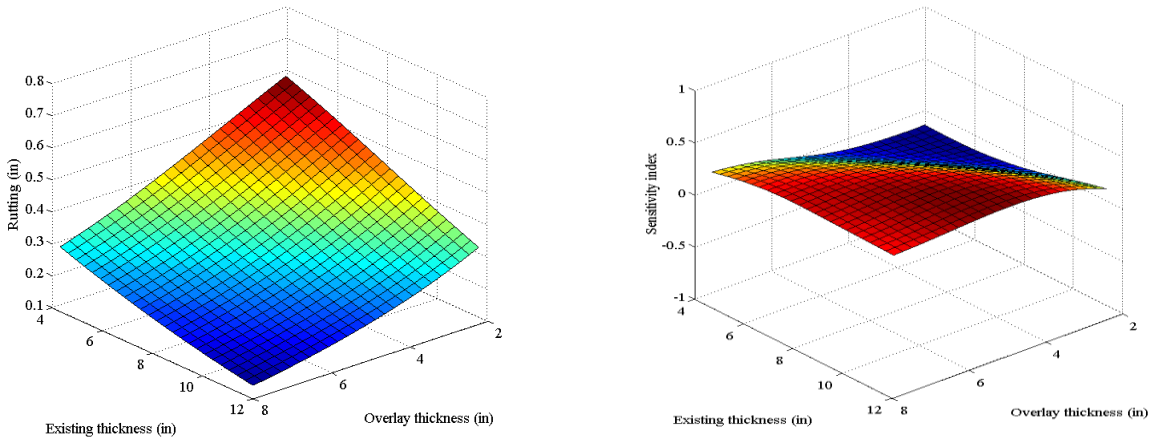

Figure B-40 Predicted interaction and NSI between existing condition and overlay thickness

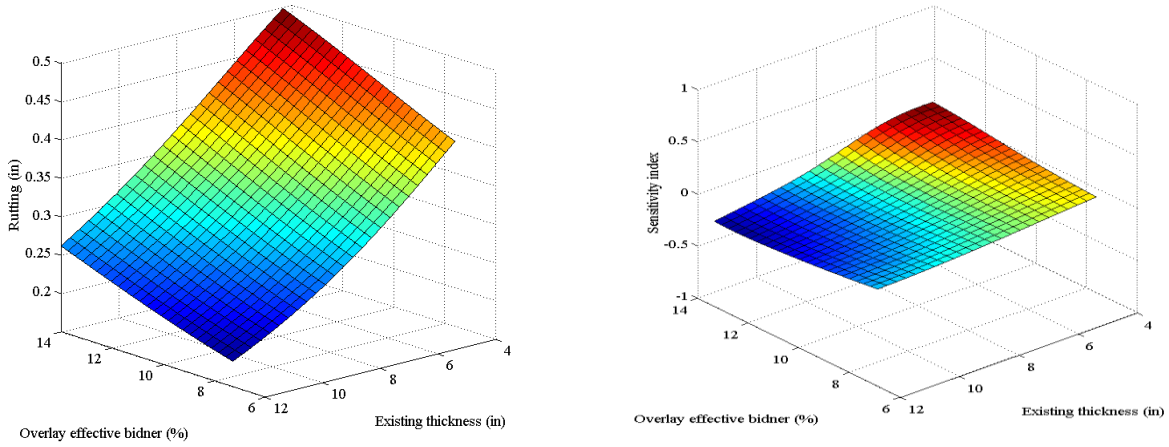

Figure B-41 Predicted interaction and NSI between existing thickness and overlay effective binder

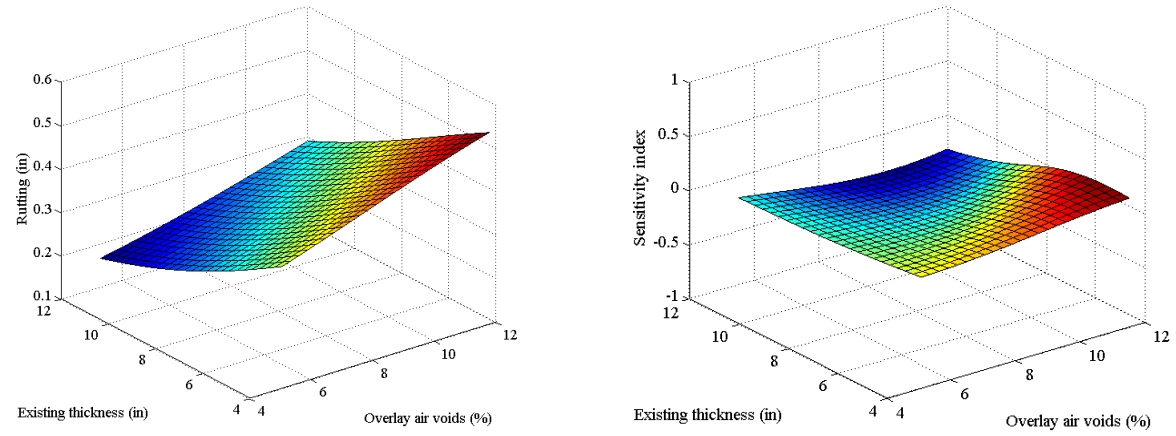

Figure B-42 Predicted interaction and NSI between existing thickness and overlay air voids

B.1.4 IRI

Inputs main effect

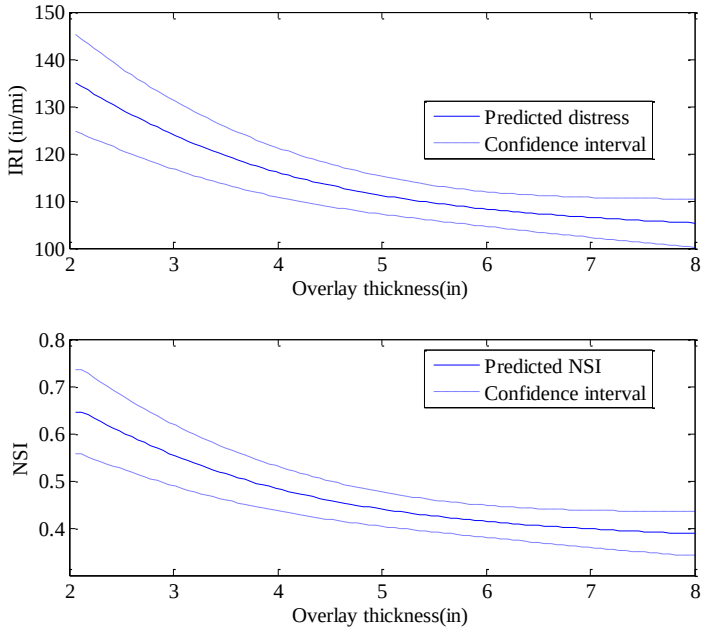

Figure B-43 Predicted IRI and NSI for overlay thickness

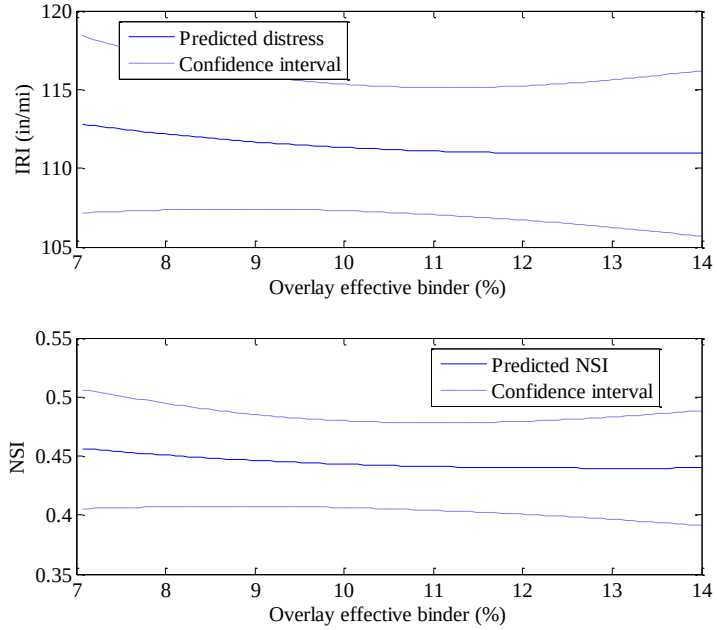

Figure B-44 Predicted IRI and NSI for overlay effective binder

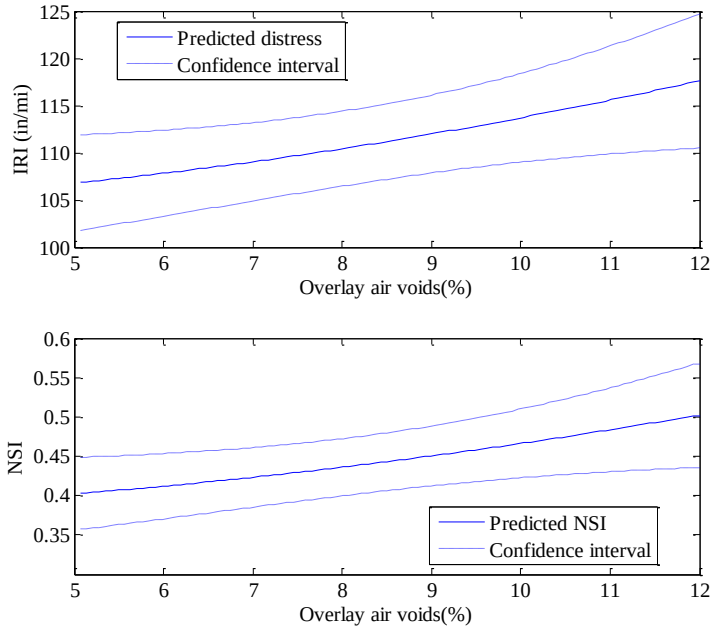

Figure B-45 Predicted IRI and NSI for overlay air voids

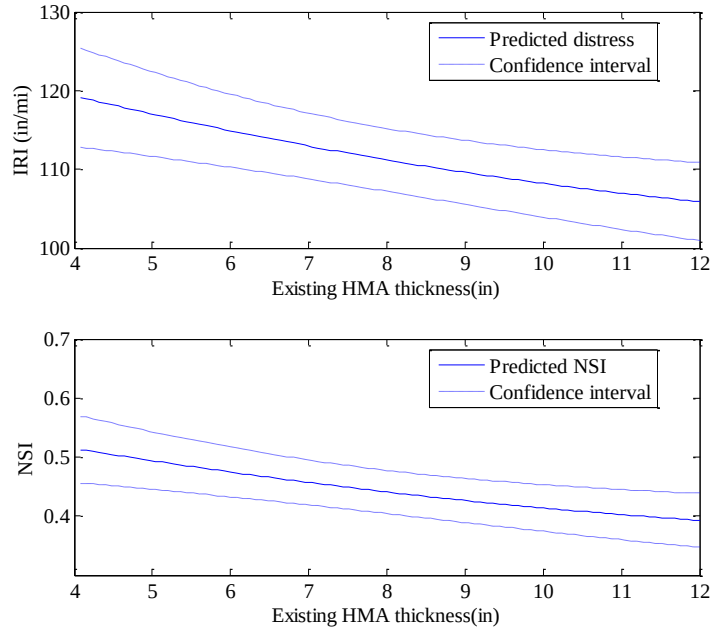

Figure B-46 Predicted IRI and NSI for overlay existing thickness

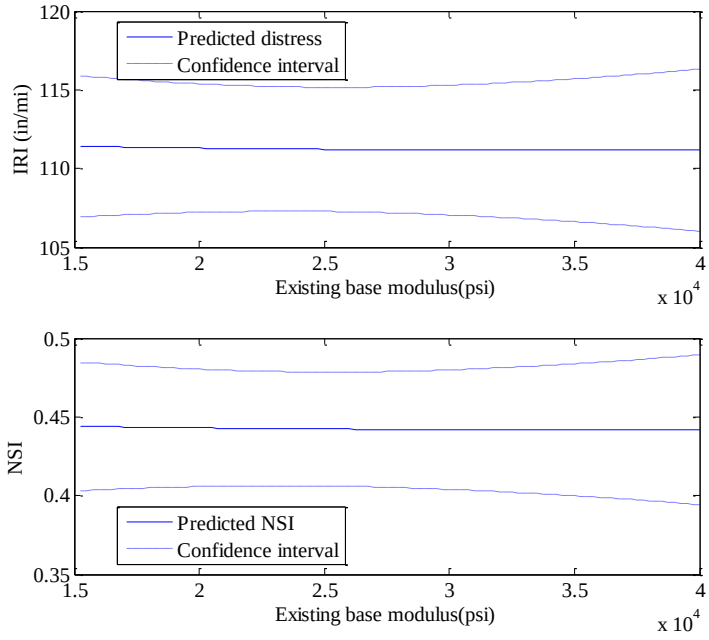

Figure B-47 Predicted IRI and NSI for base modulus

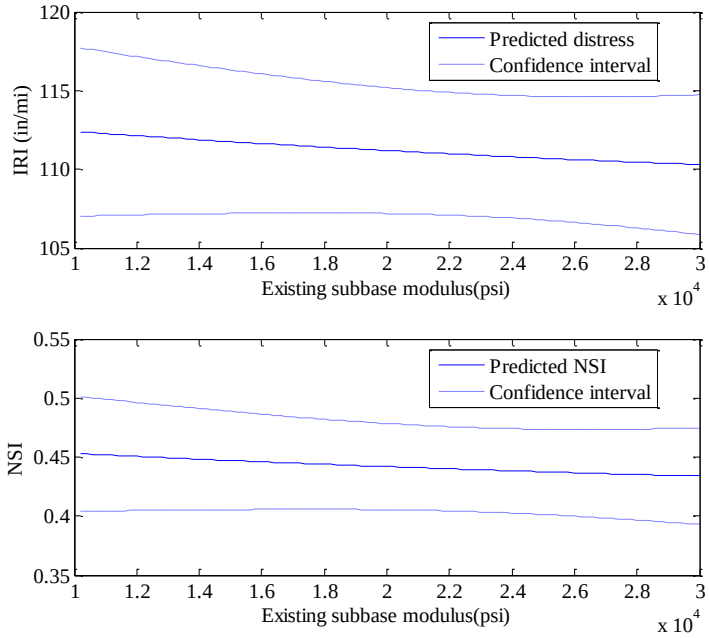

Figure B-48 Predicted IRI and NSI for subbase modulus

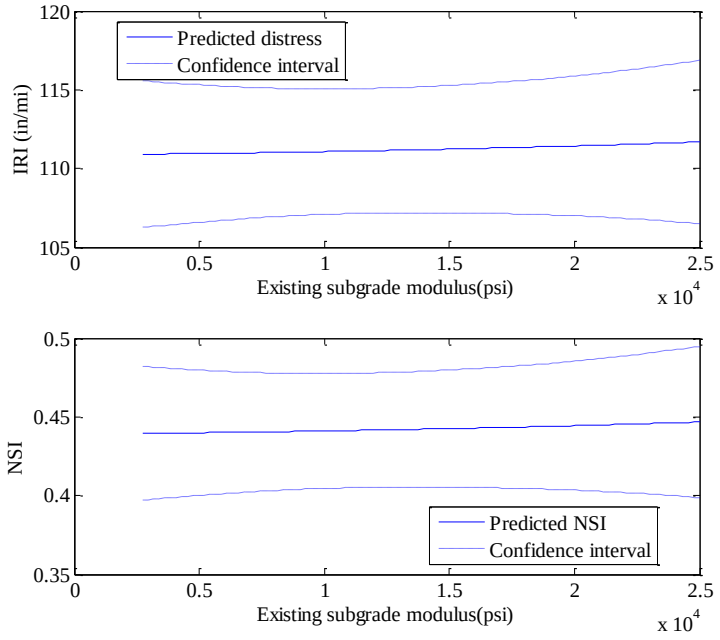

Figure B-49 Predicted IRI and NSI for subgrade modulus

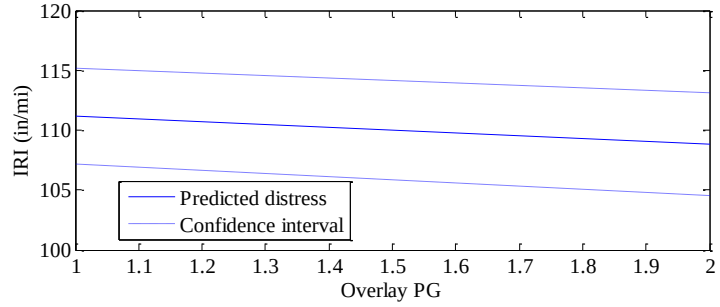

Figure B-50 Predicted IRI for overlay PG

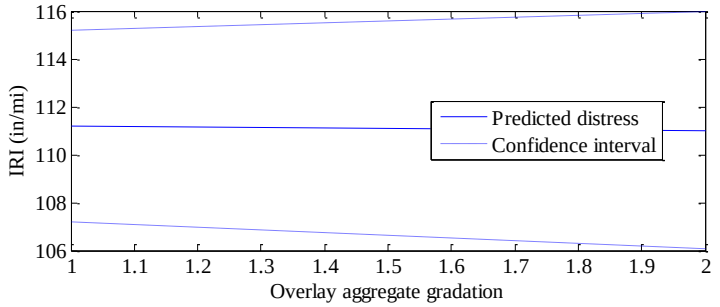

Figure B-51 Predicted IRI for overlay aggregate gradation

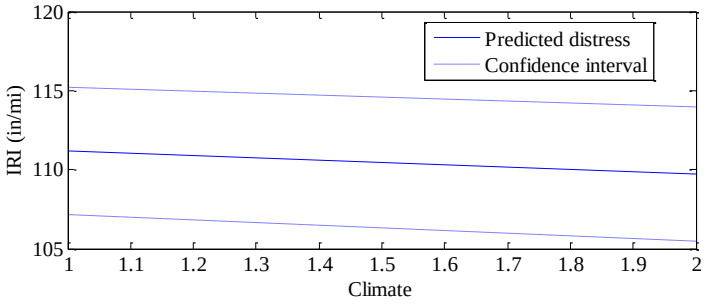

Figure B-52 Predicted IRI for climate

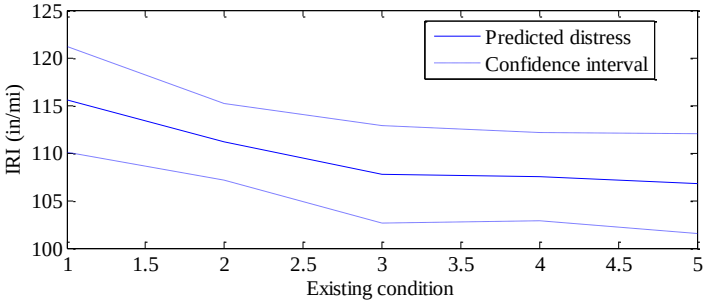

Figure B-53 Predicted IRI for existing condition

Inputs interaction effect

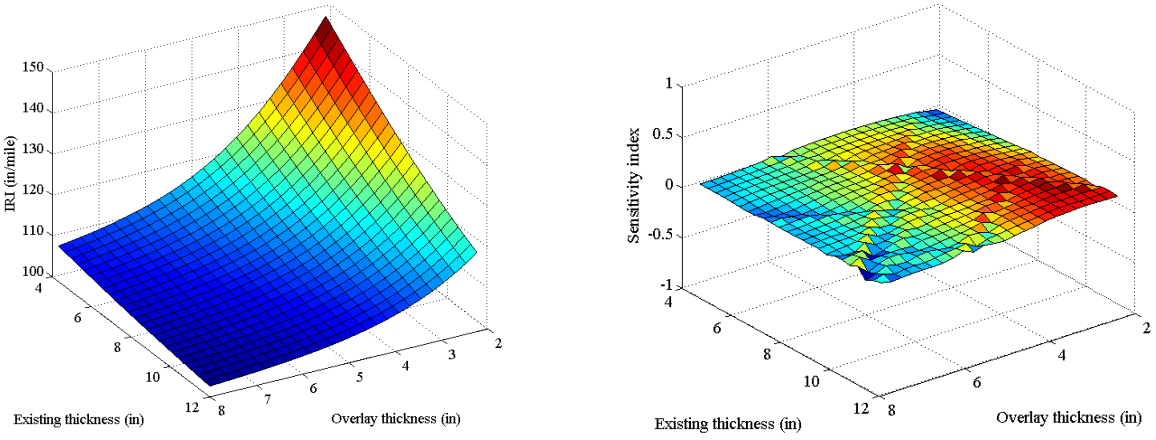

Figure B-54 Predicted interaction and NSI between existing condition and overlay thickness

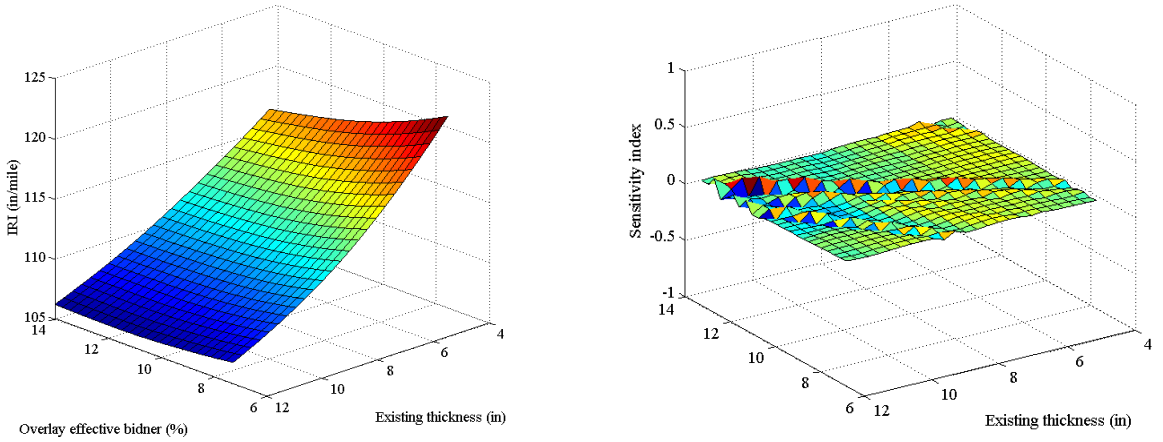

Figure B-55 Predicted interaction and NSI between existing thickness and overlay effective binder

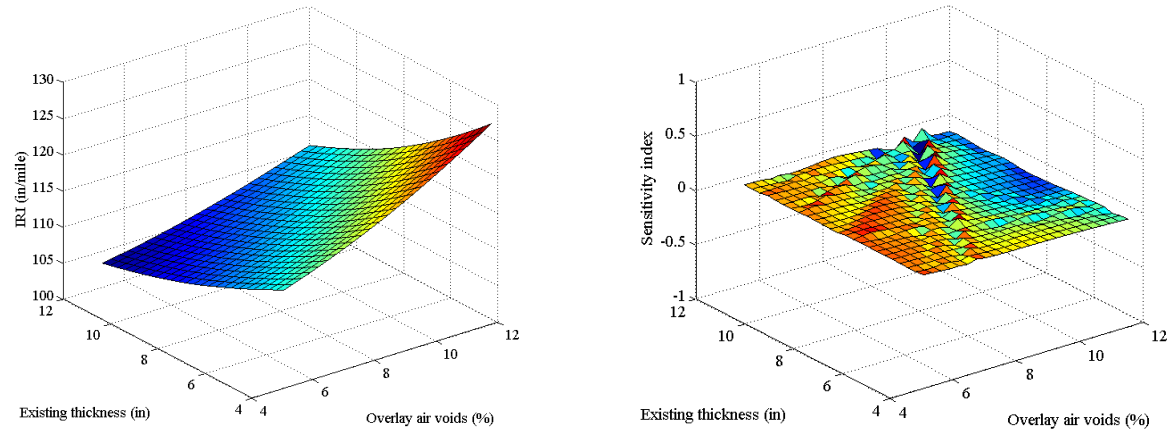

Figure B-56 Predicted interaction and NSI between existing thickness and overlay air voids

B.2 COMPOSITE OVERLAYS

B.1.5 Longitudinal Cracking

Inputs main effect

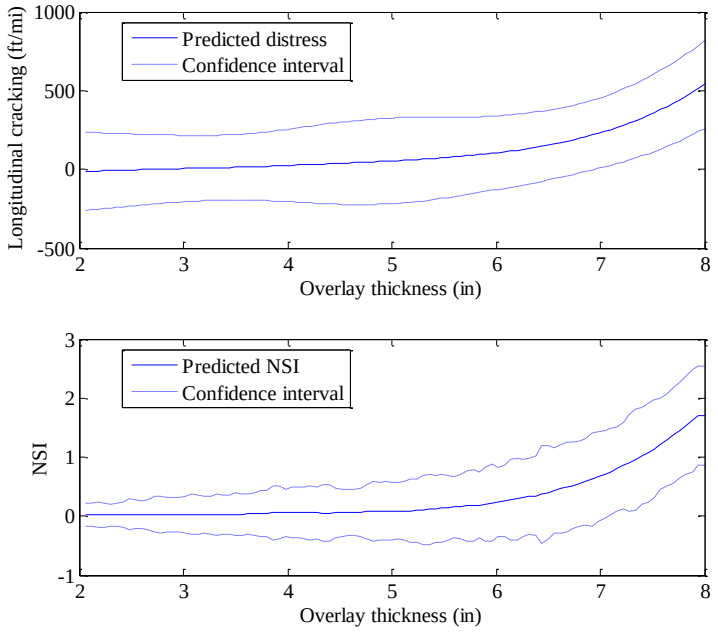

Figure B-57 Predicted longitudinal cracking and NSI for overlay thickness

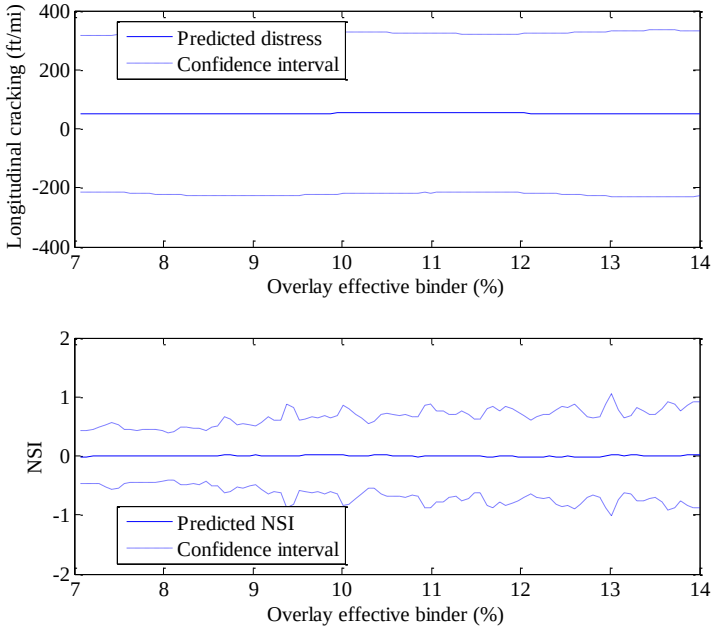

Figure B-58 Predicted longitudinal cracking and NSI for effective binder

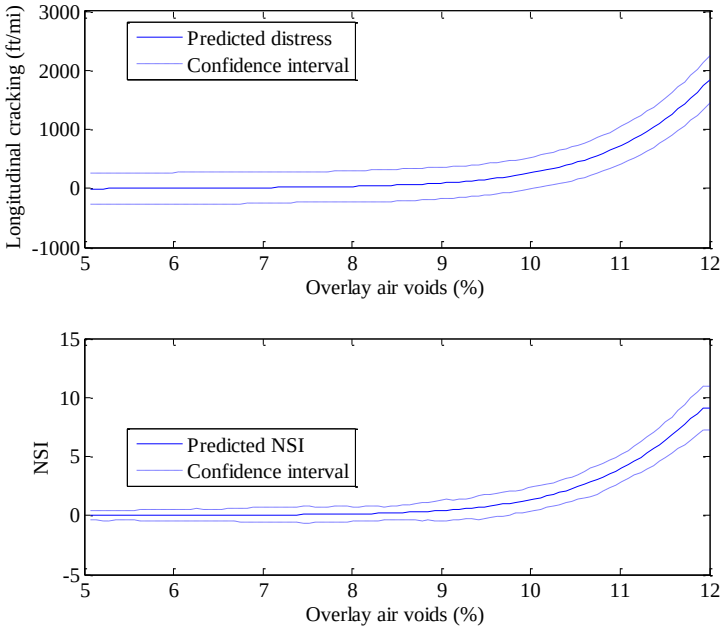

Figure B-59 Predicted longitudinal cracking and NSI for air voids

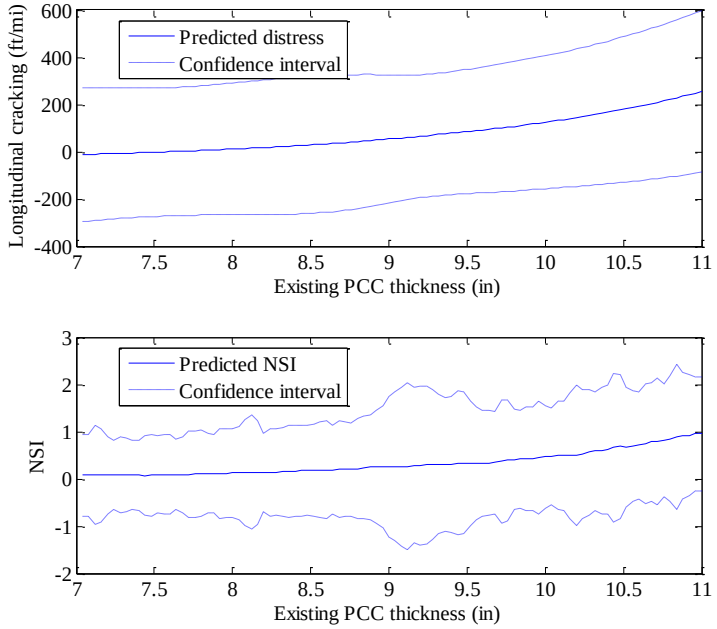

Figure B-60 Predicted longitudinal cracking and NSI for existing PCC thickness

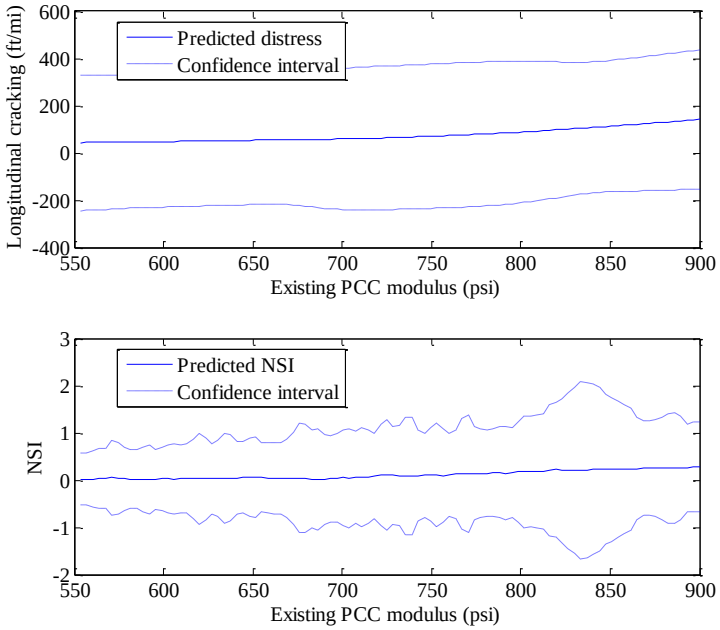

Figure B-61 Predicted longitudinal cracking and NSI for existing PCC modulus

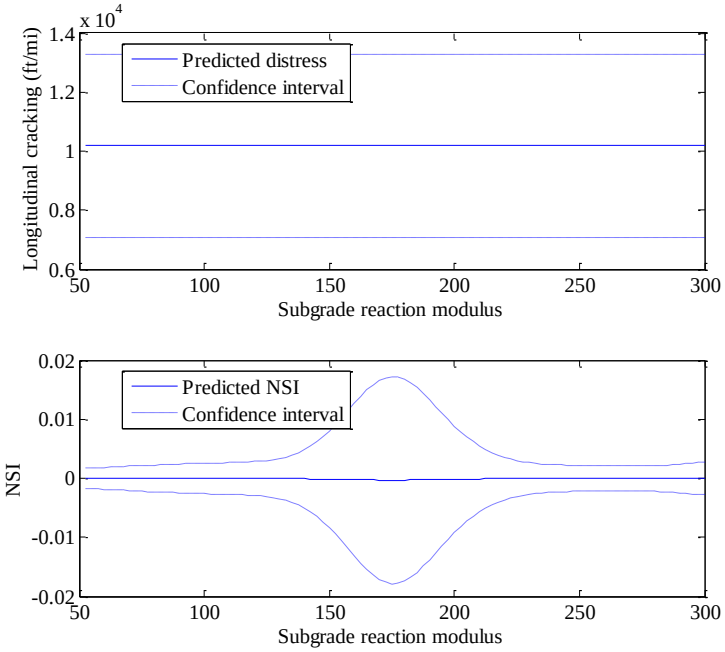

Figure B-62 Predicted longitudinal cracking and NSI for subgrade modulus reaction

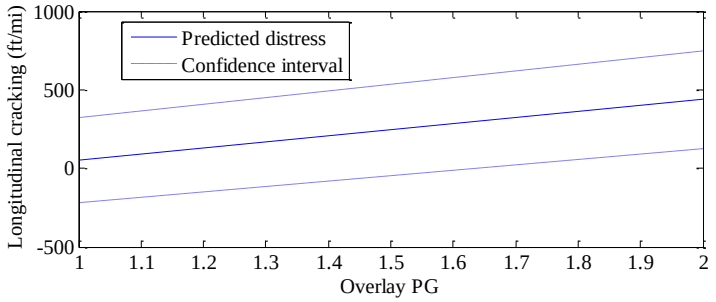

Figure B-63 Predicted longitudinal cracking for overlay PG

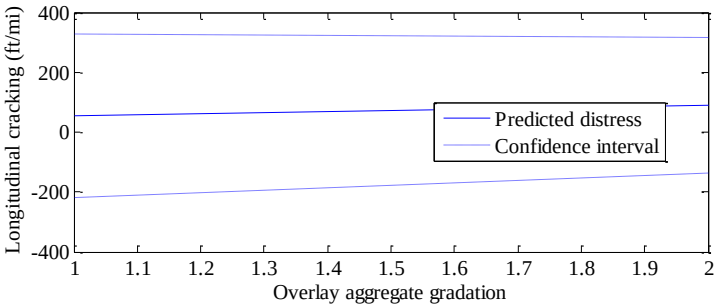

Figure B-64 Predicted longitudinal cracking for overlay aggregate gradation

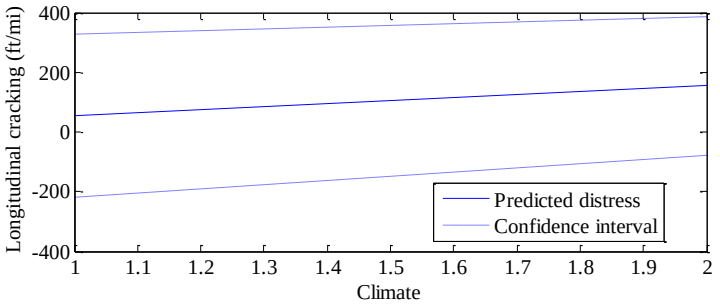

Figure B-65 Predicted longitudinal cracking for climate

Inputs interaction effect

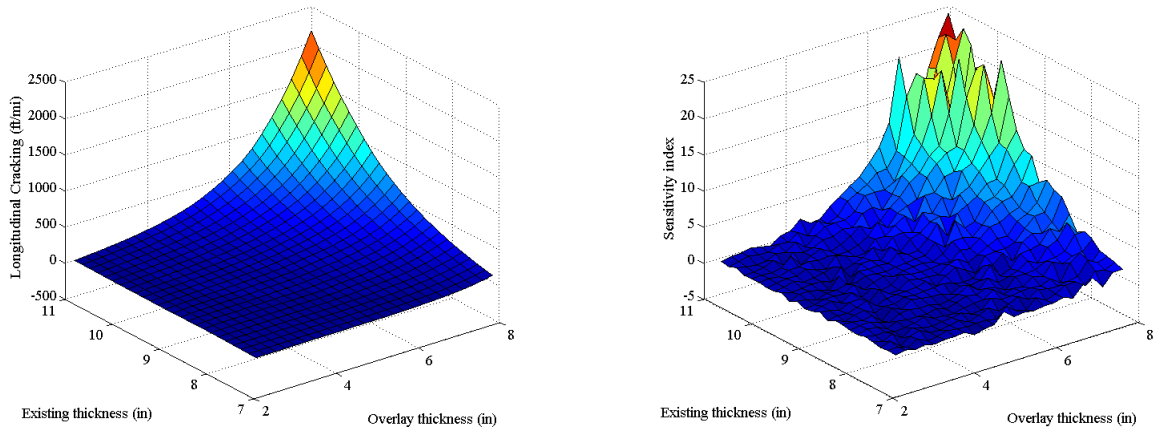

Figure B-66 Predicted interaction and NSI between existing thickness and overlay thickness

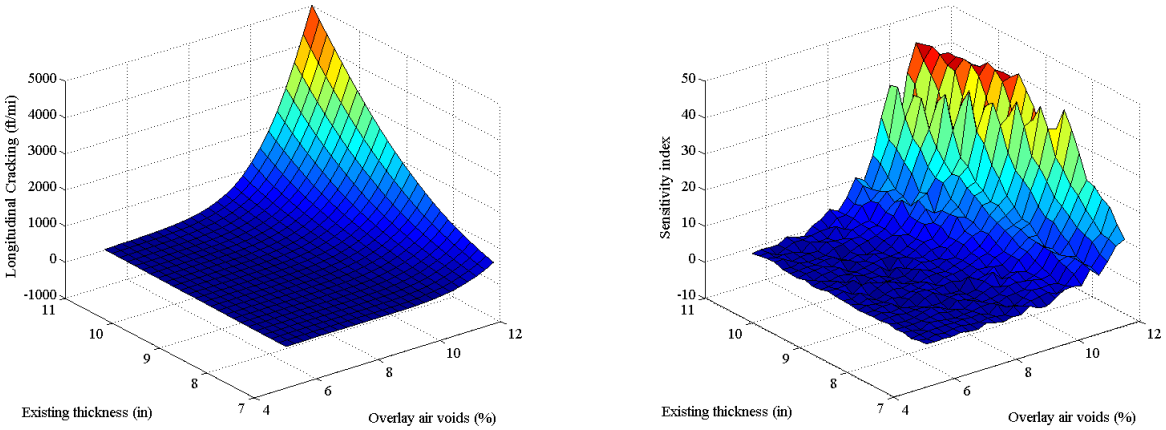

Figure B-67 Predicted interaction and NSI between existing thickness and overlay air voids

B.1.6 Rutting

Inputs interaction effect

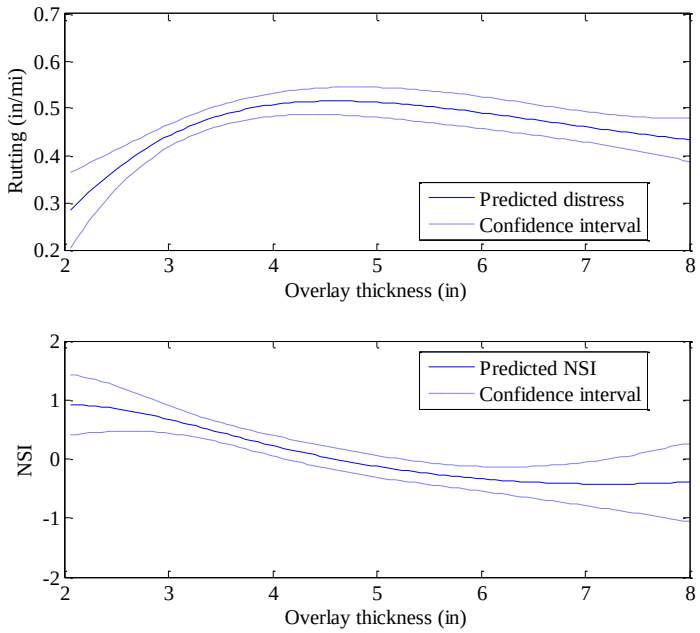

Figure B-68 Predicted rutting and NSI for subgrade overlay thickness

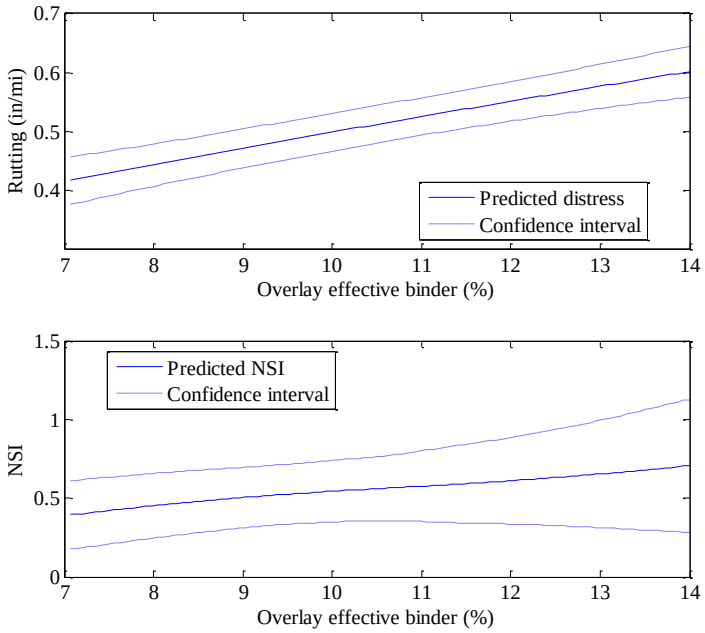

Figure B-69 Predicted rutting and NSI for overlay effective binder

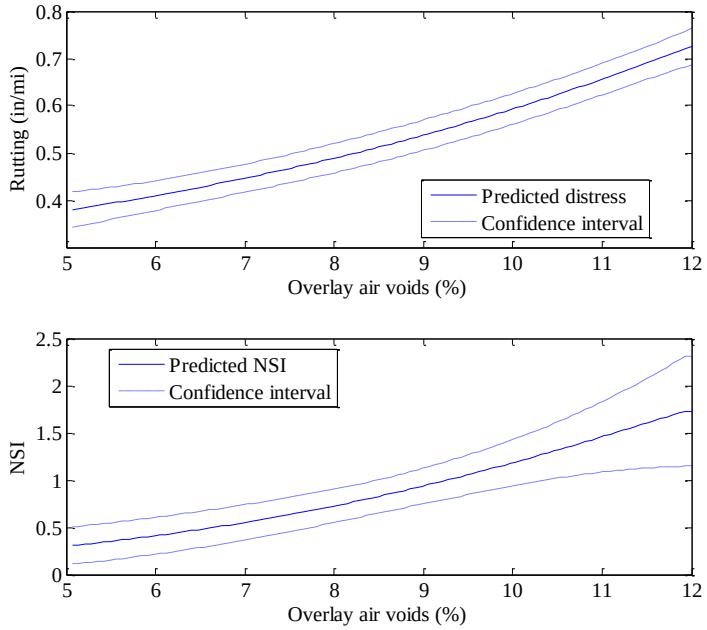

Figure B-70 Predicted rutting and NSI for subgrade overlay air voids

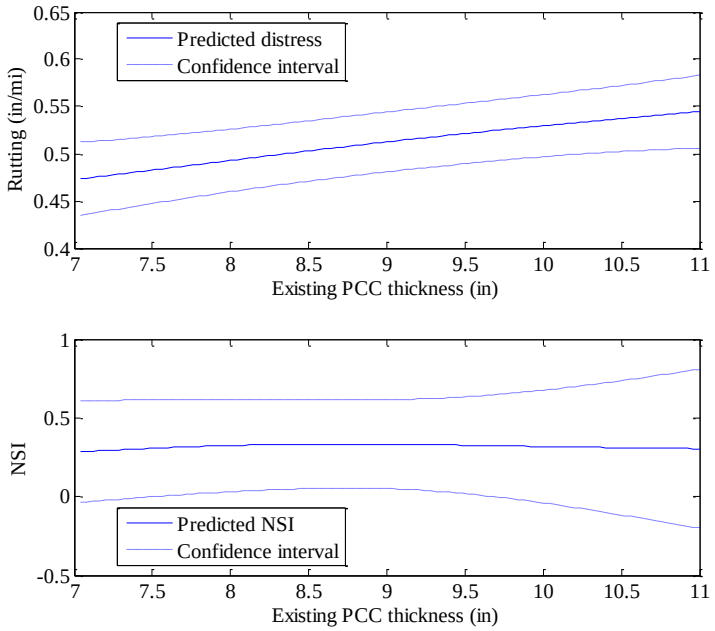

Figure B-71 Predicted rutting and NSI for existing PCC thickness

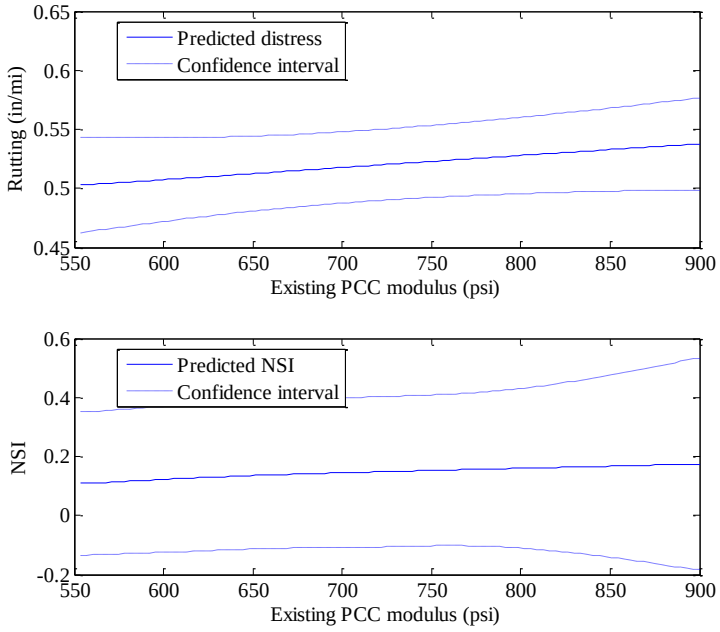

Figure B-72 Predicted rutting and NSI for existing PCC modulus

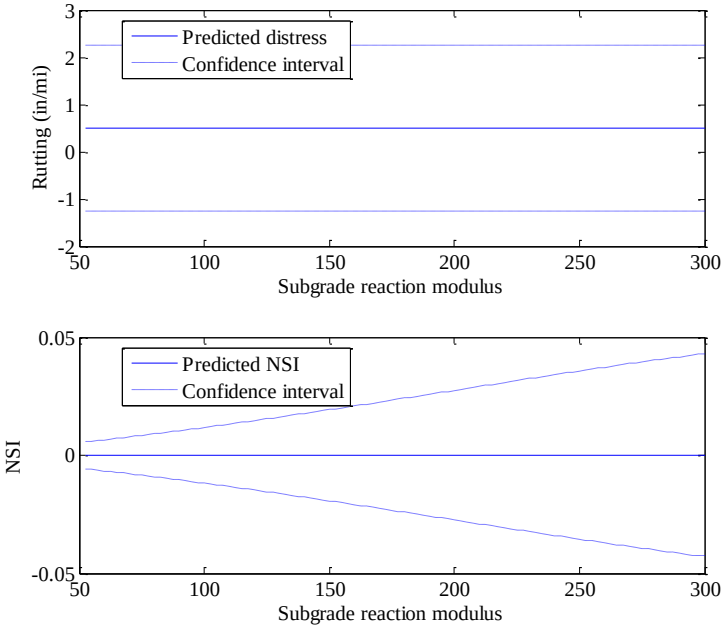

Figure B-73 Predicted rutting and NSI for subgrade reaction modulus

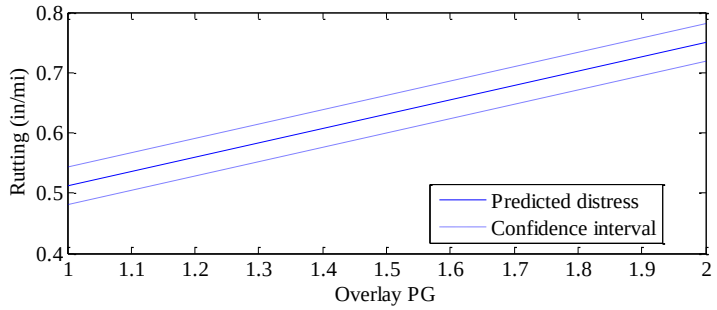

Figure B-74 Predicted rutting for overlay PG

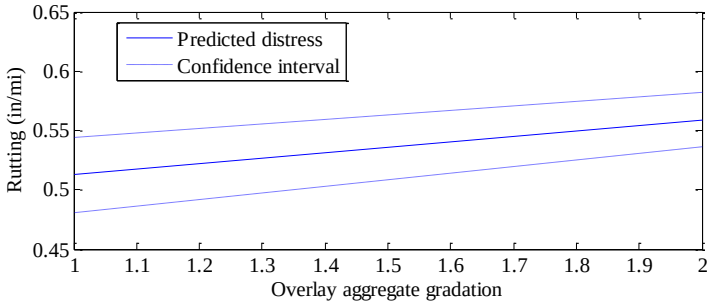

Figure B-75 Predicted rutting for overlay aggregate gradation

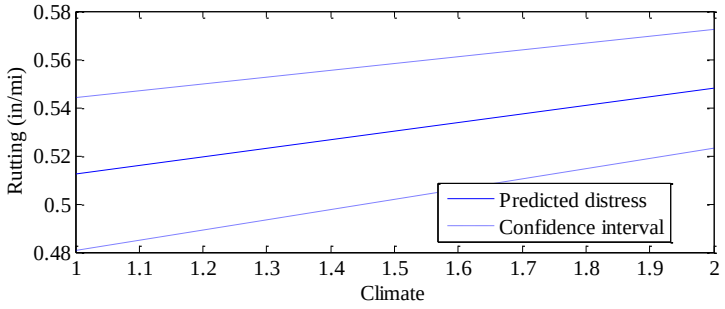

Figure B-76 Predicted rutting for climate

Inputs interaction effect

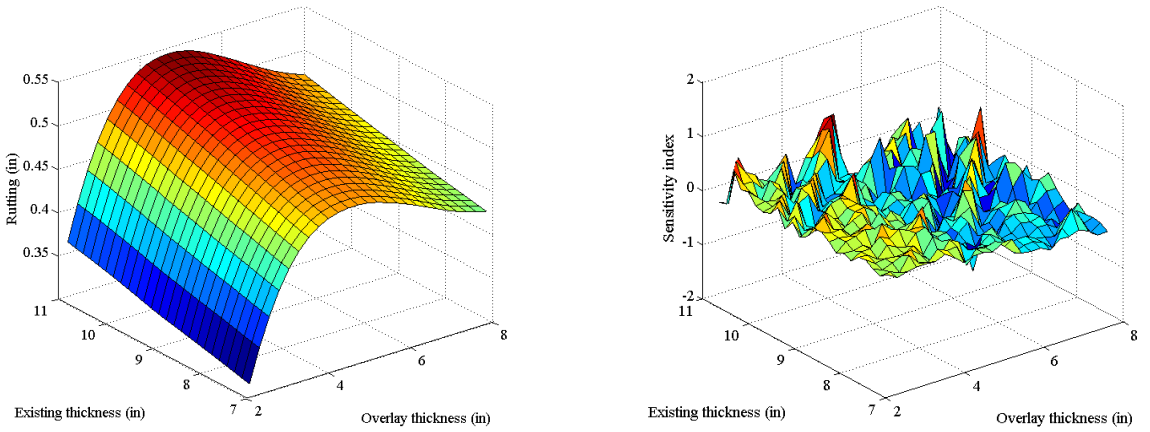

Figure B-77 Predicted interaction and NSI between existing thickness and overlay thickness

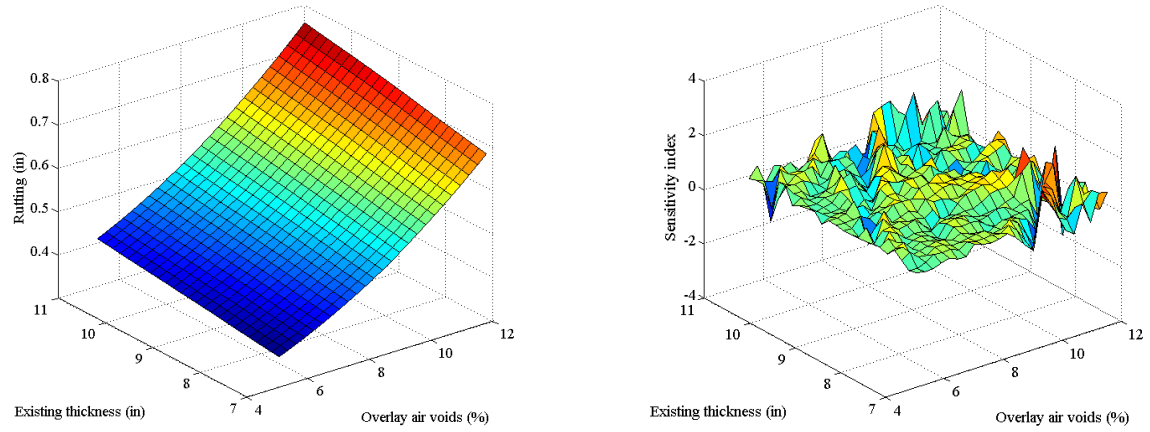

Figure B-78 Predicted interaction and NSI between existing thickness and overlay air voids

B.1.7 IRI

Inputs main effect

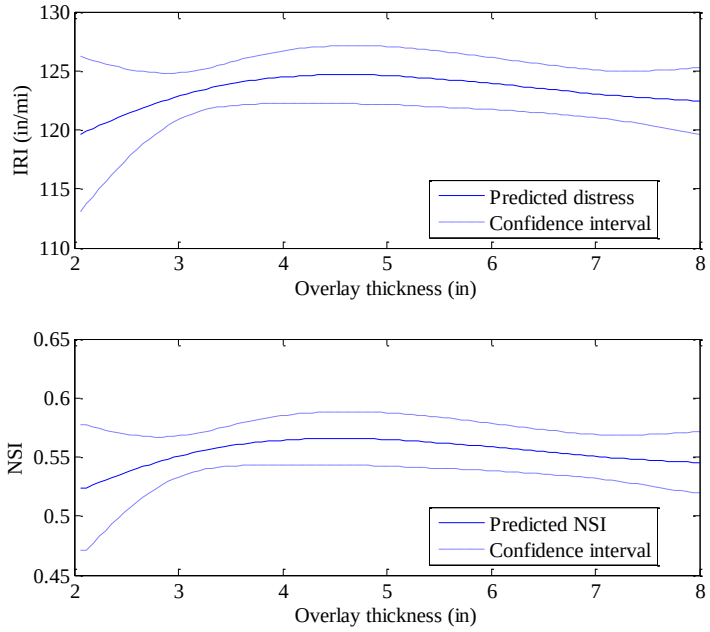

Figure B-79 Predicted IRI and NSI for overlay thickness

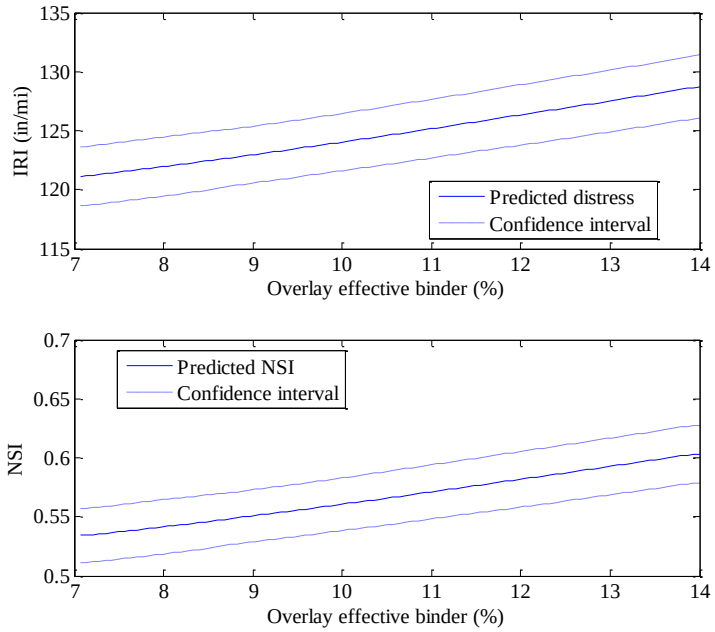

Figure B-80 Predicted IRI and NSI for overlay effective binder

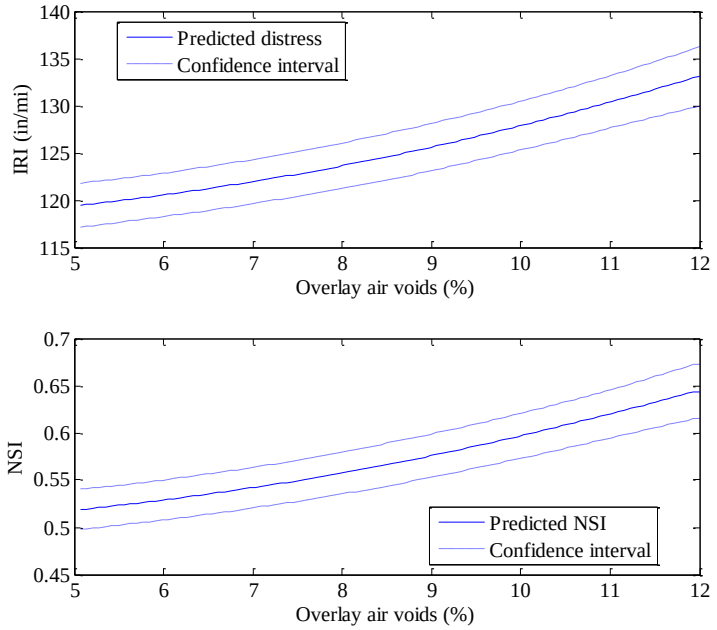

Figure B-81 Predicted IRI and NSI for overlay air voids

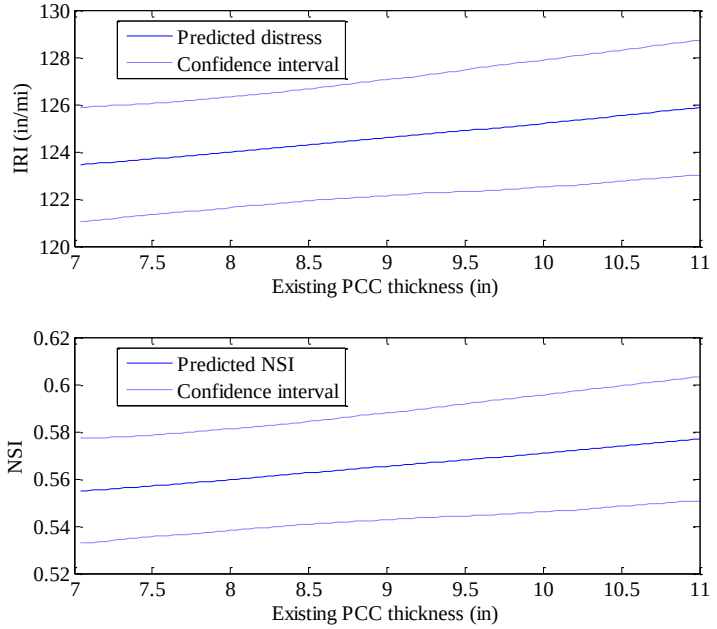

Figure B-82 Predicted IRI and NSI for existing PCC thickness

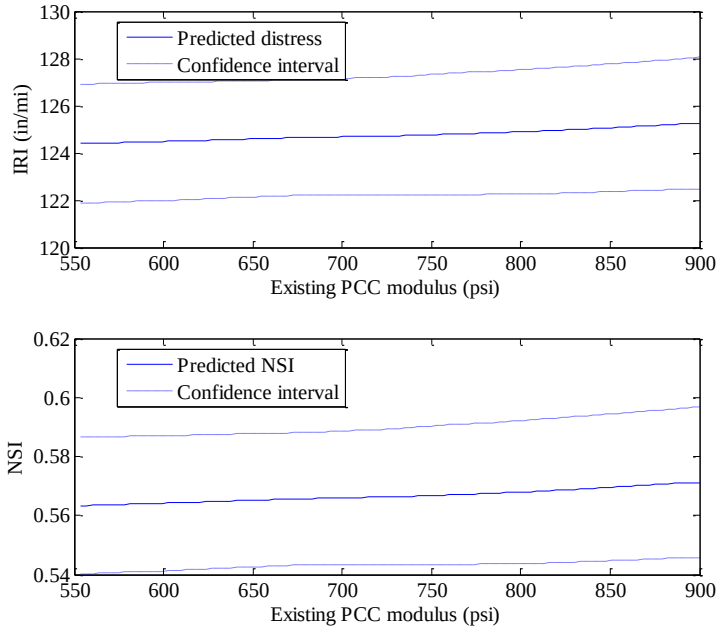

Figure B-83 Predicted IRI and NSI for existing PCC modulus

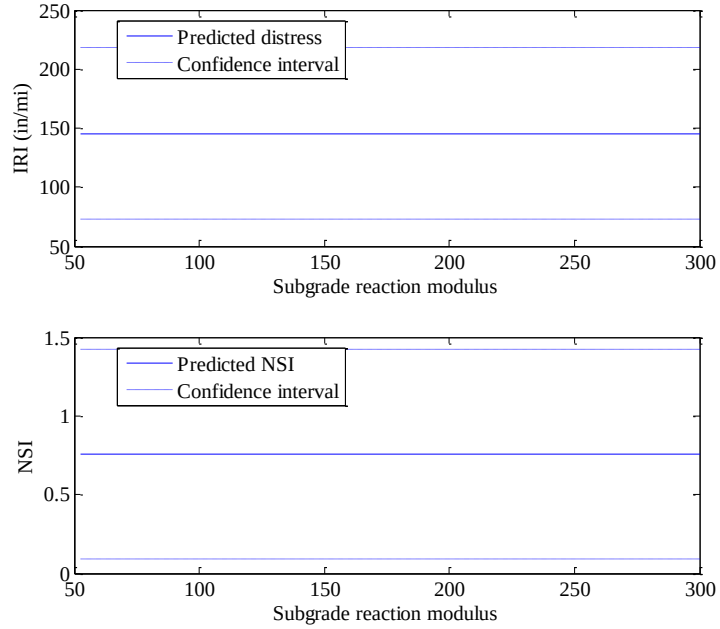

Figure B-84 Predicted IRI and NSI for subgrade reaction modulus

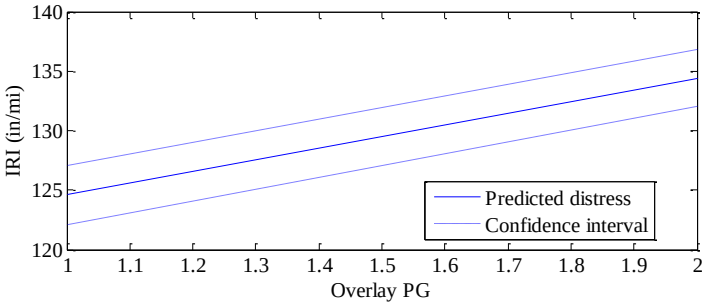

Figure B-85 Predicted IRI for overlay PG

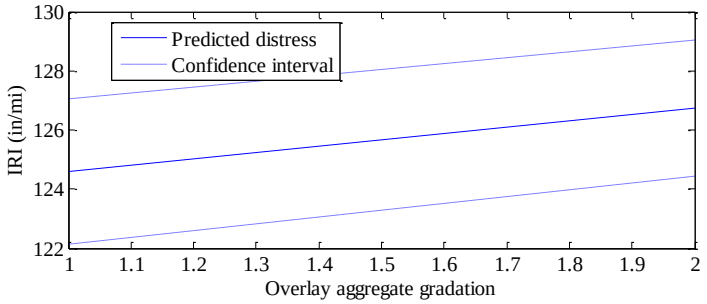

Figure B-86 Predicted IRI for overlay aggregate gradation

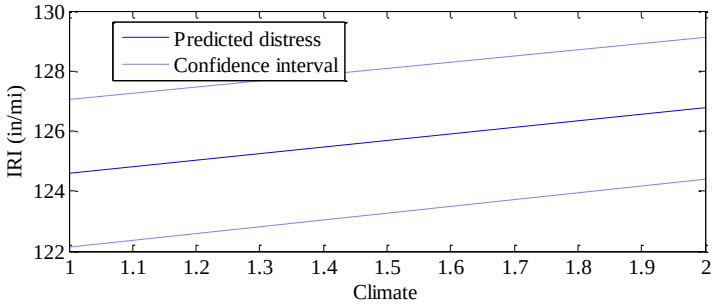

Figure B-87 Predicted IRI for climate

B.3 RUBBLIZED OVERLAYS

B.1.8 Alligator cracking

Inputs main effect

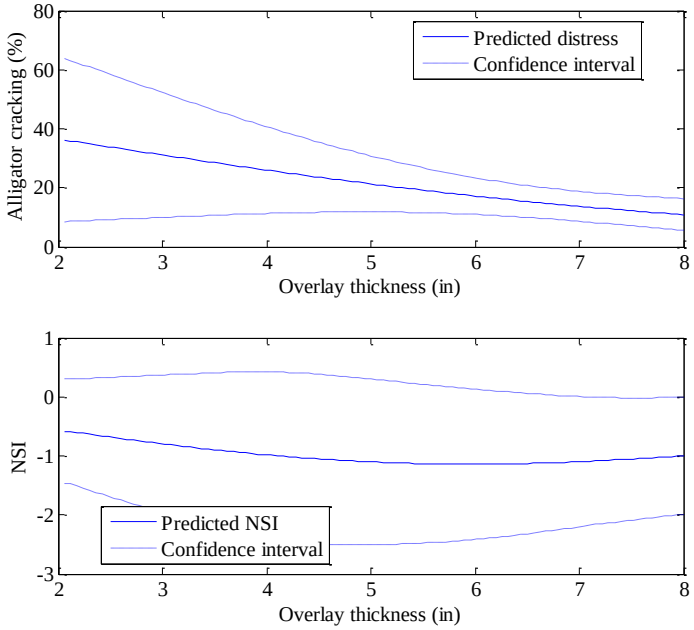

Figure B-88 Predicted alligator cracking and NSI for overlay thickness

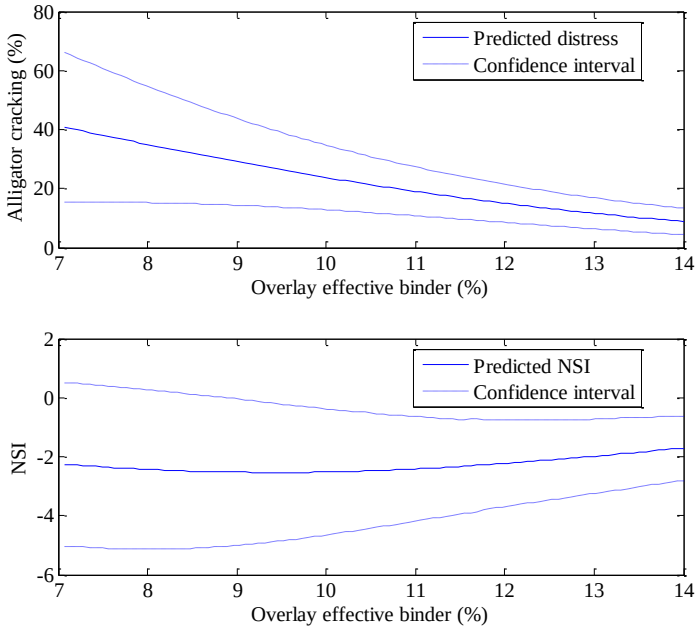

Figure B-89 Predicted alligator cracking and NSI for overlay effective binder

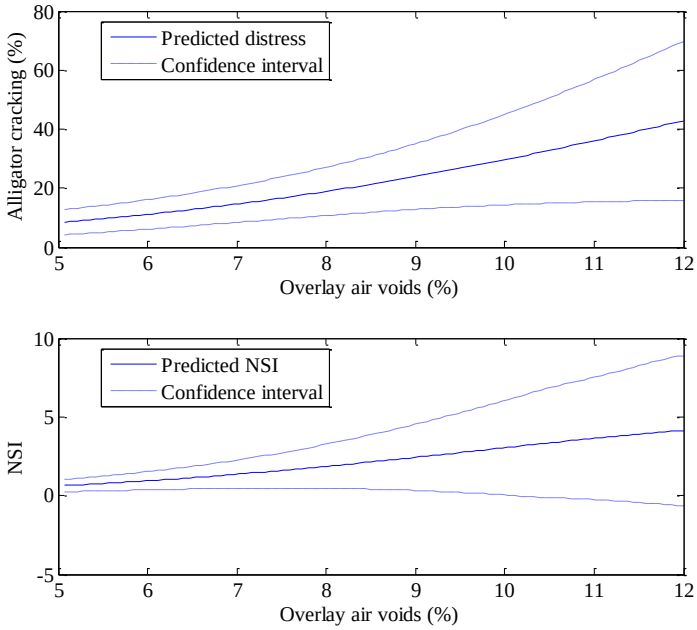

Figure B-90 Predicted alligator cracking and NSI for overlay air voids

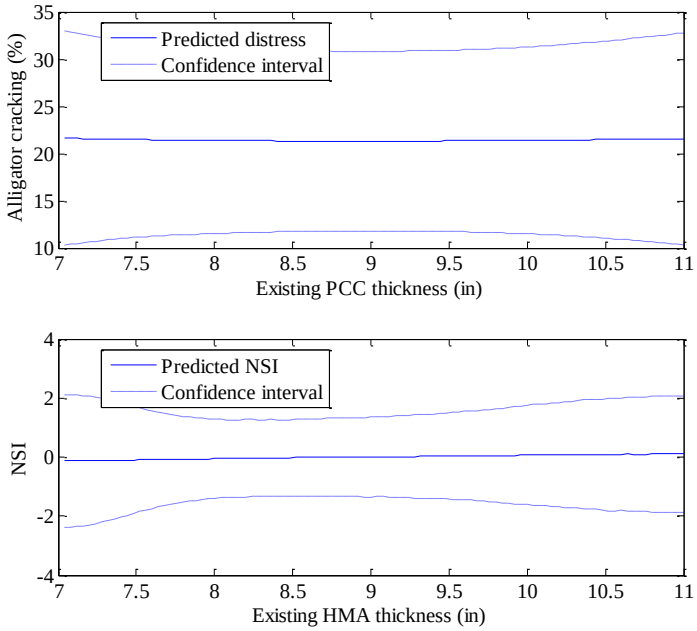

Figure B-91 Predicted alligator cracking and NSI for existing PCC thickness

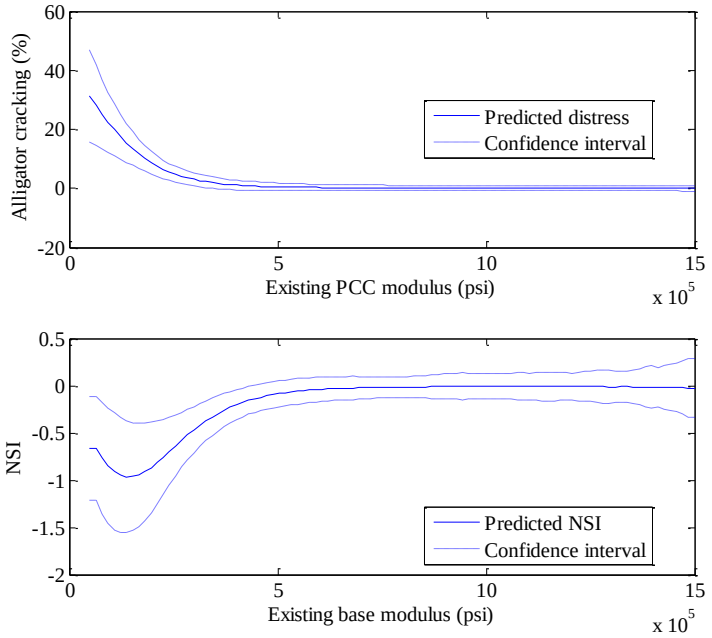

Figure B-92 Predicted alligator cracking and NSI for existing PCC modulus

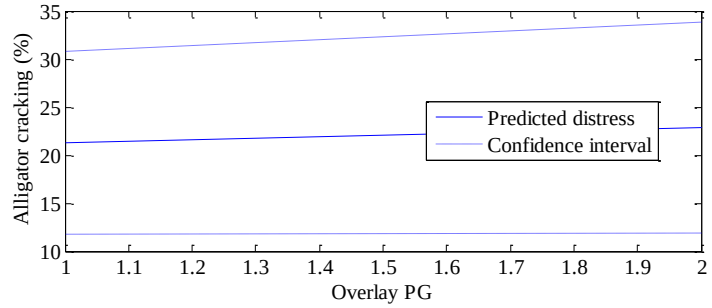

Figure B-93 Predicted alligator cracking for overlay PG

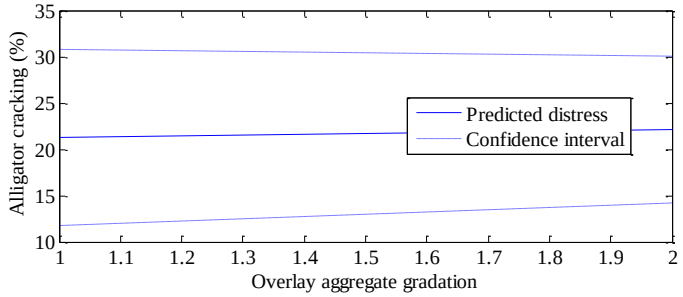

Figure B-94 Predicted alligator cracking for overlay aggregate gradation

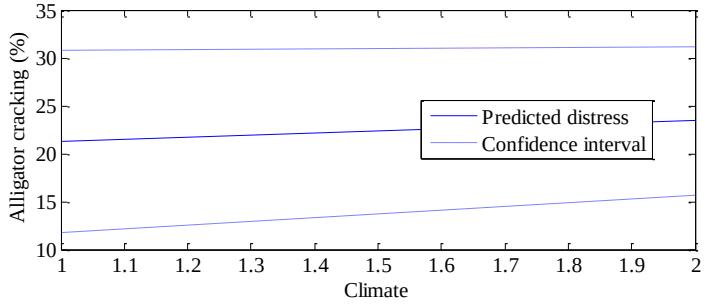

Figure B-95 Predicted alligator cracking for climate

Inputs interaction effect

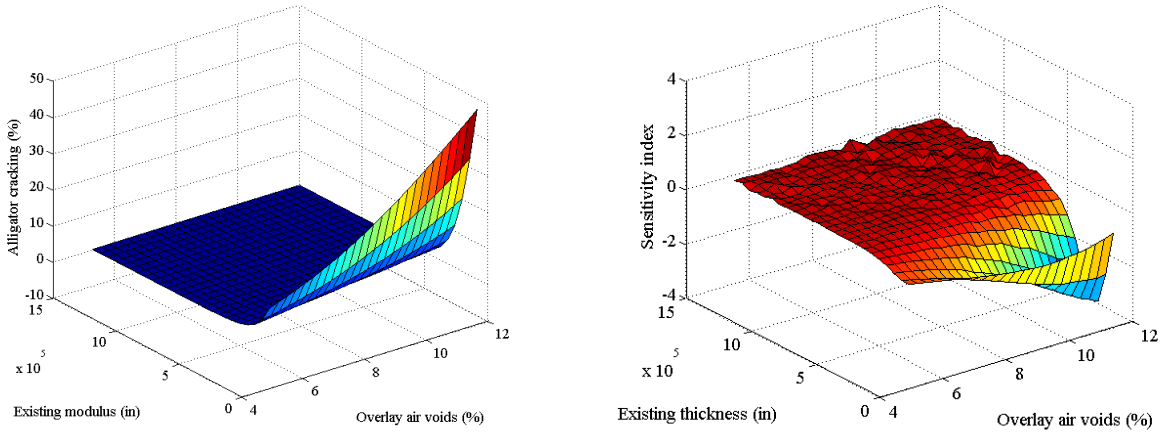

Figure B-96 Predicted interaction and NSI between existing modulus and overlay air voids

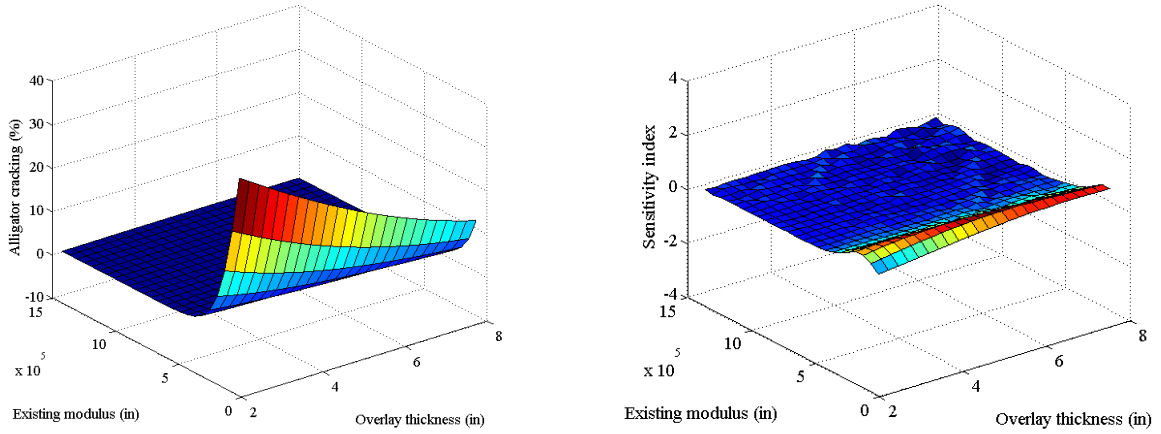

Figure B-97 Predicted interaction and NSI between existing modulus and overlay thickness

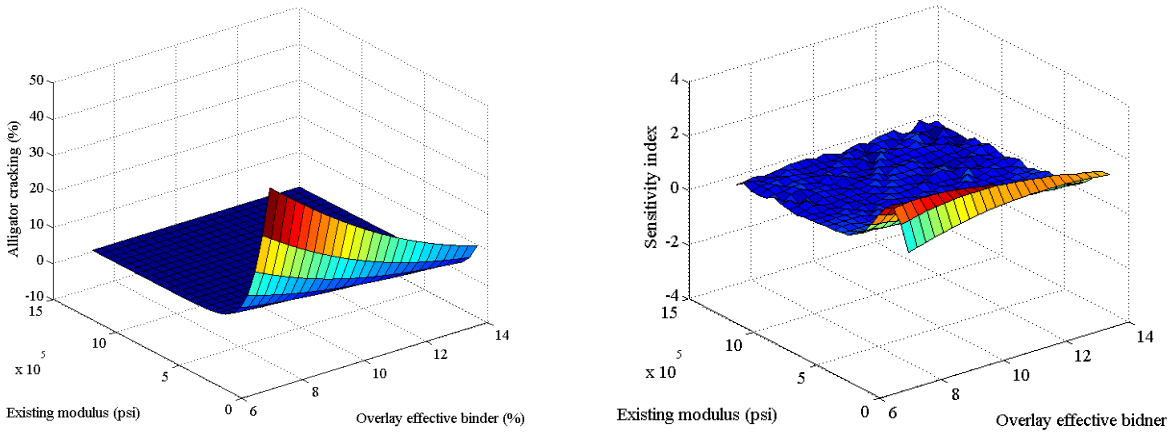

Figure B-98 Predicted interaction and NSI between existing modulus and overlay effective binder

B.1.9 Longitudinal cracking

Inputs main effect

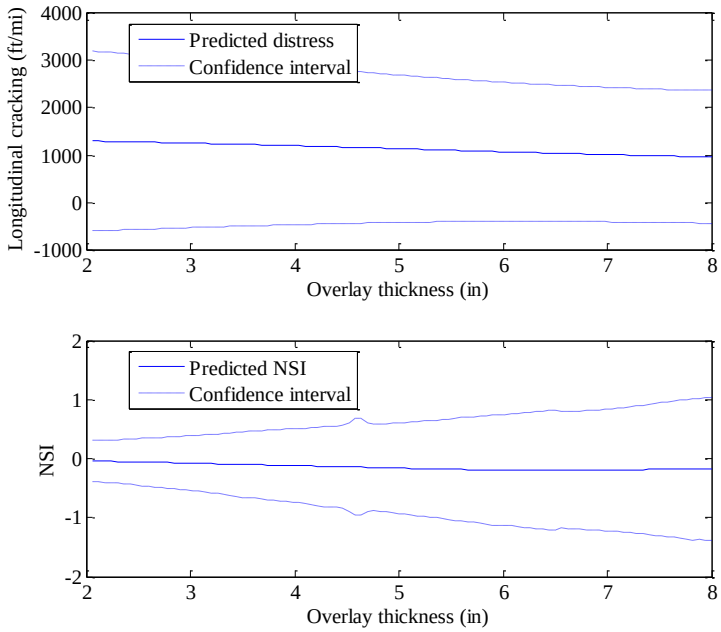

Figure B-99 Predicted longitudinal cracking and NSI for overlay thickness

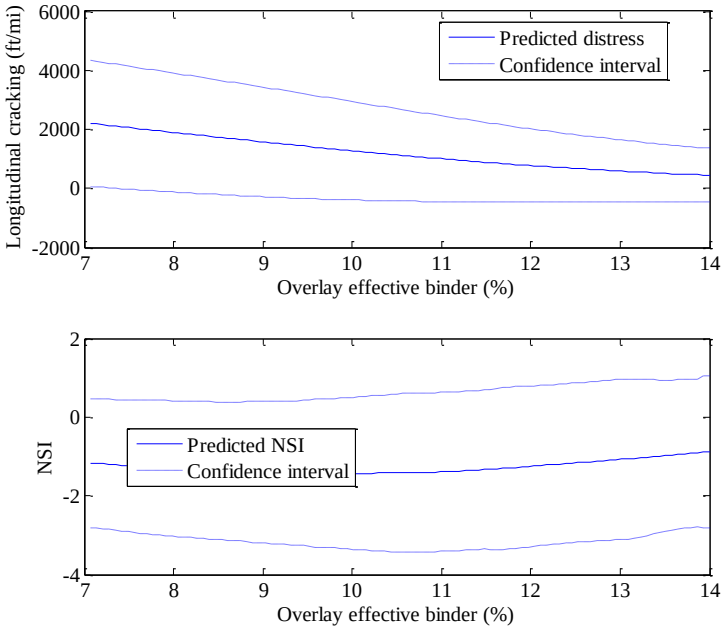

Figure B-100 Predicted longitudinal cracking and NSI for overlay effective binder

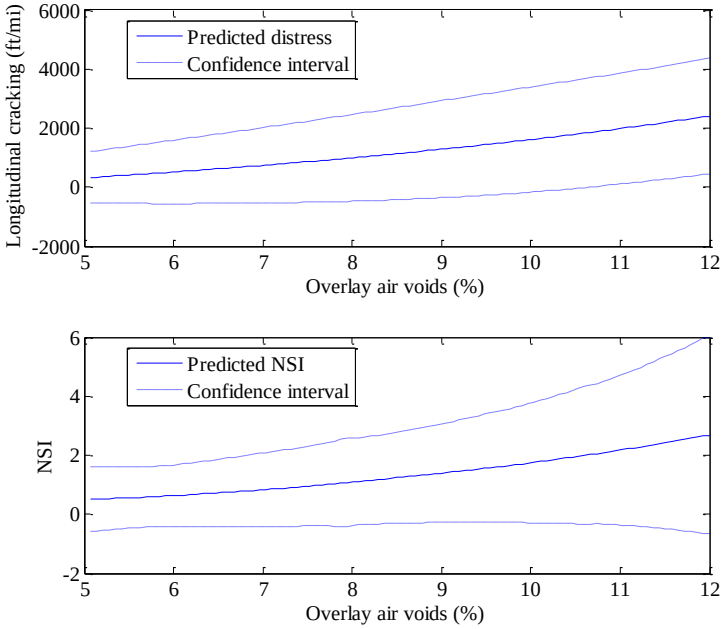

Figure B-101 Predicted longitudinal cracking and NSI for overlay air voids

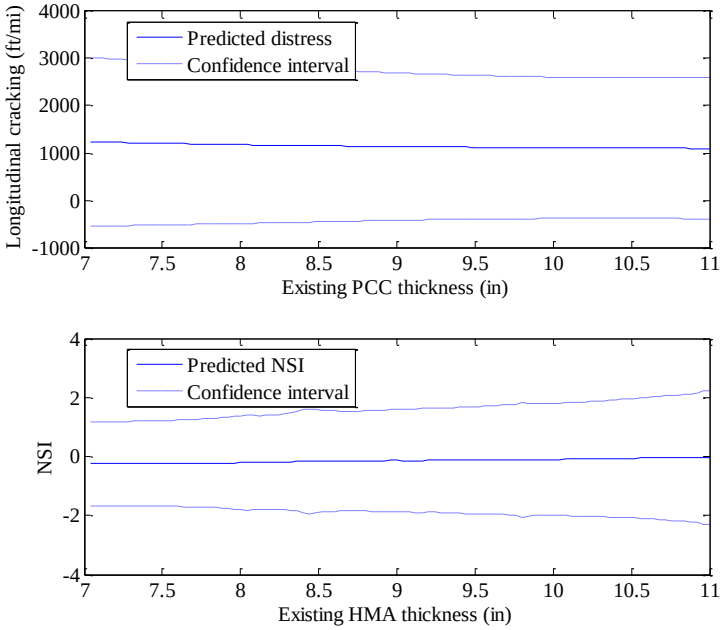

Figure B-102 Predicted longitudinal cracking and NSI for existing PCC thickness

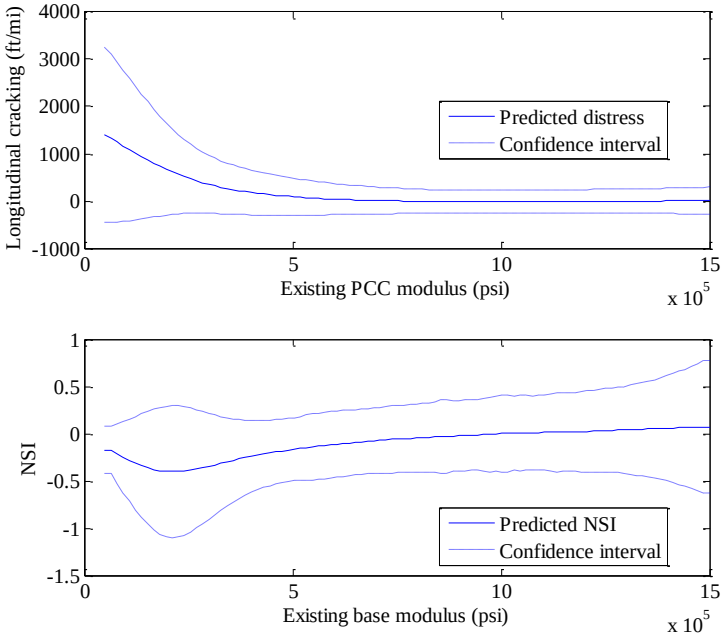

Figure B-103 Predicted longitudinal cracking and NSI for existing PCC modulus

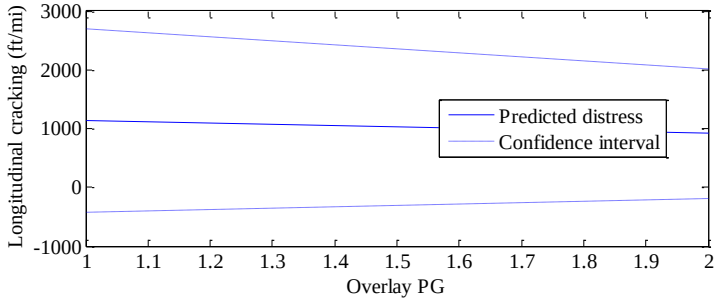

Figure B-104 Predicted longitudinal cracking and NSI for overlay PG

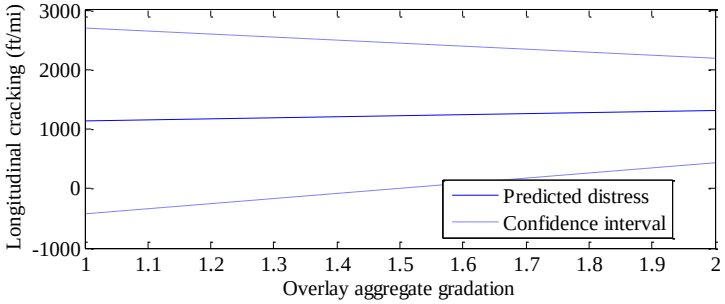

Figure B-105 Predicted longitudinal cracking and NSI for overlay aggregate gradation

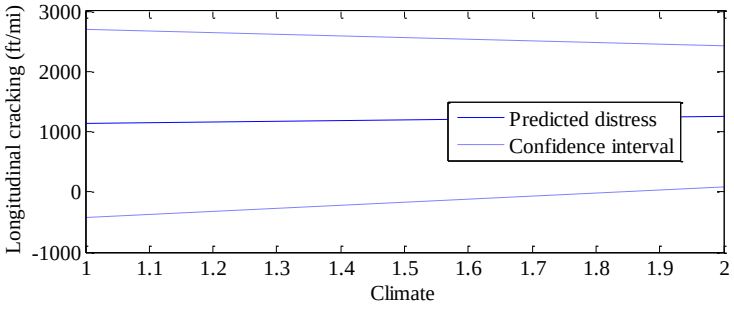

Figure B-106 Predicted longitudinal cracking and NSI for climate

Inputs interaction effect

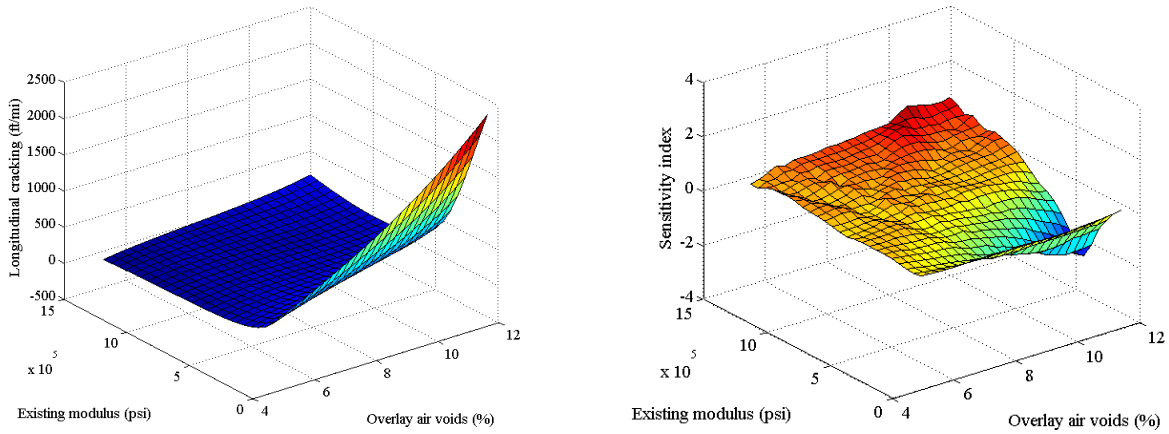

Figure B-107 Predicted interaction and NSI between existing modulus and overlay air voids

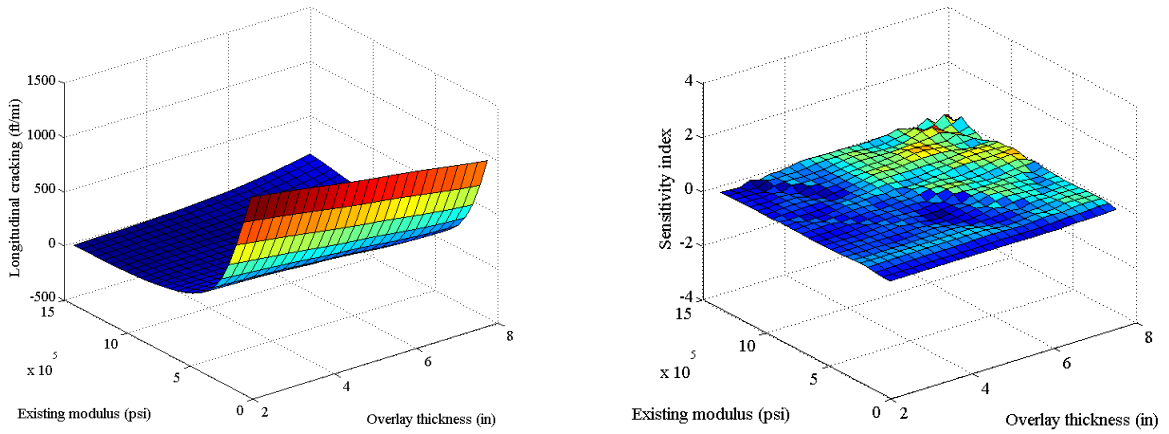

Figure B-108 Predicted interaction and NSI between existing modulus and overlay thickness

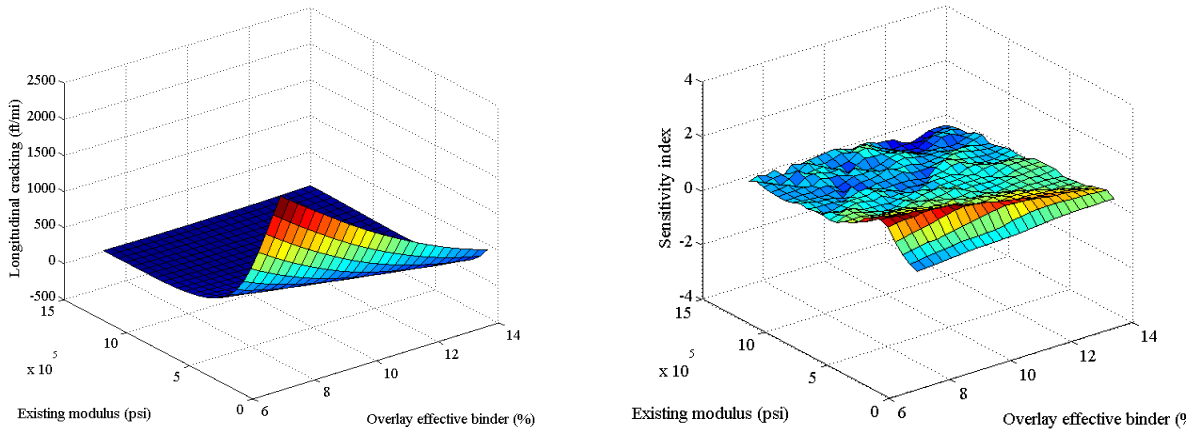

Figure B-109 Predicted interaction and NSI between existing modulus and overlay effective binder

B.1.10 Rutting

Inputs main effect

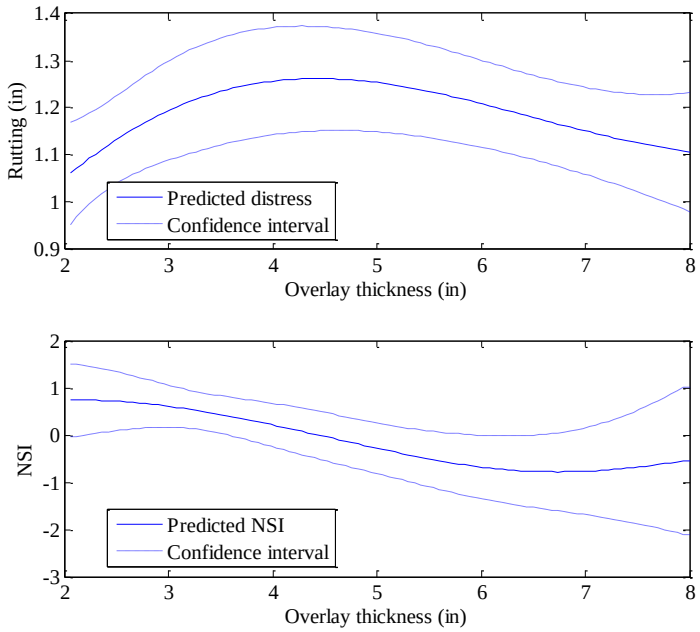

Figure B-110 Predicted rutting and NSI for overlay thickness

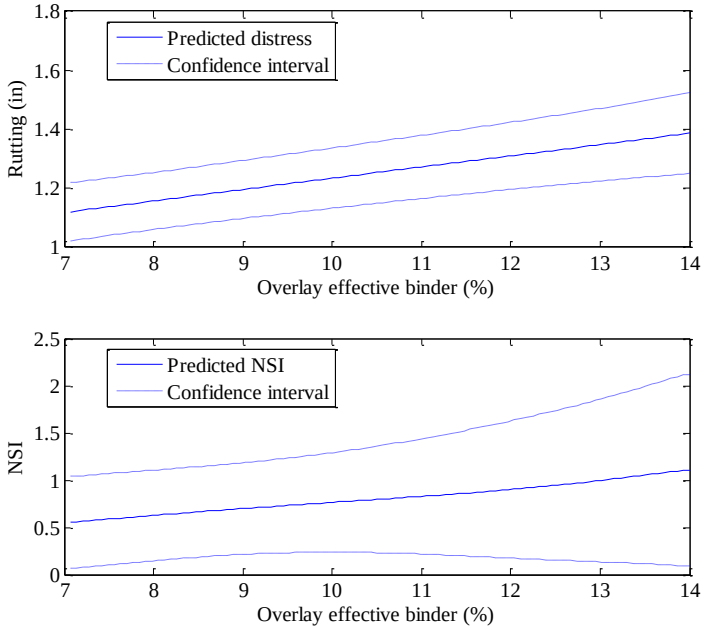

Figure B-111 Predicted rutting and NSI for overlay effective binder

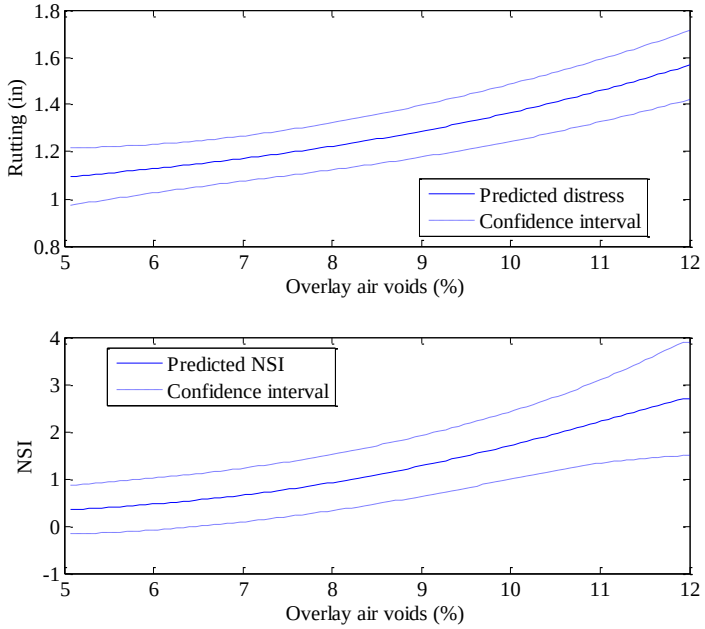

Figure B-112 Predicted rutting and NSI for overlay air voids

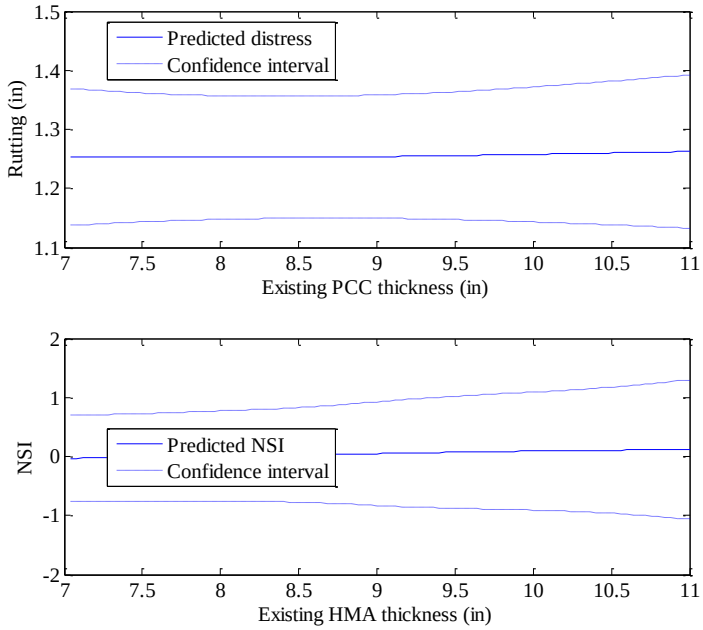

Figure B-113 Predicted rutting and NSI for existing PCC thickness

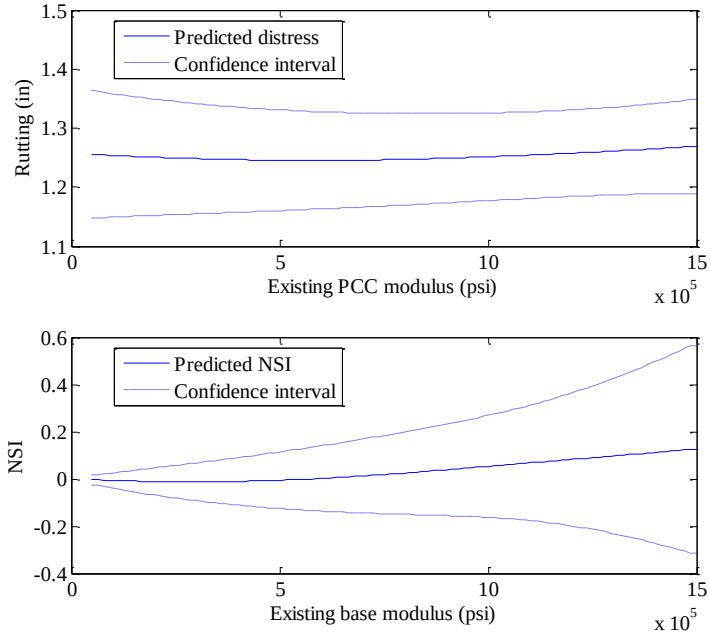

Figure B-114 Predicted rutting and NSI for existing PCC modulus

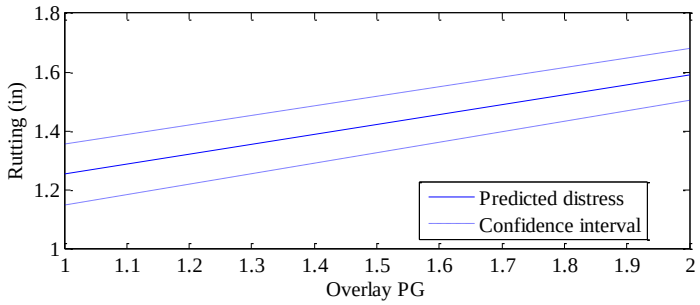

Figure B-115 Predicted rutting for overlay PG

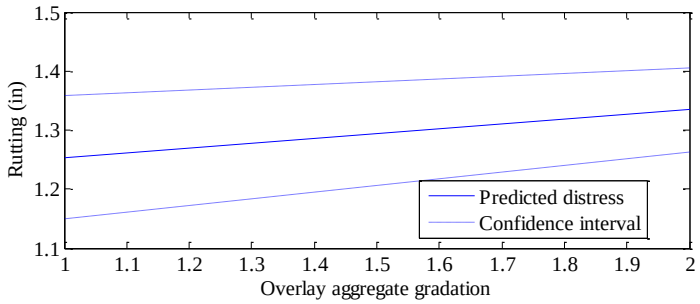

Figure B-116 Predicted rutting for overlay aggregate gradation

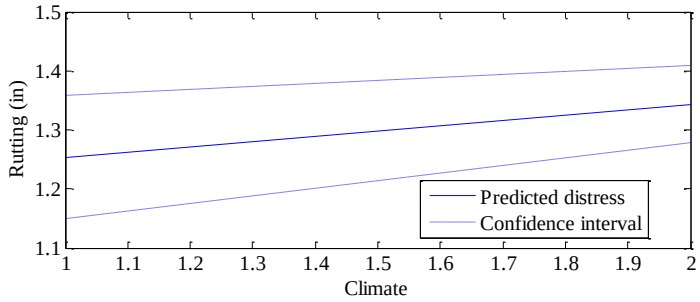

Figure B-117 Predicted rutting for climate

Inputs interaction effect

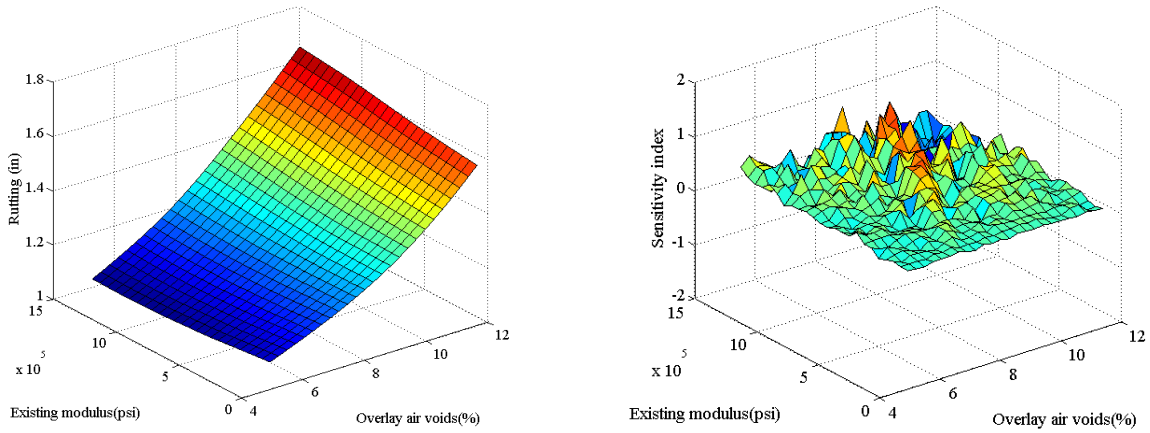

Figure B-118 Predicted interaction and NSI between existing modulus and overlay air voids

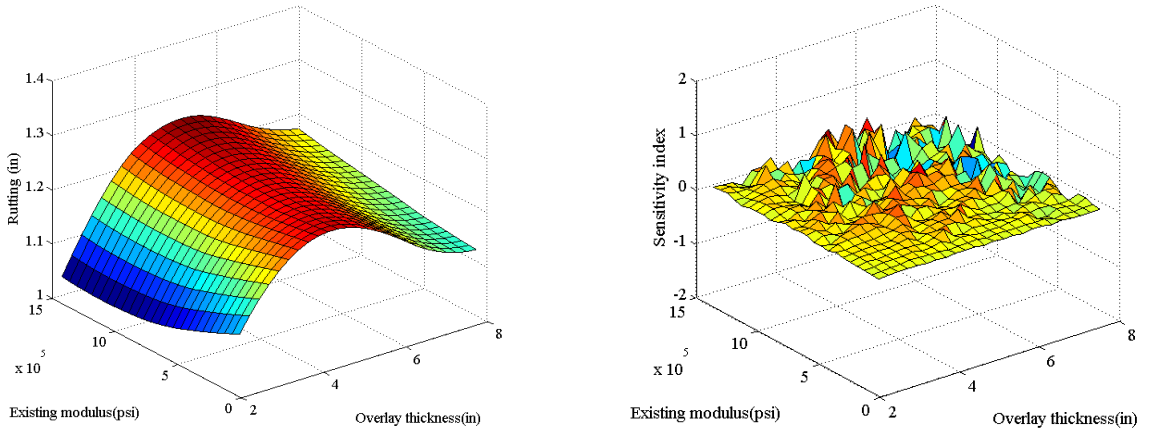

Figure B-119 Predicted interaction and NSI between existing modulus and overlay thickness

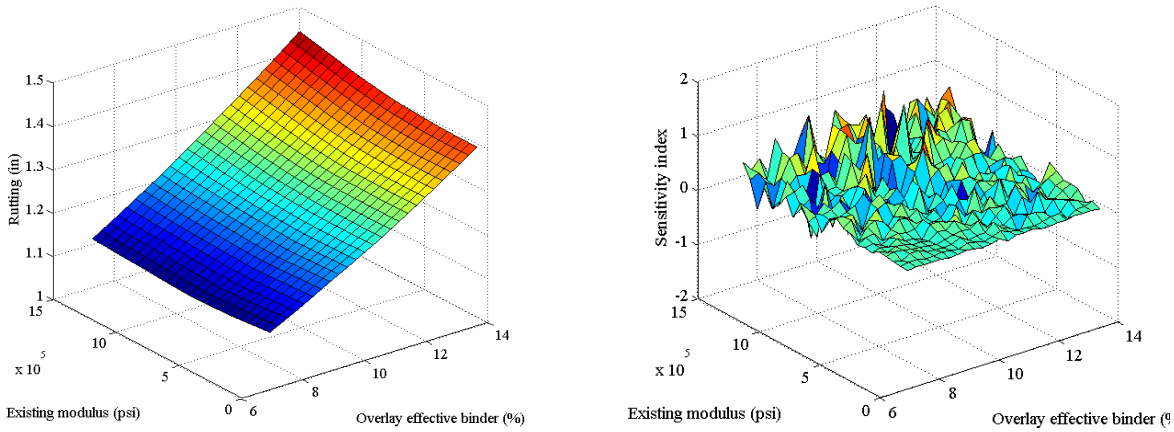

Figure B-120 Predicted interaction and NSI between existing modulus and overlay effective binder

B.1.11 IRI

Inputs main effect

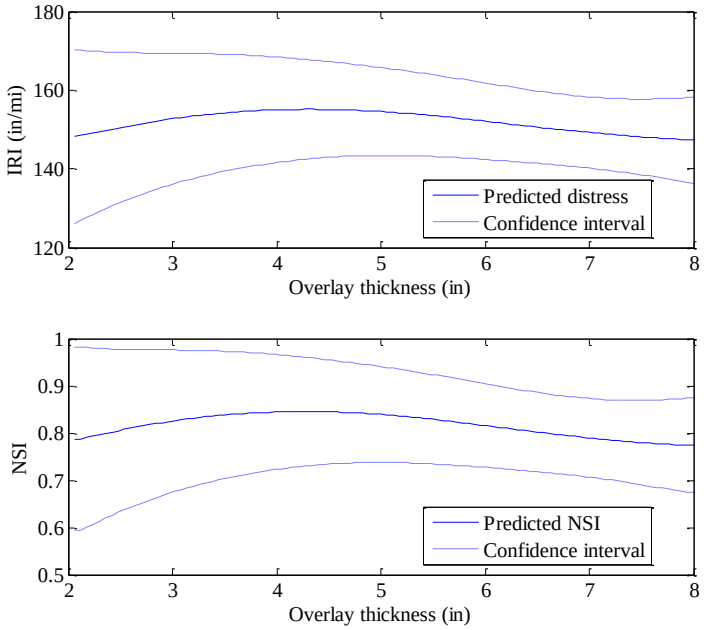

Figure B-121 Predicted IRI and NSI for overlay thickness

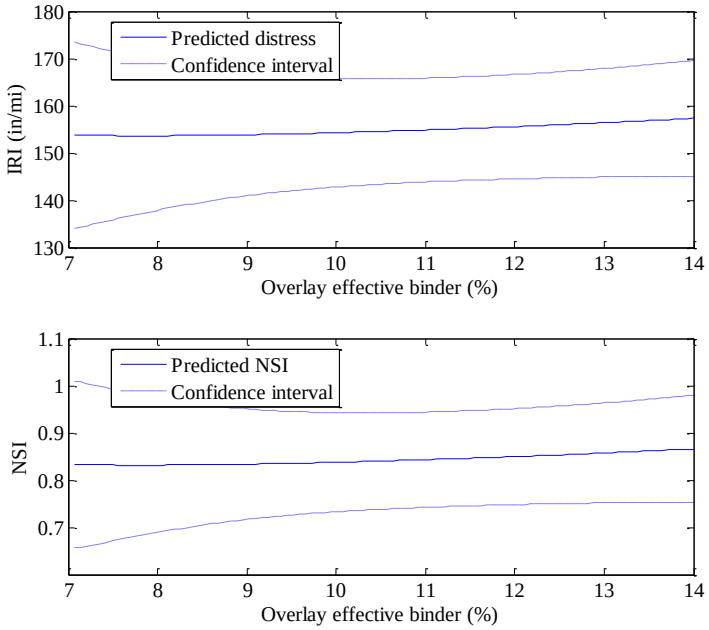

Figure B-122 Predicted IRI and NSI for overlay effective binder

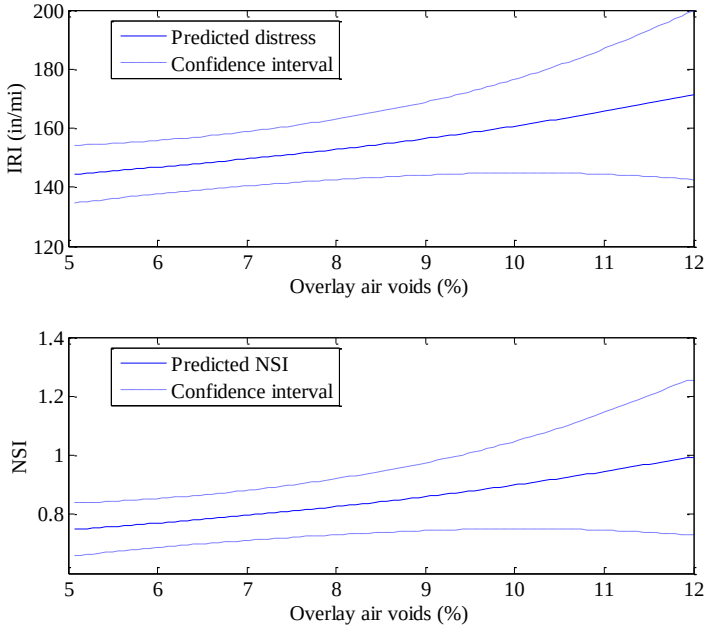

Figure B-123 Predicted IRI and NSI for overlay air voids

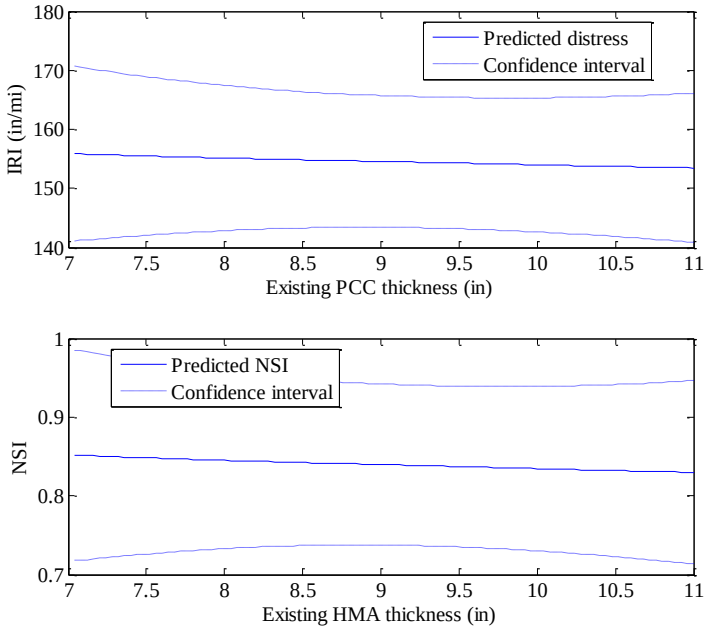

Figure B-124 Predicted IRI and NSI for existing PCC thickness

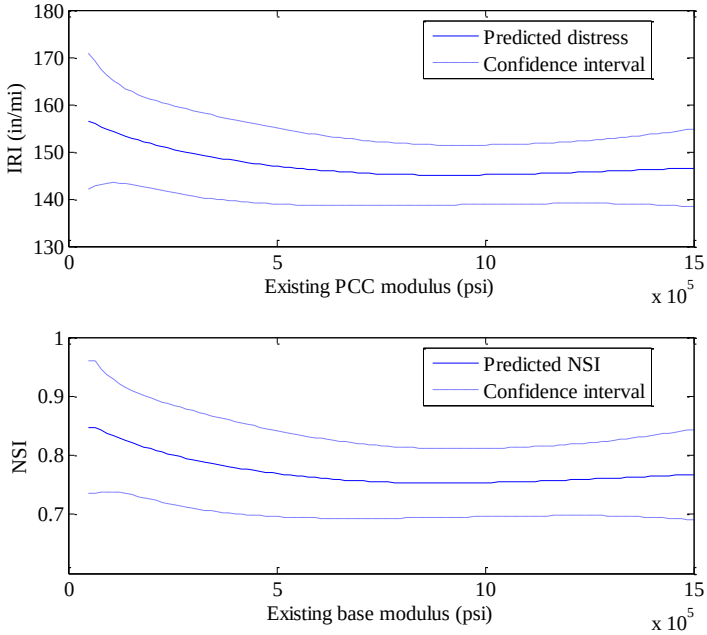

Figure B-125 Predicted IRI and NSI for existing PCC modulus

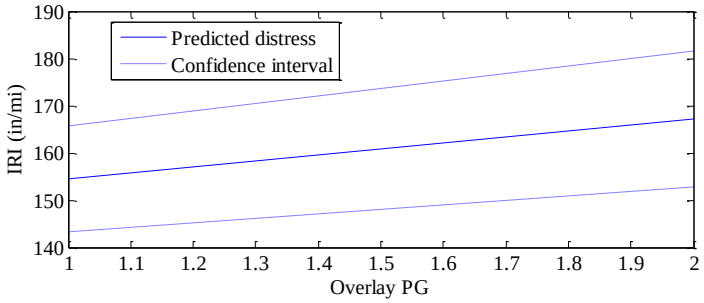

Figure B-126 Predicted IRI and NSI for overlay PG

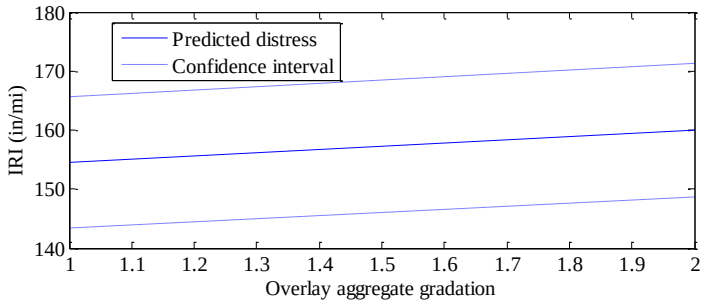

Figure B-127 Predicted IRI and NSI for overlay aggregate gradation

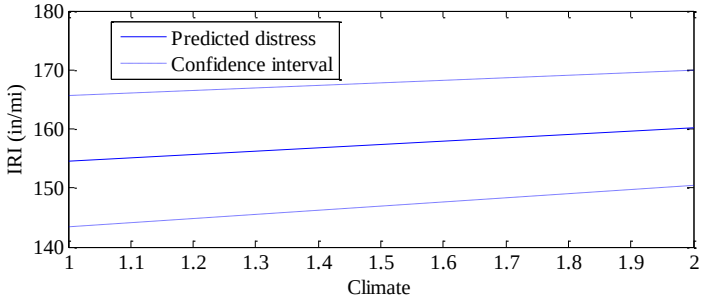

Figure B-128 Predicted IRI and NSI for climate

Inputs interaction effect

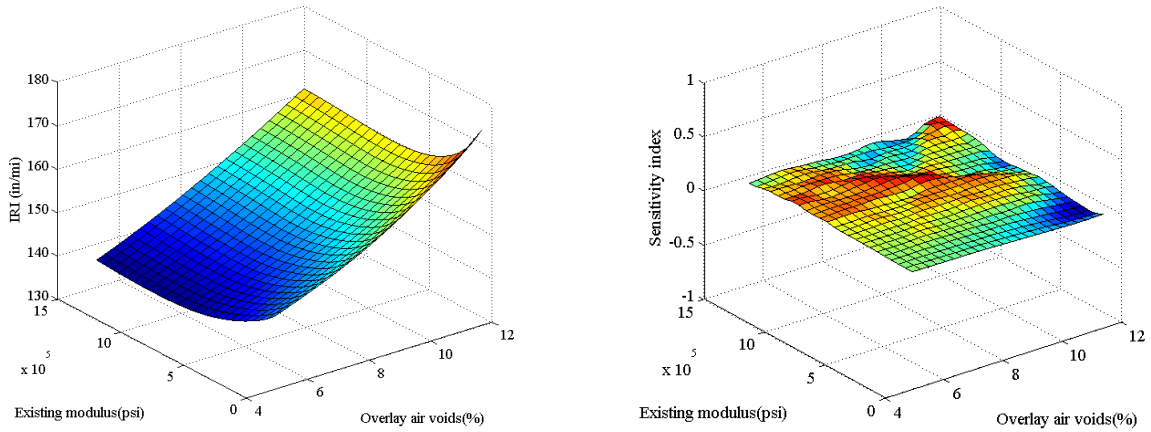

Figure B-129 Predicted interaction and NSI between existing modulus and overlay air voids

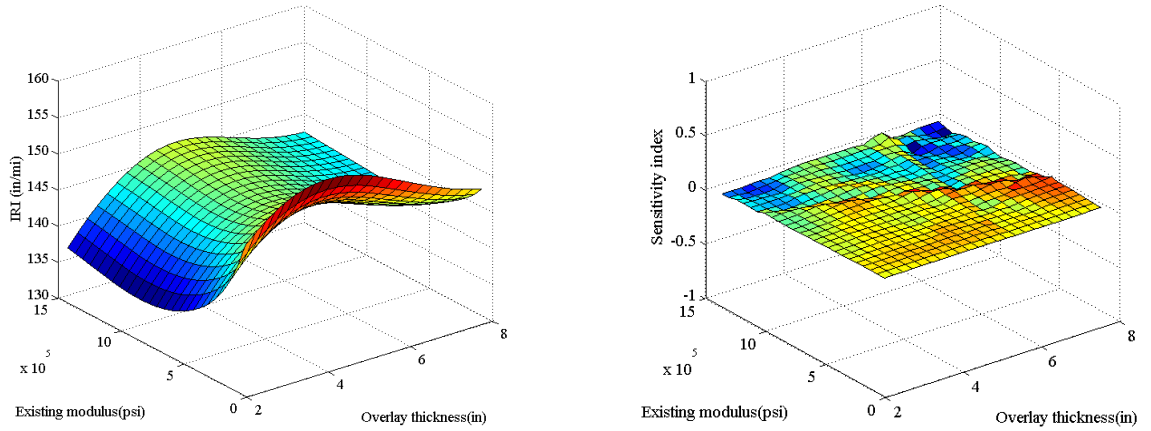

Figure B-130 Predicted interaction and NSI between existing modulus and overlay thickness

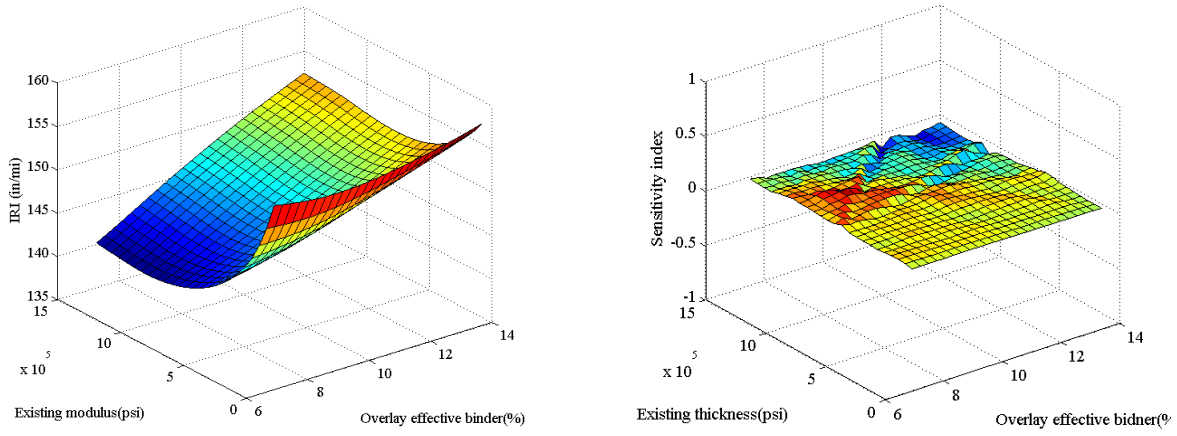

Figure B-131 Predicted interaction and NSI between existing modulus and overlay effective binder

B.4 UNBONDED OVERLAYS

B.1.12 Cracking

Inputs main effect

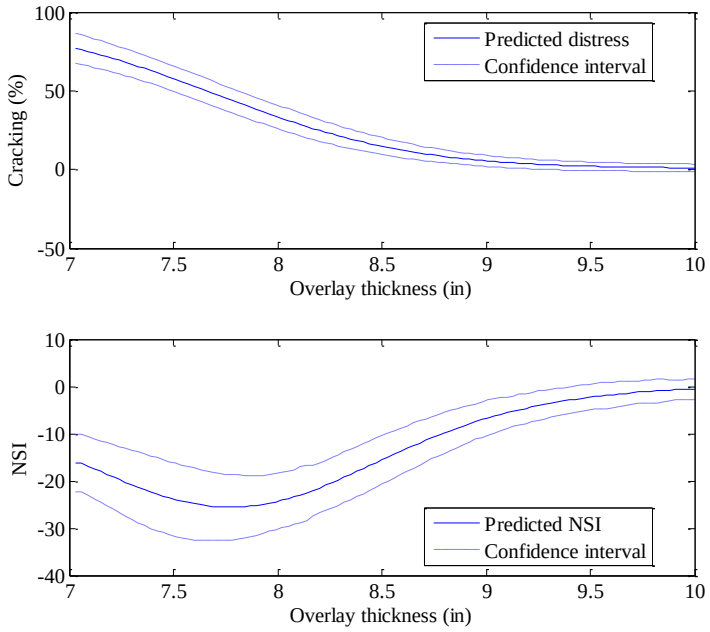

Figure B-132 Predicted cracking and NSI for overlay thickness

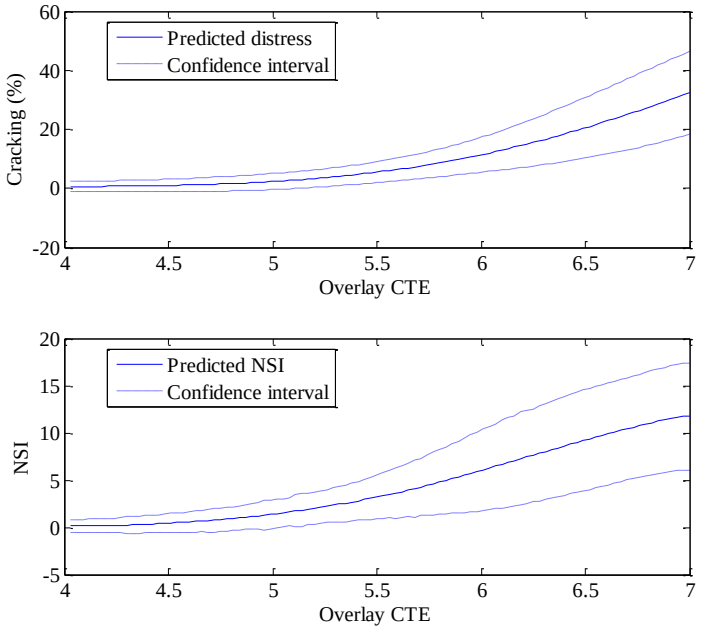

Figure B-133 Predicted cracking and NSI for overlay CTE

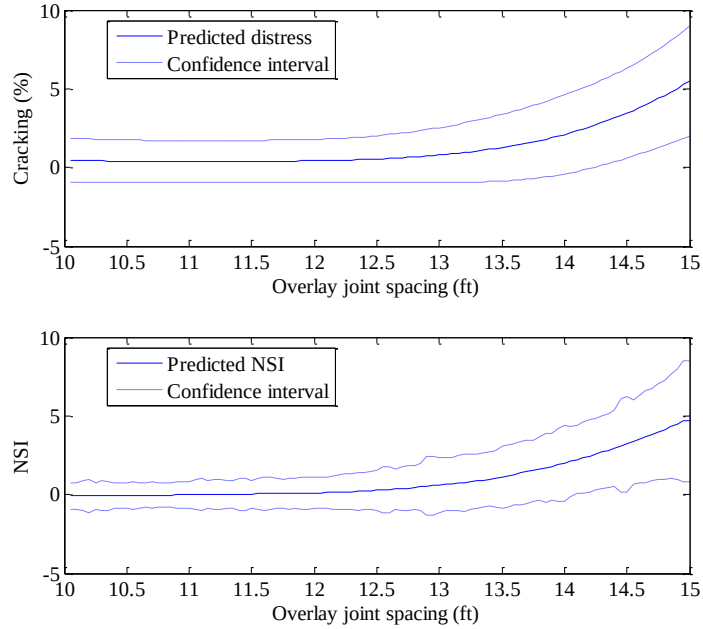

Figure B-134 Predicted cracking and NSI for overlay joint spacing

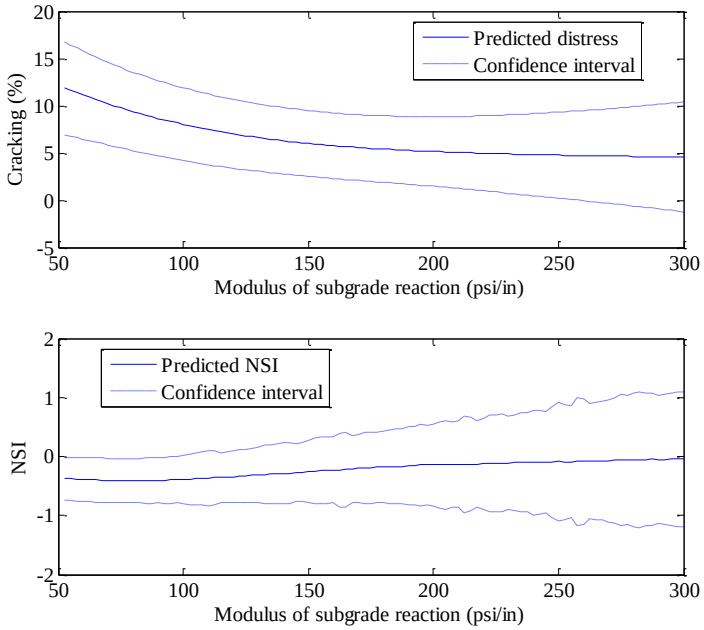

Figure B-135 Predicted cracking and NSI for modulus of subgrade reaction

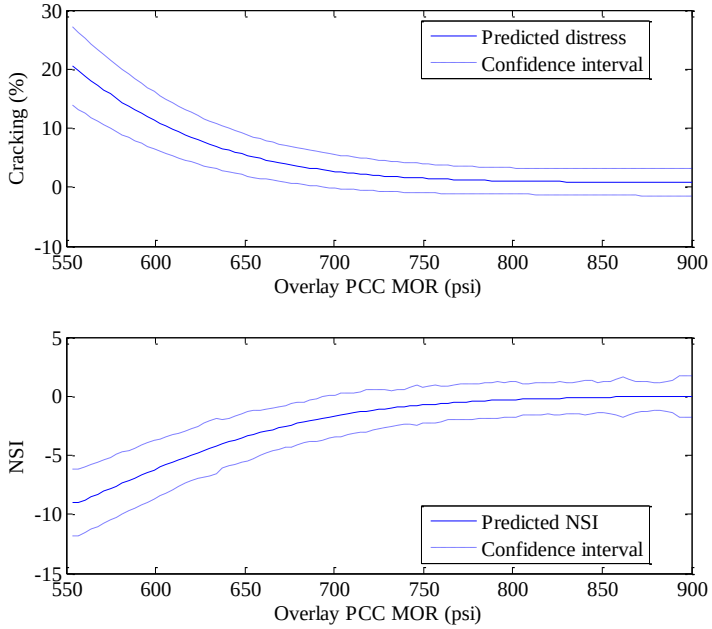

Figure B-136 Predicted cracking and NSI for overlay PCC MOR

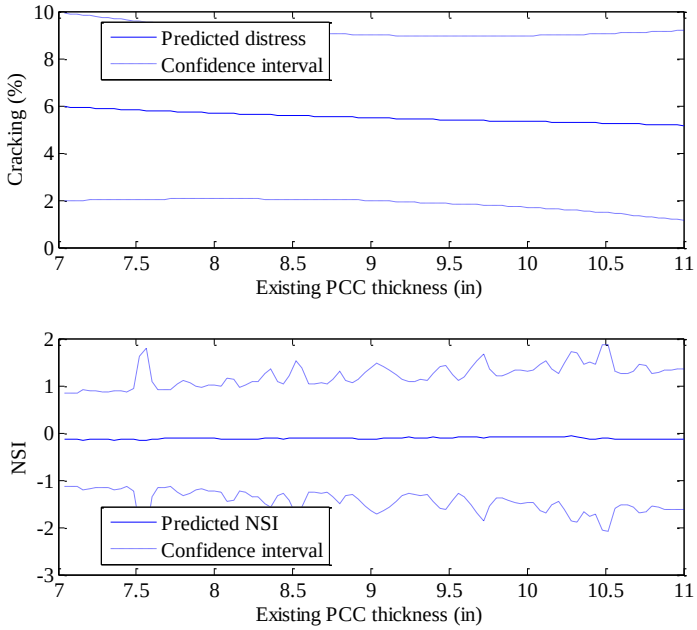

Figure B-137 Predicted cracking and NSI for existing PCC thickness

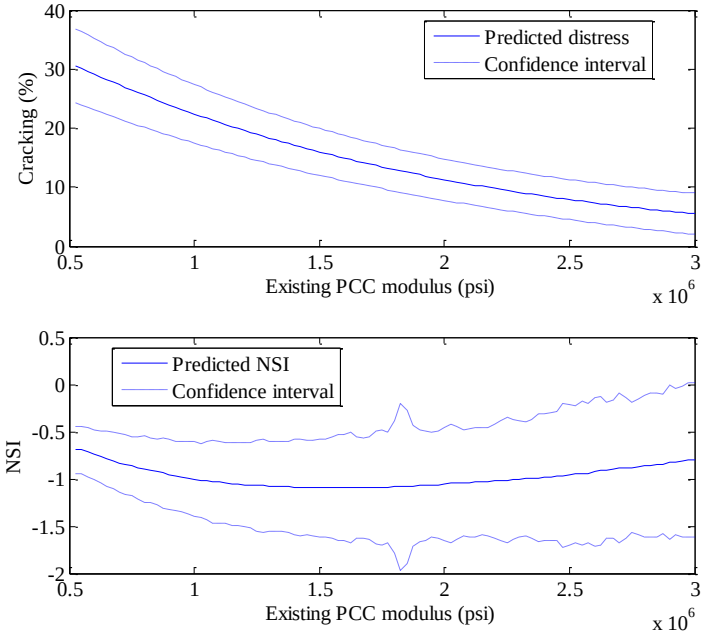

Figure B-138 Predicted cracking and NSI for existing PCC modulus

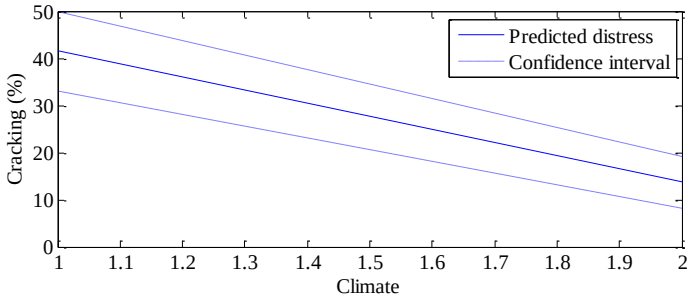

Figure B-139 Predicted cracking for climate

Inputs interaction effect

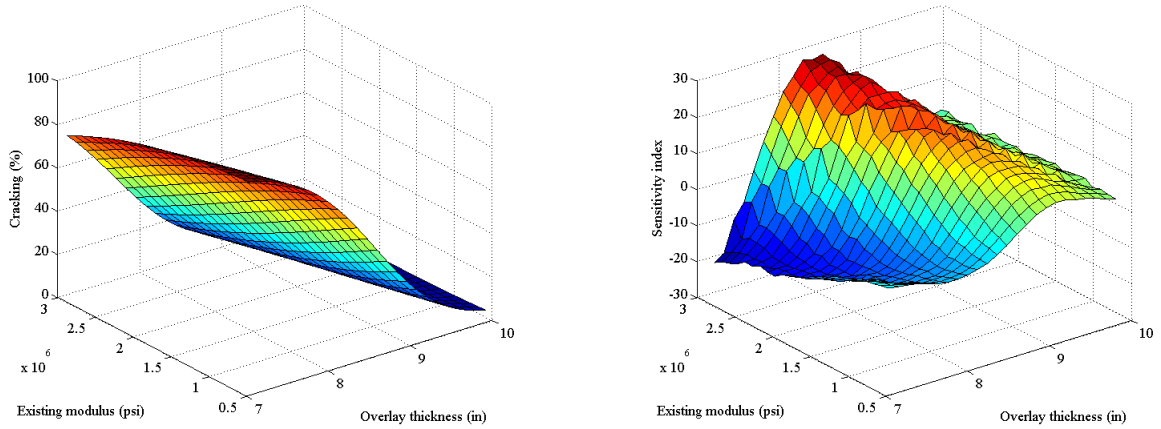

Figure B-140 Predicted interaction and NSI between existing modulus and overlay thickness

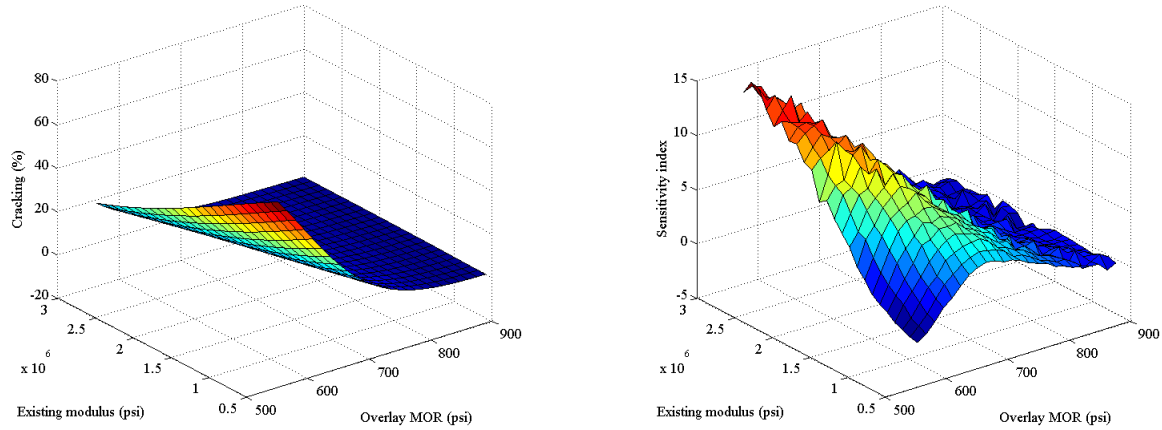

Figure B-141 Predicted interaction and NSI between existing thickness and overlay MOR

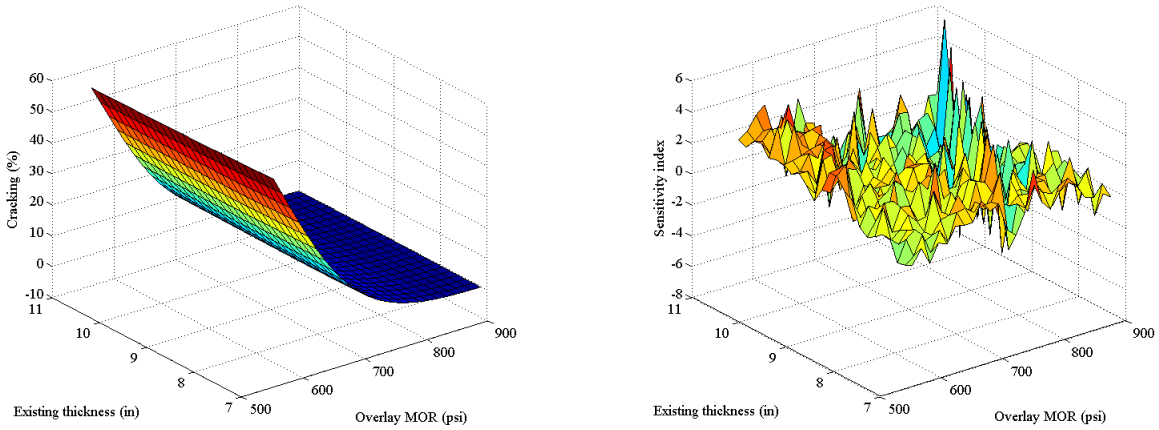

Figure B-142 Predicted interaction and NSI between existing thickness and overlay MOR

B.1.13 Faulting

Inputs main effect

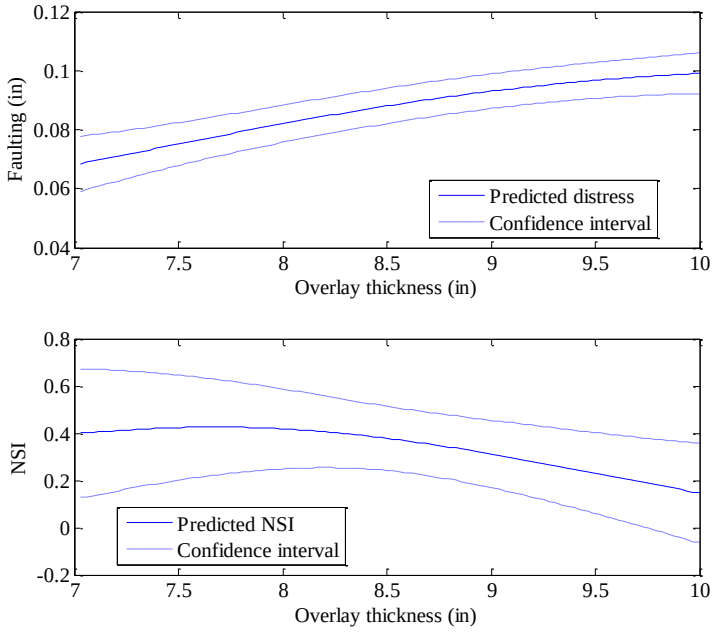

Figure B-143 Predicted faulting and NSI for overlay thickness

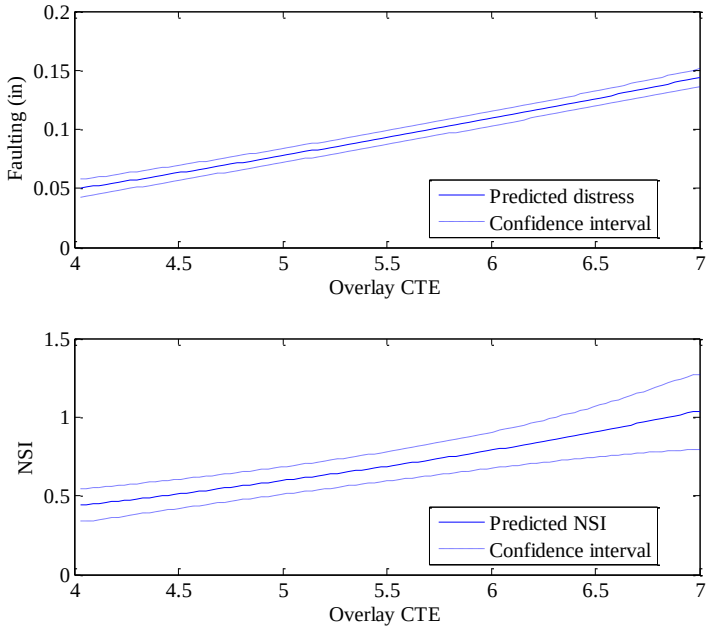

Figure B-144 Predicted faulting and NSI for overlay CTE

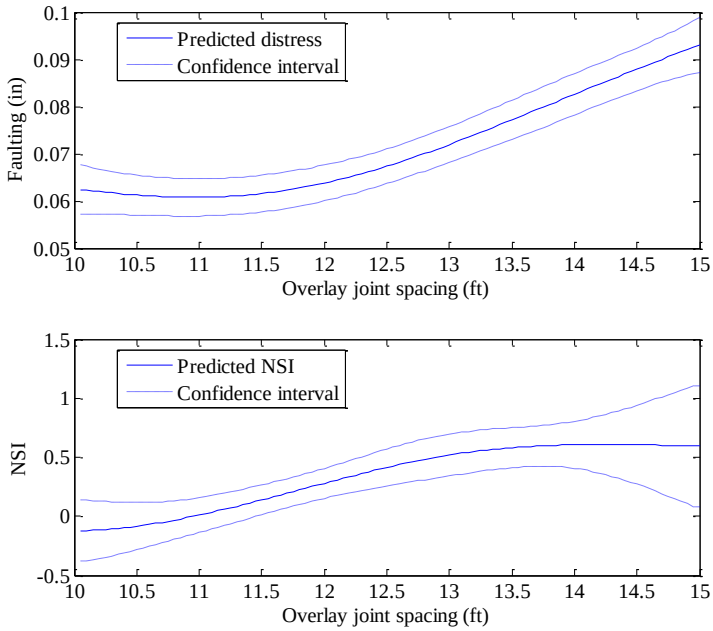

Figure B-145 Predicted faulting and NSI for overlay joint spacing

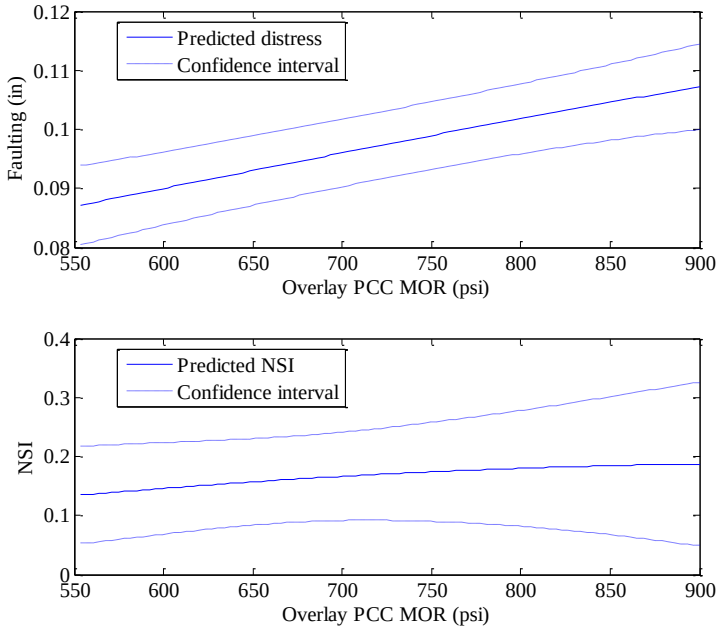

Figure B-146 Predicted faulting and NSI for overlay PCC MOR

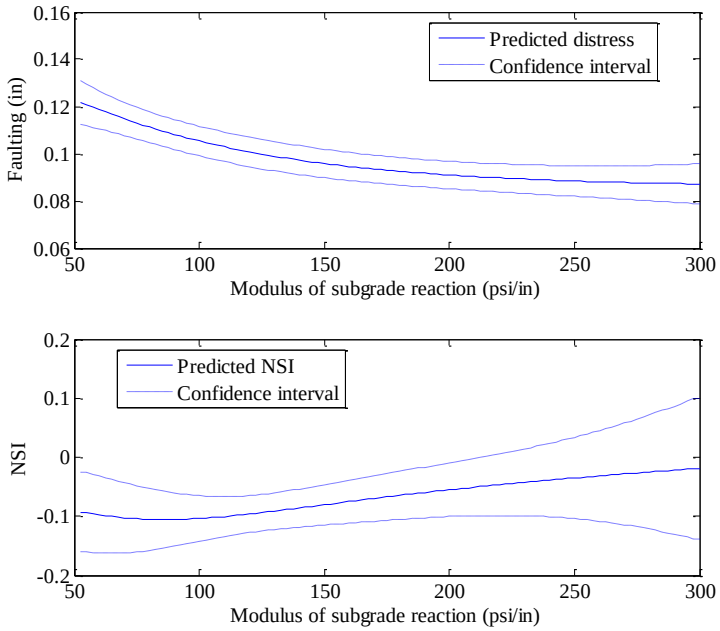

Figure B-147 Predicted faulting and NSI for modulus of subgrade reaction

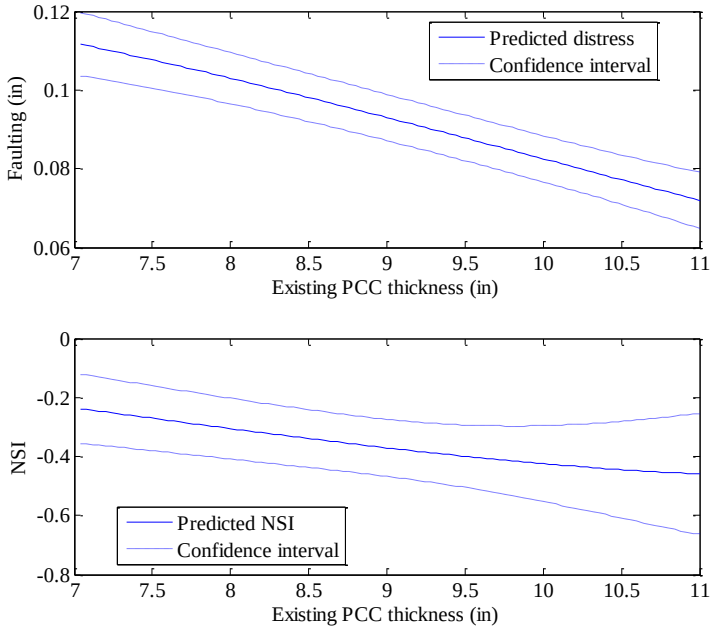

Figure B-148 Predicted faulting and NSI for PCC thickness

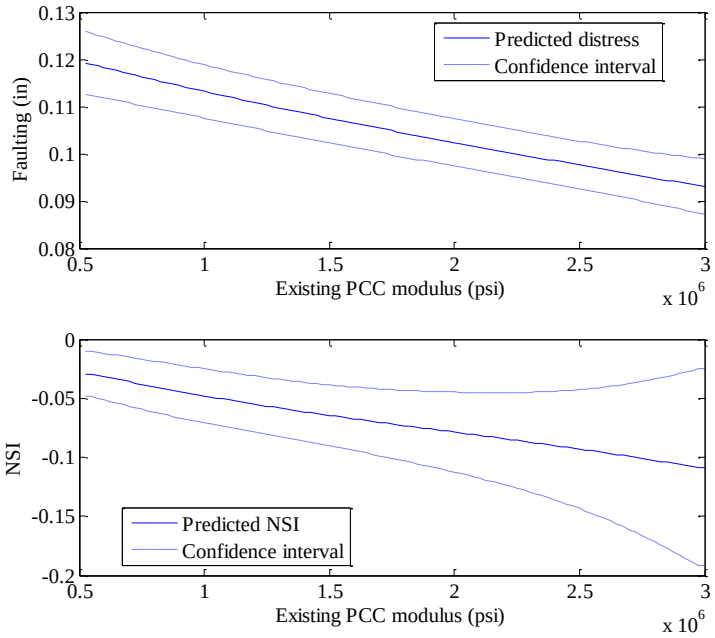

Figure B-149 Predicted faulting and NSI for PCC modulus

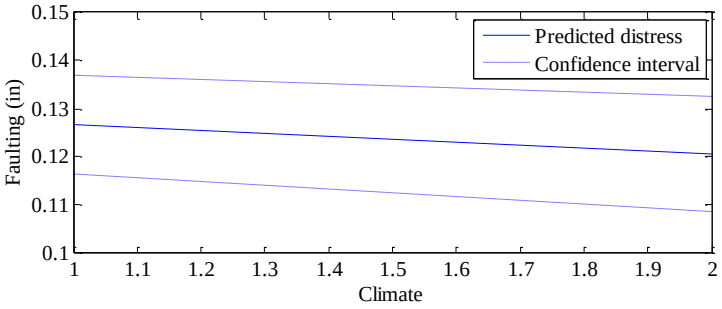

Figure B-150 Predicted faulting for climate

Inputs interaction effect

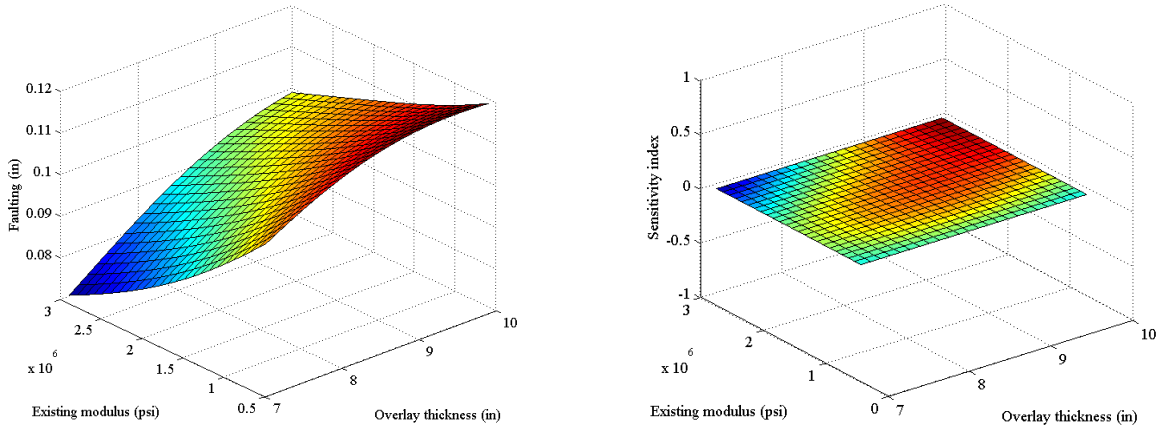

Figure B-151 Predicted interaction and NSI between existing modulus and overlay thickness

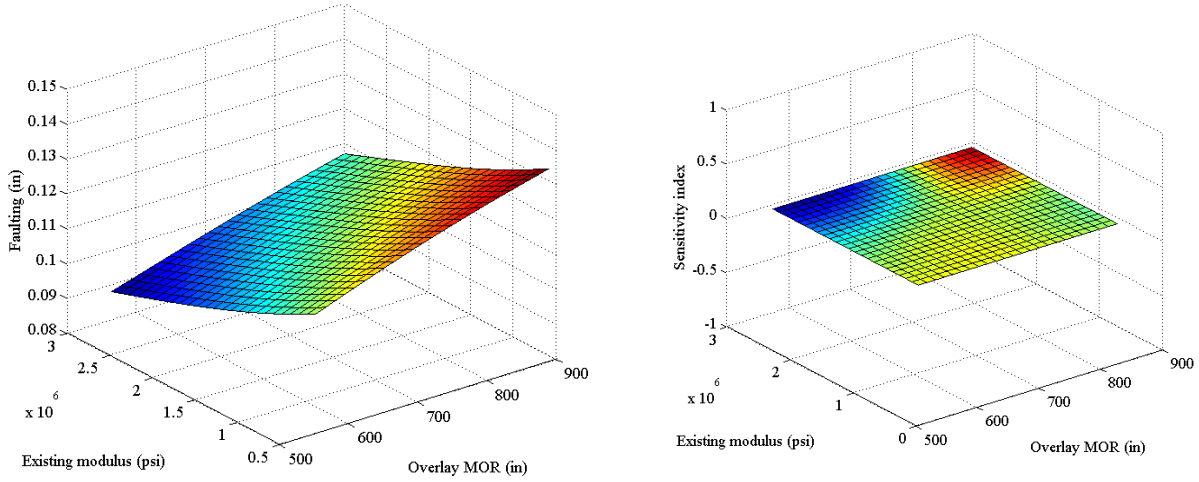

Figure B-152 Predicted interaction and NSI between existing thickness and overlay MOR

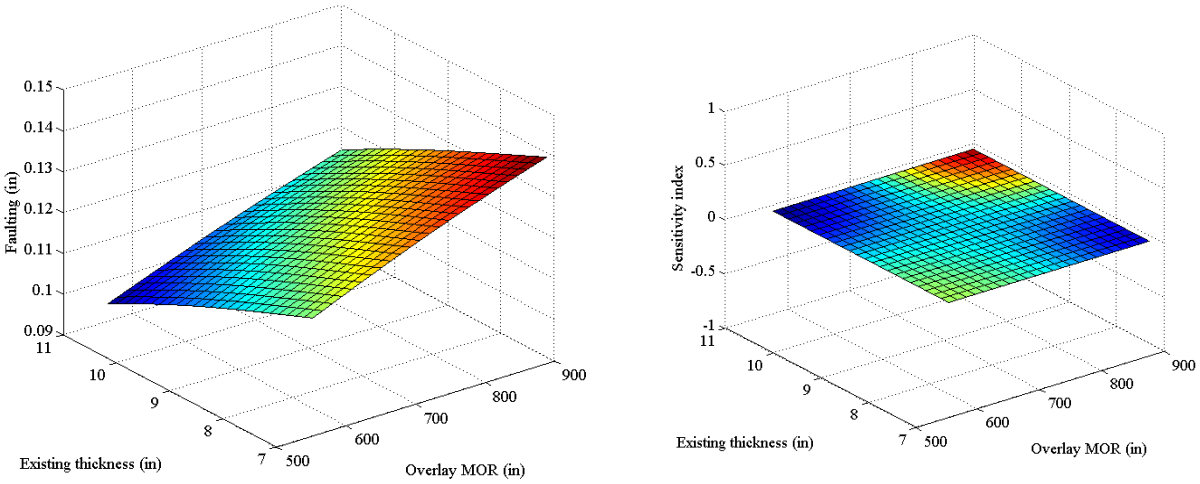

Figure B-153 Predicted interaction and NSI between existing thickness and overlay MOR

B.1.14 IRI

Inputs main effect

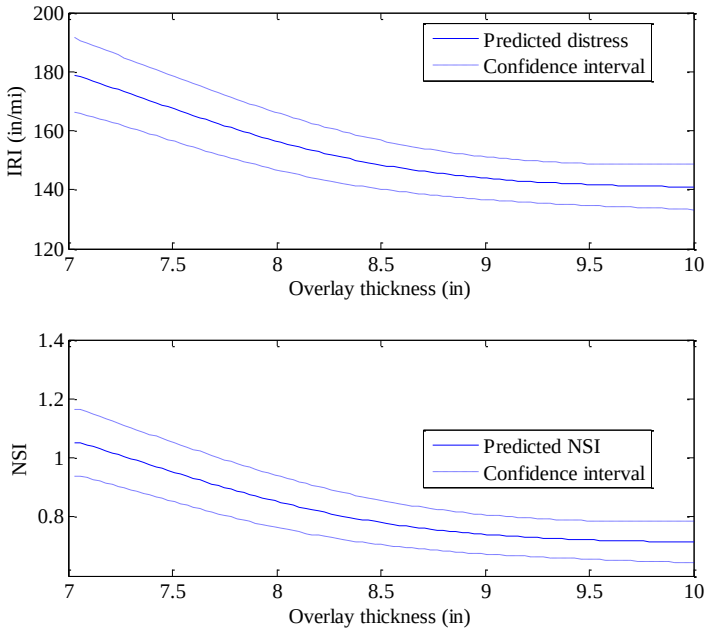

Figure B-154 Predicted IRI and NSI for overlay thickness

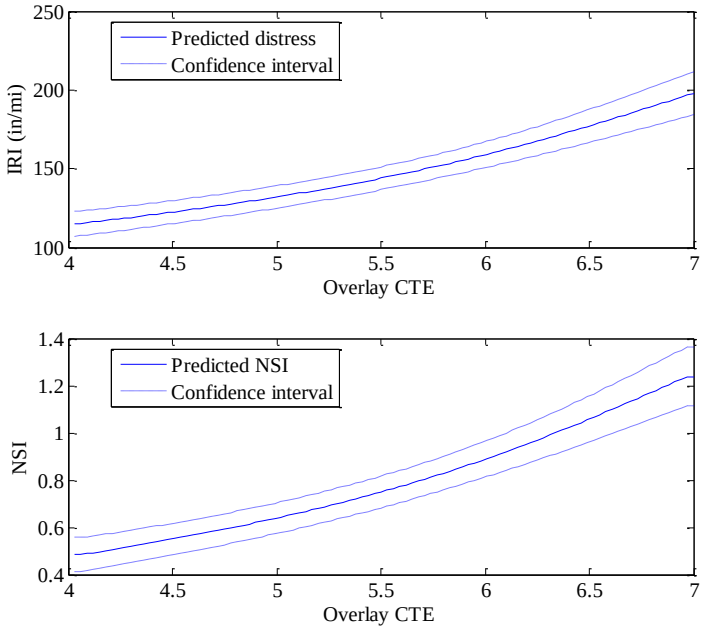

Figure B-155 Predicted IRI and NSI for overlay CTE

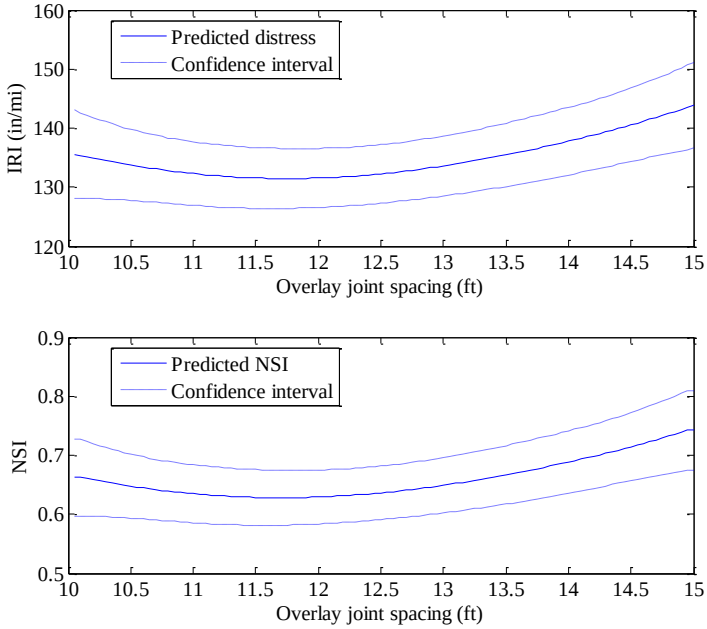

Figure B-156 Predicted IRI and NSI for overlay joint spacing

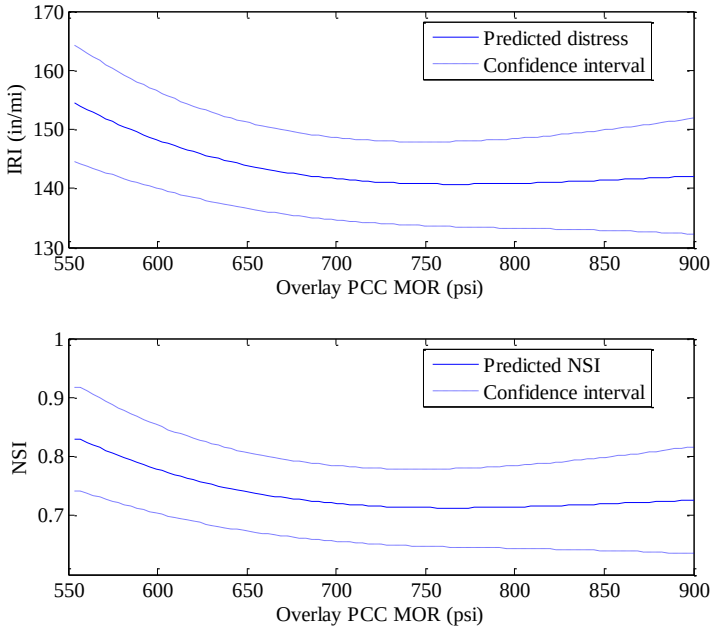

Figure B-157 Predicted IRI and NSI for overlay PCC MOR

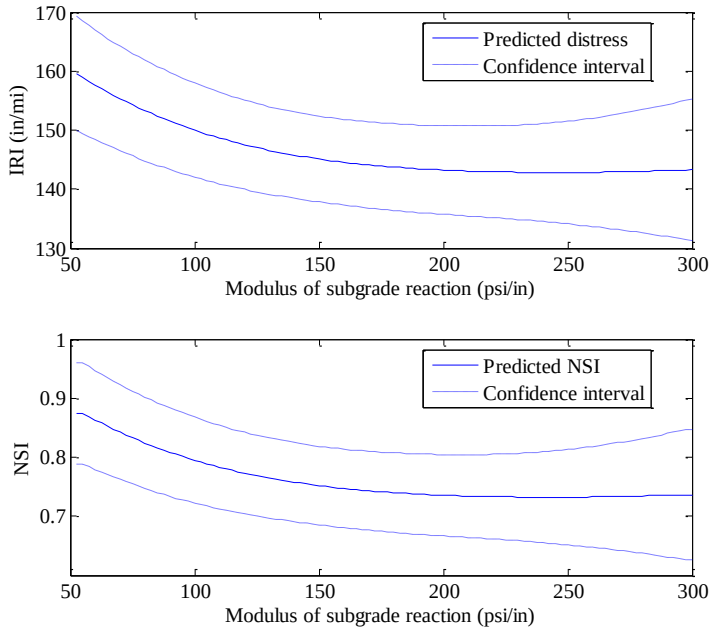

Figure B-158 Predicted IRI and NSI for modulus of subgrade reaction

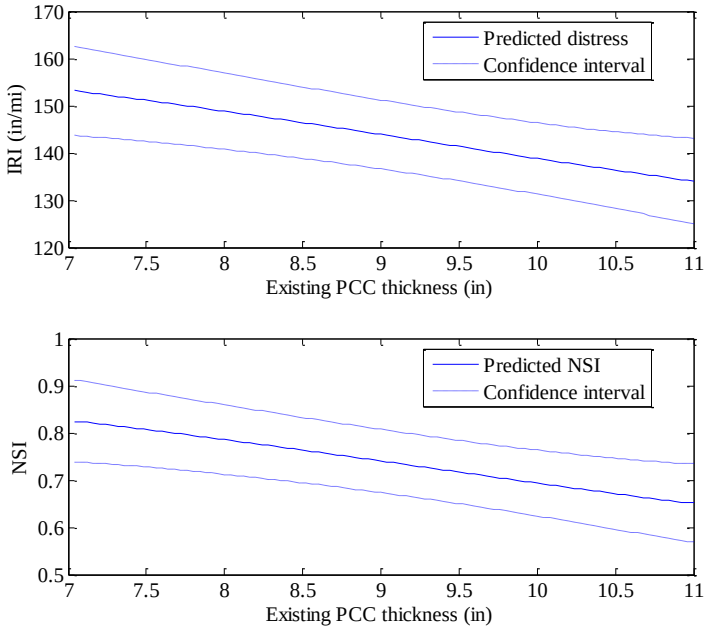

Figure B-159 Predicted IRI and NSI for existing PCC thickness

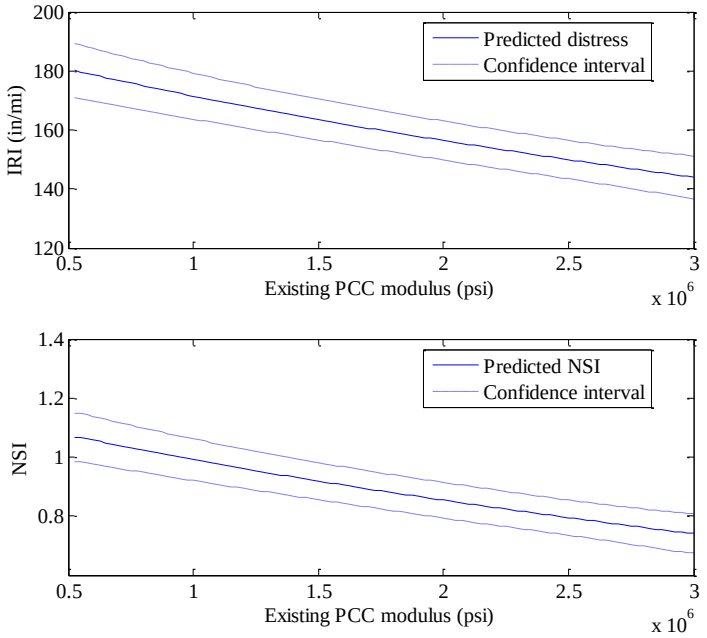

Figure B-160 Predicted IRI and NSI for existing PCC modulus

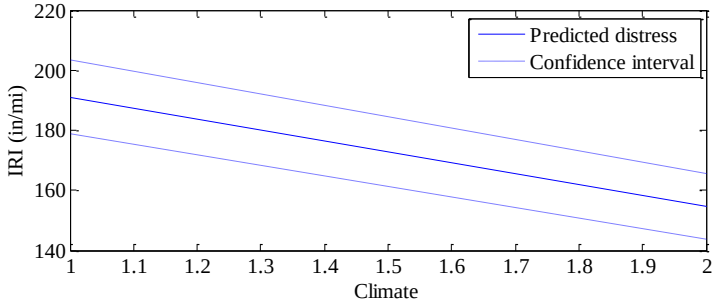

Figure B-161 Predicted IRI for climate

Inputs main effect

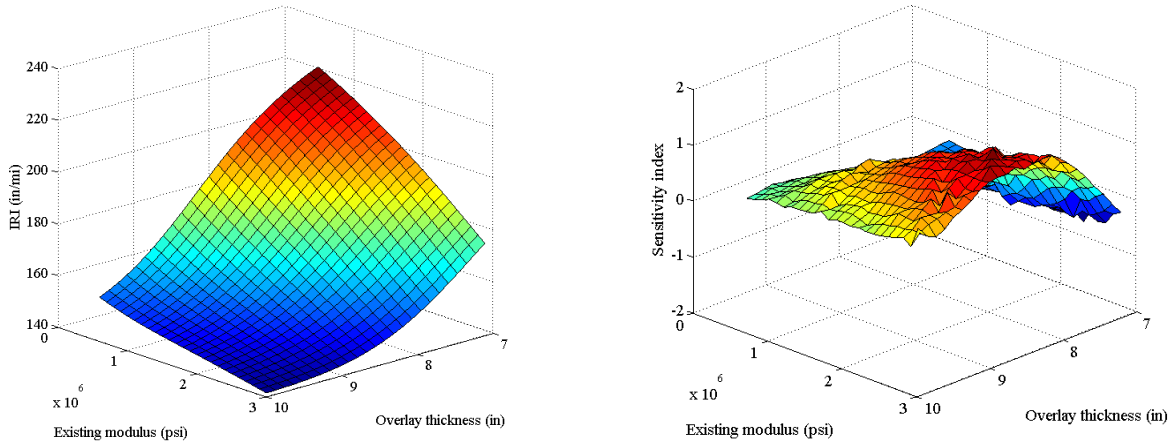

Figure B-162 Predicted interaction and NSI between existing modulus and overlay thickness

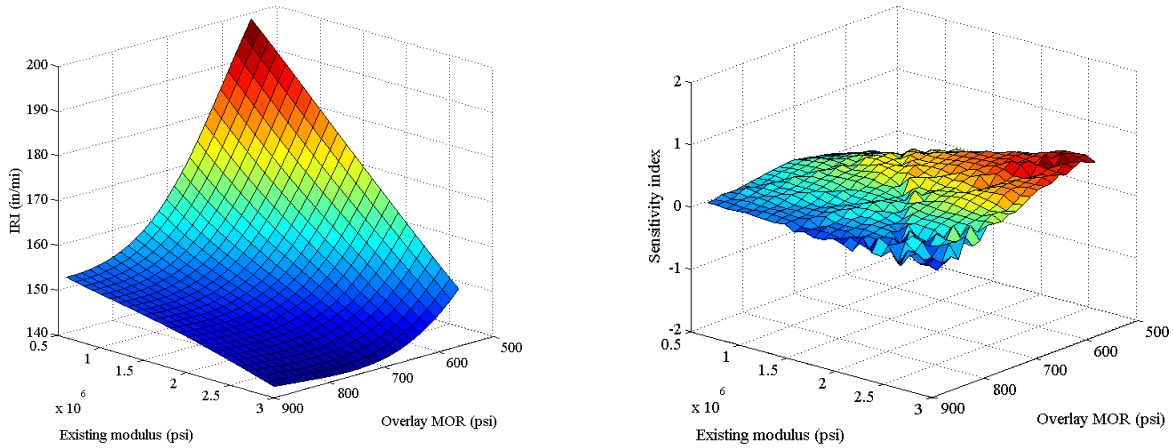

Figure B-163 Predicted interaction and NSI between existing thickness and overlay MOR

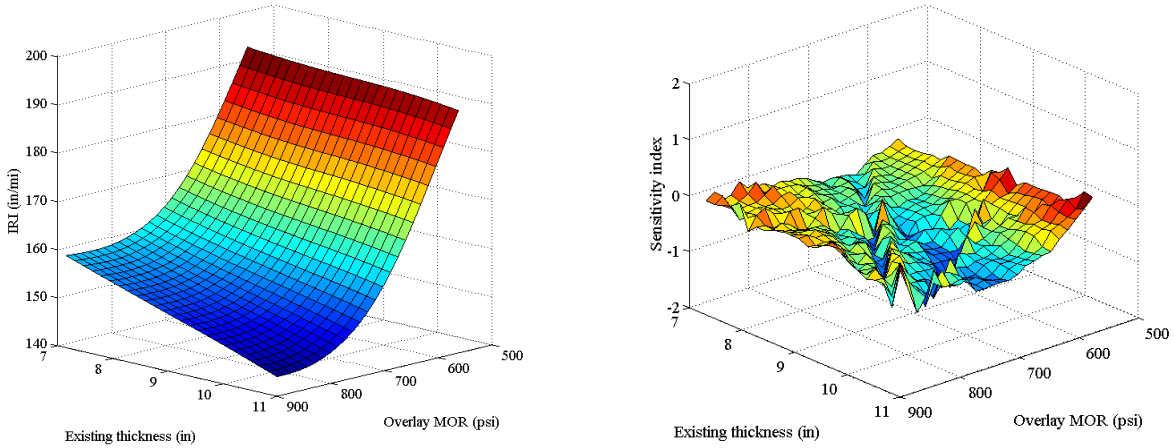

Figure B-164 Predicted interaction and NSI between existing thickness and overlay MOR